LA-UR- 99-1190

Approved for public release; distribution is unlimited.

Title: LATE QUARTERLY FAULTING ON THE PAJARITO FAULT, WEST OF LOS ALAMOS NATIONAL LABORATORY, NORTH-CENTRAL, NEW MEXICO, RESULTS OF SEVEN TRENCHES EXCAVATED IN SUMMER OF 1998

Author(s): JAMES P. McCaplin, GEO-HAZ, Consulting Inc.

Submitted to:

Los Alamos
NATIONAL LABORATORY

Los Alamos National Laboratory, an affirmative action/equal opportunity employer, is operated by the University of California for the U.S. Department of Energy under contract W-7405-ENG-36. By acceptance of this article, the publisher recognizes that the U.S. Government retains a nonexclusive, royalty-free license to publish or reproduce the published form of this contribution, or to allow others to do so, for U.S. Government purposes. Los Alamos National Laboratory requests that the publisher identify this article as work performed under the auspices of the U.S. Department of Energy. Los Alamos National Laboratory strongly supports academic freedom and a researcher's right to publish; as an institution, however, the Laboratory does not endorse the viewpoint of a publication or guarantee its technical correctness.

Form 836 (10/96)

GEO-HAZ Consulting, Inc.

LATE QUATERNARY FAULTING ON THE PAJARITO FAULT, WEST OF LOS ALAMOS NATIONAL LABORATORY, NORTH-CENTRAL NEW MEXICO

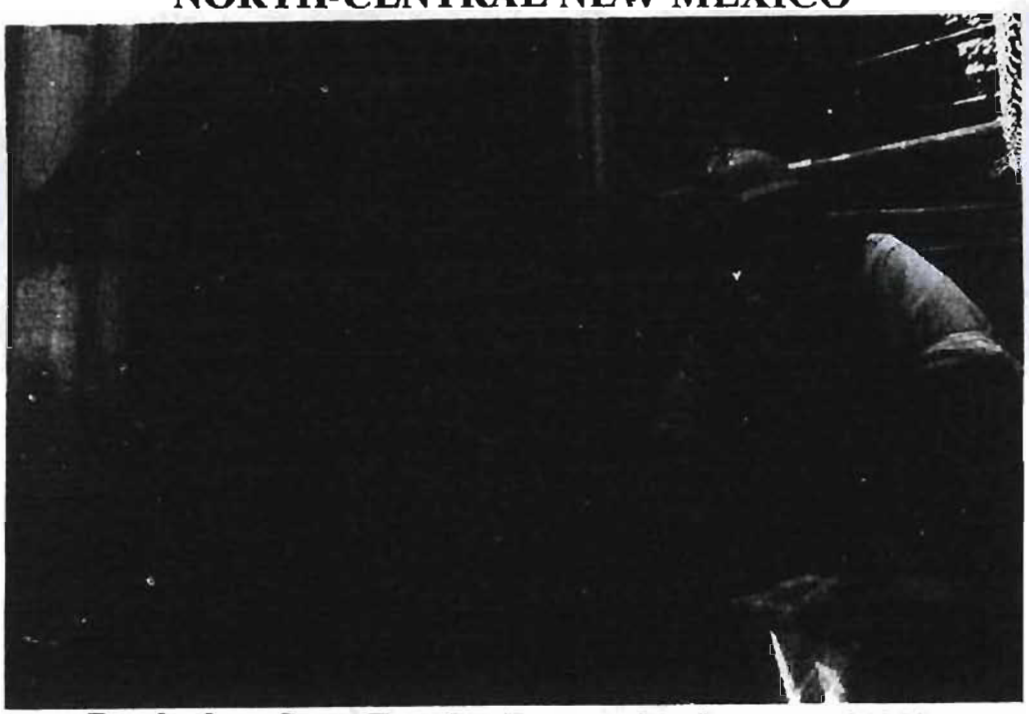

Results from Seven Trenches Excavated in Summer of 1998

Final Report, March 10, 1999

Submitted by:
James P. McCalpin
GEO-HAZ Consulting, Inc.
P.O. Box 1377
1221 Graves Avenue
Estes Park, CO 80517

Prepared for:
Douglas E. Volkman, P.E.
EES-1, MS M984
Los Alamos National Laboratory
Los Alamos, NM 87545

F:\GEOHAZ\LANL\PAJARITO98\98TRENCH.DOC 03/08/99

LATE QUATERNARY FAULTING ON THE PAJARITO FAULT, WEST OF LOS ALAMOS NATIONAL LABORATORY, NORTH-CENTRAL NEW MEXICO

Results from Seven Trenches Excavated in Summer of 1998

Final Report

March 10, 1999

Submitted by:
James P. McCalpin
GEO-HAZ Consulting, Inc.
P.O. Box 1377
1221 Graves Avenue
Estes Park, CO 80517

Prepared for:
Douglas E. Volkman, P.E.
EES-1, MS M984
Los Alamos National Laboratory
Los Alamos, NM 87545

Table of Contents **Page**

List of Figures 4
List of Tables 6
List of Appendices 6

1. EXECUTIVE SUMMARY 7

2. INTRODUCTION 9
   2.1 Purpose and Scope of The Trenching Study 9
   2.2 Trench Locations and Rationale 11
   2.3 Field Methods 12
   2.4 Laboratory Methods 15
   2.5 Acknowledgments 16

3. RESULTS 18
   3.1 Geomorphology of the Intermediate-Age Alluvial Fan 18
   3.2 Trench 1a 25
      3.2.1 Geomorphology 25
      3.2.2 Stratigraphy 25
      3.2.3 Soils 28
      3.2.4 Structure 28
      3.2.5 Geochronology 29
   3.3 Trench 1b 29
      3.3.1 Geomorphology 29
      3.3.2 Stratigraphy 29
      3.3.3 Soils 32
      3.3.4 Structure 32
      3.3.5 Geochronology 32
   3.4 Trench 2 32
      3.4.1 Geomorphology 32
      3.4.2 Stratigraphy 32
      3.4.3 Soils 36
      3.4.4 Structure 37
      3.4.5 Geochronology 37
   3.5 Trench 3 37
      3.5.1 Geomorphology 37
      3.5.2 Stratigraphy 37
      3.5.3 Soils 40
      3.5.4 Structure 40
      3.5.5 Geochronology 40
   3.6 Overall Interpretation of the Alluvial Fan Trenches 40
   3.7 Trench 4 42
      3.7.1 Geomorphology 42

3.7.2 Stratigraphy 46
3.7.3 Soils 50
3.7.4 Structure 50
3.7.5 Geochronology 51
3.7.6 Paleoseismic Interpretation 52
3.8 Trench 5 57
3.8.1 Geomorphology 57
3.8.2 Stratigraphy 61
3.8.3 Soils 67
3.8.4 Structure 69
3.8.5 Geochronology 71
3.8.6 Paleoseismic Interpretation 72
3.9 Trench 6 74
3.9.1 Geomorphology 74
3.9.2 Stratigraphy 76
3.9.3 Soils 78
3.9.4 Structure 78
3.9.5 Geochronology 79
3.9.6 Paleoseismic Interpretation 79

4. INTERPRETATION 81
4.1 Timing of the Most Recent Faulting Event 81
4.3 Recurrence Intervals Between Paleoearthquakes 83
4.4 Displacement per Event 85

5. CONCLUSIONS AND RECOMMENDATIONS 88
5.1 Conclusions 88
5.2 Implications of the 1998 Trenching Results on Quaternary Slip rates for the Pajarito fault 88
5.3 Timing of the MRE on the PF, GMF, and RCF 90
5.4 Recommendations 90

6. REFERENCES 92

7. APPENDICES 96
7.1 Seismic refraction survey results
7.2 Report by PaleoResearch Labs on content of radiocarbon samples
7.3 Explanation for reconnaissance geologic map of the main Pajarito fault scarp west of LANL (Reneau, 1996)

List of Figures

Fig. 1. Map of major fault strands of the Pajarito fault zone and location of paleoseismic trenches from this study and previous studies 10

Fig. 2. Reconnaissance geologic maps along the main scarp of the Pajarito fault west of LANL. (a)- Area between Pajarito Canyon and Canon de Valle; (b) Area between the Water Tanks and NM Highway 4; (c) Explanation. All mapping from Reneau (1996). 19

Fig. 3. Geologic map of the intermediate-age alluvial fan south of Pajarito Canyon and location of Trenches 1a, 1b, 2, and 3. 22

Fig. 4. Longitudinal topographic profile down the intermediate-age alluvial fan. Trenches 2 and 3 are on the line, Trenches 1a and 1b are projected from south of the line.The gradient of the upper fan is less than that of the lower fan. Vertical exaggeration= 5x 24

Fig. 5. Photographs of Trench 1a. (a)- View east down the trench axis; (b) South wall from 4-7 mH. 26

Fig. 6. Log of Trench 1a. 27

Fig. 7. Photographs of Trench 1b. (a) View to SE, Trench 1b in foreground, Trench 1a in background; (b) South wall centered about 12 mH; orange flags at left mark soil horizon boundaries in profile at 13 mH. 30

Fig. 8. Log of Trench 1b. 31

Fig. 9. Photographs of Trench 2. (a) View east down trench axis. 33

Fig. 9b. South wall from 9 mH to east end. Level line at center is -3 mV. Unit 4a with light-colored pumice stringers is just above lower level line at lower right. 34

Fig. 10. Log of Trench 2. 35

Fig. 11. Photographs of Trench 3. (a) View west down trench axis; note fault scarp in distance; (b) South wall, centered at 6.1 mH; orange flags mark soil horizon boundaries. 38

Fig. 12. Log of Trench 3. 39

Fig. 13. Schematic longitudinal section of the alluvial fan. Distance between three Trenches at right is not to scale. 41

Fig. 14. Geologic map of the intermediate-age alluvial fan at the base of the Western Splay fault, and location of Trench 4. 43

Fig. 15. Photographs of Trench 4. (a)- Clearing trench footprint in the dense oak grove before excavation 44

Fig. 15b. View west down trench axis. 45

Fig. 16. Log of Trench 4 47

Fig. 17. Photograph of steeply-dipping tuff slabs at the head of Trench 4 48

Fig. 18. Geologic map of the main Pajarito fault scarp west of the intermediate age alluvial fan south of Pajarito Canyon, the head of which (and Trench 3) is at right center. 58

Fig. 19. Photographs of Trench 5. (a)- View east down the trench axis, from the upslope end of the middle fault block (at center).The upper pocket is out of photo to the lower right, the lower pocket is at upper left. 59

Fig. 19b. The upper pocket, view to west 60

Fig. 20. Log of Trench 5 62

Fig. 21. Photograph of the lower pocket and its fine-grained fissure fill. View to west. Shadowed area at the base of the left (south) trench wall is the void space termed the "Rat Hole". 63

Fig. 22. Photographs of Trench 5. (a)- Unit 4l (the "beach sand") showing the fine, east-dipping bedding and the small conjugate normal faults. Finger is pointing to the subvertical contact between units 4l (to left) and 3l (to right) at ca. 29 mH. 64

Fig. 22b. Photograph of fault zone A in Trench 5, between 30 and 31 mH at the -12 mV line. Upper part of photo shows light-colored unit 4l, lower part shows darker and more hackly unit 2-4l. 66

Fig. 23. Geologic map of the main Pajarito fault scarp where NM Highway 4 ascends the scarp. Trench 6 is at center. 75

Fig. 24. Log of Trench 6 77

Fig. 25. Space-time diagram of faulting events in Trenches 4, 5, and 6 82

Fig. 26. Schematic cross-section of the Hansel Valley, UT fault scarp affected by coseismic slumping 87

List of Tables

Table 1. Time schedule of trench excavation and logging, summer 1998. 12
Table 2. SDI age estimates for trenches 1a, 1b, 2, 3, 4, 5, and 6 excavated in 1998. 14
Table 3. Summary Table of Radiocarbon Dates 17
Table 4. Slip rates used for the PF in the WCFS 1995 Logic Tree 80

List of Appendices

Appendix 1. Seismic refraction survey results. A1-1
Appendix 2. Report by PaleoResearch Labs on content of bulk radiocarbon samples. A2-1
Appendix 3. Explanation for reconnaissance geologic map of the main Pajarito fault A3-1

1. EXECUTIVE SUMMARY

In June 1998 we excavated seven trenches across strands of the Pajarito fault zone to characterize the most recent faulting event (MRE), and to refine characterization of previous faulting events. Our strategy was two-fold: 1) to determine whether a late Quaternary alluvial fan was offset by faulting, and 2) to characterize the latest few faulting events on several well-defined fault traces at the base of high scarps of the Pajarito fault. Four of the seven trenches were located on a late Quaternary alluvial fan south of Pajarito Canyon, with the remainder on scarps farther south.

The four trenches on the alluvial fan did not expose any faults within their 5 m depth. Instead, alternating beds of fluvial gravel and debris flow deposits extended along the entire lengths of the trenches. Fan gradient decreased toward the head, suggesting that the entire fan may be backtilted toward the Pajarito fault.

The remaining 3 trenches all exposed complex zones of faulting and/or folding. Trench 4, at the base of the western splay scarp, exposed complex folding and thrust faulting in the western (upslope) part of the trench, while beds farther east were undisturbed. This compressional deformation is inferred to be the toe of a landslide coming from the scarp face. Trench 5 contained two deep pull-apart zones filled with fine-grained deposits that had been subsequently deformed by fissuring and "domino style" rotational normal faulting. Trench 6 also contained a deep pull-apart and domino faulting, but also contained some smaller high-angle faults that displaced post-pull-apart colluvium near the surface,

The MRE in Trenches 4, 5 and 6 appears to fall in a relatively broad age range between ca. 2-3 ka (age of the surface soil) and 12-20 ka (age of the uppermost buried soil). The vertical displacement on individual structures in these trenches tends to be small (10-35 cm), and the net vertical displacement for the MRE in a given trench ranges from 35-55 cm. These displacements constitute the minimum per-event displacement across the entire fault zone during the MRE, and imply (via empirical relations) minimum earthquake magnitude of Mw 6.5-6.6 and surface rupture lengths of 25-28 km on the Pajarito fault.

The record of older paleoearthquakes was partially reconstructed in Trenches 4, 5, and 6. The penultimate event (PE) ranged from quite young (8.7-18.9 ka) in Trench 4 to much older (41-58 ka) in Trench 6, and had displacements as large as 1.4-2.8 m in Trench 5, where the age is roughly bracketed between 11-19 ka and 25-42 ka. The recurrence time between the MRE and PE was smallest at Trench 4 (5-11.6 ka), intermediate in Trench 5 (11.3-21.6 ka), and longest in Trench 6 (28.6-48.9 ka). This variation in recurrence time roughly correlates with the difference in geomorphic expression of faulting among the three trench sites, with Trench 4 (inferred short recurrence) excavated across a high scarp in young (post-El Cajete) deposits, whereas at Trench 6 (inferred long recurrence) no scarp currently exists; however, scarp morphology may also be sensitive to other factors.

The MRE dated between 2-3 ka and 12-20 ka could conceivably be contemporaneous with the MRE dated in four of the 1997 trenches farther north on the PFZ, based on a

comparison of constraining radiocarbon dates rather than soil PDI age estimates. In addition, the PE in Trench 4 (8.7-18.9 ka) overlaps the age ranges of the MRE in Trenches 5 and 6, and could conceivably be the same event. The age range for the MRE in the 1998 trenches is sufficiently broad that it covers the age ranges of both the MRE on the Guaje Mountain fault, (dated at Cabra Canyon at 4-6 ka; Gardner et al, 1990) and the MRE on the Rendija Canyon fault (dated at either 8 ka or 23 ka; Wong et al, 1995). Thus, age control from the 1998 trenches is insufficiently precise to permit a correlation among MREs between the three major faults of the PFZ. Much of this imprecision results from our necessary reliance on PDI age estimates to bracket faulting events. The PDI method assumes that changes in soil development at a given site are solely a function of time, but due to the complex patterns of erosion, deposition, and infiltration operating on faults scarps, this is unlikely to be true.

Our trenches do not show evidence on the Pajarito fault for a second (or third) Holocene earthquake aside from the MRE. However, the older half of the Holocene (5-10 ka), and the youngest part of the Pleistocene, are generally not represented by deposits in our trenches, but instead were periods of nondeposition or soil formation. Thus, it is conceivable that one (or more) small-displacement events could have occurred between ca. 4 ka and 20 ka and not be detectable in our trenches. The slip rates for the PFZ implied by the single Holocene characteristic earthquake that we can definitely identify fall within the range of slip rates used in the PSHA of Wong et al. (1995).

2. INTRODUCTION

This report summarizes the paleoseismic trenching study of the Pajarito fault performed by James P. McCalpin and co-workers during the summer of 1998. Contained herein are the trench logs and the interpretation of deformation events deduced from these logs.

2.1 Purpose and Scope of The Trenching Study

The primary purpose of this trenching study was to date the most recent faulting event (MRE) on the main trace of the Pajarito fault (PF) (Fig. 1). Previous studies of the Pajarito fault zone (PFZ) (Gardner et al., 1990; Wong et al., 1993,1995; Olig et al., 1996; Kelson et al., 1996) yielded relatively well - constrained ages for the MRE on the two major west-dipping faults, the Rendija Canyon fault (RCF) and Guaje Mountain fault (GMF). On the Rendija Canyon fault, the MRE was dated at either 8-9 ka (based on radiocarbon; Wong et al., 1995; Kelson et al., 1996) or 23 ka (based on TL). On the Guaje Mountain fault the MRE was dated at 4 - 6 ka (Gardner et al., 1990). In contrast, the MRE deduced from four trenches on the main trace of the Pajarito fault zone pre-dated the El Cajete pumice, and would thus be older than ca. 50 - 60 ka (Wong et al., 1995; Olig et al, 1996). Thus the Holocene (or late Pleistocene) MREs on the two smaller antithetic faults (Rendija Canyon fault and Guaje Mountain fault) evidently had no counterpart events on the master fault (Pajarito fault).

The paleoearthquake chronology outlined above could be explained in several ways: (1) The dates of MREs on all three faults were correct, indicating that separate Holocene earthquakes had occurred on the Rendija Canyon fault and Guaje Mountain fault, but that no Holocene events had ruptured the Pajarito fault; (2) there may have been a Holocene event on the Pajarito fault that matches the MRE on either the Rendija Canyon fault or Guaje Mountain fault (two separate events), but evidence of this event was not exposed in the four trenches of Wong et al. (1993); or (3) the MREs on the Rendija Canyon Fault and Guaje Mountain fault are actually the same event, poorly constrained by current dates. If so, then this MRE also may have ruptured the Pajarito fault, but that rupture was not exposed in the Wong et al. (1993) trenches.

In order to test these three hypotheses a paleoseismic program was implemented to find the MRE on the Pajarito fault. First, the PF scarp was mapped at a scale of 1:1200 (McCalpin, 1997). Based on the map, a structural model was developed for the Pajarito fault scarp, showing that the scarp consisted of an articulated monocline (ca. 50% of its length), landslide blocks (ca. 30% of its length), or a simple high-angle normal fault (ca. 20% of its length). Given this structural configuration, three possible trenching strategies were envisioned. The first was a megatrench through the ca. 50 m-thick colluvial wedge at the scarp base where the scarp was underlain by one or more high-angle normal fault. This option was given low priority due to logistical problems of megatrenching through the coarse colluvium. The second strategy consisted of seven trenches scattered along

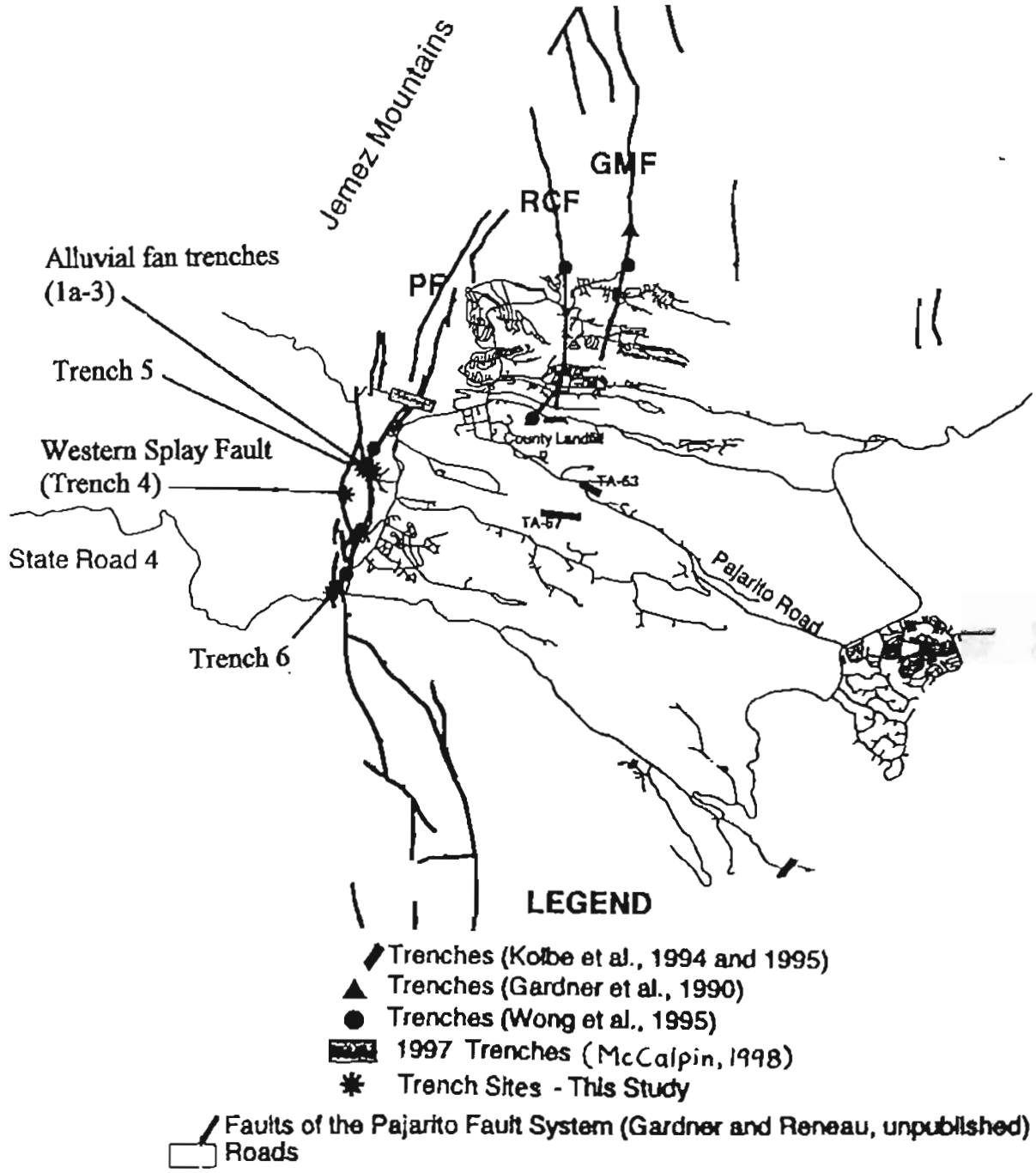

Fig. 1. Map of major fault strands of the Pajarito fault zone and location of paleoseismic trenches from this study and previous studies.

strike on the PF scarp, but on different structures. Although this strategy was logistically feasible, rupture events (including the MRE) might be missed due to the scattered locations of trenches. The third strategy, which was considered to have the highest potential for success, involved a transect of seven trenches across all major component scarps of the PF at a given latitude. That strategy was considered the best for capturing evidence of the MRE on the PF, and was executed during the summer of 1997 (see McCalpin, 1998).

The 1997 transect of trenches revealed that the MRE in 4 of the 7 trenches was bracketed rather tightly between about 1.5 and 2.5 ka. Earlier events were difficult to date due to lack of charcoal for radiocarbon dating, but soils suggest that the penultimate event occurred about 20 ka, and prior events had recurrence intervals of ca. 20-60 ka. However, the best paleoseismic chronologies came from minor, west-facing scarps created by subsidiary faulting. Thus, it was unclear whether there may have been additional faulting events on the larger, east-facing scarps that were not detected in the 1997 trenches.

Given the ambiguity above, in 1998 we pursued the second trenching strategy as conceived in 1996, consisting of seven trenches scattered along strike on the PF scarp. Four of these trenches (1a, 1b, 2, and 3) crossed subtle lineations or fault projections across a late Quaternary alluvial fan, mapped by Reneau (1996) as mainly older than the El Cajete pumice. The remaining three trenches (4, 5, and 6) were across large, east-facing scarps.

2.2 Trench Locations and Rationale

The adopted trenching strategy relied heavily on our understanding of the structural geometry of the Pajarito fault. Trenches 1a, 1b, 2, and 3 were placed on the largest alluvial fan complex at the base of the main fault scarp, across projections of fault scarps or structurally-controlled stream reaches from north and/or south of the fan. At this latitude just south of Pajarito Canyon the Pajarito fault is composed of a 2 km-wide zone of east-facing fault scarps, toppled blocks, tension fissures, and fracture zones. Given the distributed nature of deformation in this wide zone, we hoped that faint lineaments on the fan would be underlain by minor down-to-the-east normal faults that displaced beds of El Cajete pumice and/or younger fan deposits. Such young displacements would be attributable to the Most Recent (faulting) Event (MRE) or possibly the Penultimate (faulting) Event (PE) on the Pajarito fault.

The other three trenches were each excavated for a different reason. Trench 4 was excavated across the Western Splay fault, a previously untrenched, 30-35 m-high east-facing fault scarp that lies 0.5 km west of and parallel to the main scarp, between Pajarito Canyon and Canon de Valle. This scarp obviously represents the result of numerous surface-faulting events, but it was not known if its paleoseismic chronology was identical to that of the main scarp. In particular, we wanted to know if the MRE on the Western Splay fault was Holocene, as dated in several of the 1997 trenches farther north, or pre-El

Cajete, as dated by Wong et al. (1995) at the nearby Pajarito Canyon and Water Tanks trench sites. The Holocene MRE in the 1997 trenches was best expressed on the western fault strands, so we surmised that faulting may be progressing westward with time, in which case the Western Splay fault may exhibit several young deformation events (this turned out to be the case).

2.3 Field Methods

Trenching: Trenches 1a through 5 were excavated by Parker Construction, Los Alamos, with a Komatsu 200 track-mounted backhoe with a 20 ft-long arm and buckets ranging in width from 24" to 30". The time schedule for excavating, cleaning, and logging the trenches is shown in Table 1. Trench 6 was excavated by a Cat 416 backhoe. Parker Construction also shored the trenches with hydraulic aluminum shores of various lengths up to 7 ft, and covered several trench walls with stucco wire. Trench walls were cleaned by J. P. McCalpin, L.C.A. Jones, T.E. Cooper, J.-C. Moya, J. Gardner, and A. Lavine. The softer, light colored Holocene sediments were best cleaned with scraping tools such as trowels or stirrup hoes. However, using these tools on hard, clay-rich Bt soil horizons resulted in smearing that obscured horizon contacts. Therefore, all hard cohesive materials were cleaned by plucking, usually using the claw end of a claw hammer. Horizontal string lines were attached to the trench walls at 1 m intervals, with every 1 m increment marked by labeled squares of duct tape. Contacts were scribed into the wall with trowels or knives. Logging contacts was done manually and the log was drawn on graph paper at a scale of 1 inch = 0.5 m (an approximate scale of 1:20). The definition and logging of units followed a mixed subjective- objective approach, as outlined in McCalpin (1996b).

Table 1. Time schedule of trench excavation and logging, summer 1998

Trench No.	Dug	Cleaned	Strung	Logged	Revised	Photographed & Sampled
1a	June 11	June 12	June 12	June 12-19		Aug. 16
1b	June 12	June 16	June 16	June 20-22		Aug. 16
2	June 15	June 17	June 17	June 20-22	July 16	Aug. 17
3	June 15	June 18	June 18	June 20-22		Aug. 17
4	June 17	June 24, 25	June 25-26	June 27-29	Aug. 17-19	Aug. 19
5	June 18	June 19	June 29-30	June 30-July 3	Aug. 20	Aug. 20
6	June 18	June 19	June 22	June 23-25	Aug. 24	Aug. 24

In many trenches, the most obvious mappable contacts in unconsolidated deposits were soil horizon boundaries rather than stratigraphic contacts. In general, stone lines within the colluvium, and soil horizon boundaries, were parallel to each other and to the modern ground surface. This parallelism suggests that mappable buried soils are probably developed on discrete stratigraphic units, and that soil horizon contacts and stratigraphic

contacts are parallel, in general. Thus, we use the same solid line map symbol for both lithologic contacts (where visible) and soil contacts. Parent material units and soil horizons are given abbreviations, with parent material numbers (at front) decreasing with increasing age, and buried soil numbers (at end) increasing with increasing age. In some trenches, faulting has uplifted parent materials and their soils across faults, after which sediments/soils were stripped from the upthrown block, and then soil formation continued on the stripped surface, thus superimposing a soil across two parent materials. Conversely, when soils merge a single parent material can be affected by B horizon development from several distinct episodes of soil formation; such soils are "welded" onto each other.

Soil Development Index: In addition to our definition of soil horizons, Eric McDonald (Desert Research Institute, Reno, NV) described vertical soil profiles at 11 locations on our logged trench walls. He also calculated Profile Development Index (PDI) and Soils Development Index (SDI) values for all soil horizons (Table 2), after the methods of Harden (1982), Harden and Taylor (1983) and Taylor (1988). The complete results of McDonald's soil study are in a separate report (McDonald, 1999).

IMPORTANT NOTE: McDonald described his soil profiles after we had logged the trenches, so in many cases his soil horizon boundaries do not exactly correspond with the boundaries of our mapping units. There are several reasons for this. First, we had to define mapping units that could be traced for long distances along the trench walls, whereas McDonald only had to define his soil horizons within a vertical strip about 20 cm wide. As a result, McDonald defined many more soil horizons at a given stratigraphic level than we map on the trench logs. Second, McDonald dug the trench wall back 15-20 cm when describing his soils. Soil contacts that are not horizontal thus shift slightly between his mapped position and our original mapping; usually these shifts are <5-10 cm. Most of McDonald's contacts between his buried soils (b1, b2, b3, etc.) do correspond with our trench log mappping units.

Radiocarbon Sampling: Organic samples analyzed by radiocarbon dating methods (Table 3) consisted of one or more discrete charcoal fragments that were either hand-picked from the trench walls, or floated and picked from bulk samples. Areas with discolored soil (suggesting the possibility of roots burned in place) or disrupted soil (such as due to animal burrows or the decay of large roots) were avoided, although the absence of distinct stratigraphy in the sampled units suggest some degree of mixing, and the possibility of bioturbation of younger charcoal into older deposits cannot be ruled out. In addition, the possibility of recycling older charcoal exists, potentially providing ages older than the sampled deposits. Where possible, multiple samples were collected from single units or single stratigraphic sections in order to provide internal checks on the analyses. Bulk samples were picked by PaleoResearch Labs, Inc. to extract and identify datable components. Their report is Appendix 2.

Table 2. PDI age estimates for trenches 1a, 1b, 2, 3, 4, 5, and 6. From McDonald, 1999.

Trench no.	Figure No.	Profile no.	Lowest Buried Soil Horizon	Depth of Soil (cm)	Trench Unit[a]	Soil PDI	PDI Age Estimate: Best Age (ka)	Lower Range (ka)	Upper Range (ka)
PC-1a	13	P10.6	Bw2	52	1	7.6	2.3	1.8	2.9
			Bt5b1	201	2, 3	50.8	42	33	53
			Btb2	276	4	69.6	66	54	86
			Bt2b3	367	4, 5	102.9	125	99	157
			Bt3b4	475	5	140.6	202	161	255
PC-1b	15	P13.0	Bw	41	1	6.8	1.9	1.5	2.4
			BCb1	259	2,3	52.9	45	36	56
T2	16	P7.8	Bw	33	1	6.5	1.8	1.4	2.2
			C3b1	490	2,3,4	57.6	51	41	64
T3	17	P8.1	BA	52	1	6.7	1.9	1.5	2.4
			CB2b1	444	2, 3	49.4	40	32	51
T4	18	P6.6	Bt2	62	1, 2C	9.1	3.0	2.4	3.8
			Bt3b1	133	3C2	34.4	23	18	29
			C2b2	307	3C3-3C5	58.1	52	41	65
T4	19	P6.4	Bw	51	1, 2C	6.3	1.7	1.4	2.1
			Bt3b1	133 (219)b	3C2	47.7	38	30	48
			Bt3b2	297 (275)b	3C3-3C5	73.2	74	59	63
T4 Composite[c]		P6.4 + P6.6	Bw	51	1, 2C	6.3	1.7	1.4	2.1
			"b1"	219	2C2, 3C1	47.7 (38.4)d	38 (25)d	30 (20)d	48 (32)d
			"b2"	290	3C2	72.9 (52.8)d	73 (46)d	58 (36)d	92 (56)d
			"b3"	474	3C3	96.7 (65.9)d	113 (63)d	90 (50)d	143 (79)d
T4	20	P27.2	Bw1	39	1A, 1B	6.6	1.8	1.5	2.3
			Btb1	96	2a, 3Bt, 4Bt	19.5	10.0	7.9	12.6
			CB2b2	354	3a4, 4a2	48.9	40	32	50
			Bt2b3	423	5a	66.7	80	63	101
T5	21	P7.4	Bt	40	9c	9.1	3.0	2.4	3.7
			Btb1	78	7u	22.7	12.0	9.7	15.0
			Bt3b2	142	4Lb	47.4	38	30	48
			Bt2b3	209	4ub	69.9	69	55	67
			Bt1b4	264	3u3	88.7	98	79	124
			Bt2b5	340	3u3	120.5	159	128	200
			Bt2b6	386	3u3	137.6	195	154	246
T5	22	P30.7	Bt2	54	9c	17.3	8.1	6.4	10.2
			Btb1	85	7lu	30.5	19	15	24
			Btb2	114	2-4l	42.1	32	25	40
T5	23	P31.6	Bt	46	9c	9.3	3.1	2.5	3.9
			Btb1	75	7lu	21.2	11	9	14
			Bt3b2	187	2-4l	52.3	44	35	55
T5	24	P32.7	Bt1	41	7lu	8.2	2.5	2.0	3.2
			Btb2	112	4l	36.3	25	20	32
T6	25	P2.7	Bw2	53	1	6.8	1.9	1.5	2.4
			Bt3b1	133	2a, 3Bt, 4Bt	35.0	24	19	30
			Bt1b2	176	4Bt	48.7	41	32	51
			Bt1a3	214	5Bt	62.8	58	46	74
			Bt1b4	258	6aBt	76.8	78	62	98
T6	26	P8.8	Bw2	36	1	8.4	2.7	2.1	3.4
			Btb1	128	2b	27.1	16	13	20

a: Trench unit designations from McCalpin (1996b).
b: Depth adjusted for total thickness of soil b1.
c: Stratigraphic composite section composed of most complete soil sections from Profiles 6.5 MD 5.4.
d: PDI values adjusted for no change in texture, color, and metal concentration due to saturation.

Luminescence sampling: Luminescence samples were collected from trench walls, in daylight conditions, by first scraping 5-10 cm of material from the trench wall at the sampling location. A 3-5 cm-diameter steel sampling tube was then quickly driven into the freshly-exposed trench wall. Upon extraction the open end of the tube was immediately sealed. In the laboratory both ends of samples thus collected are discarded, and only the central part is used for luminescence analysis. Care was taken to avoid recognizable krotovinas.

Surveying: The locations of seismic refraction lines and trenches were surveyed by J.N. Gardner and A. Lavine (LANL) using a Geodimeter total station. All survey locations were tied to fixed reference points whose coordinates were determined from the Los Alamos Geographic Information System (FIMAD), in coordinates of the New Mexico Central Zone State Plane Coordinate System (in feet), 1983 North American Datum. Accuracy of the surveyed points is within about 3 feet in absolute 3-dimensional space.

Post-Trenching Seismic Refraction Survey: These surveys were performed by Craig V. Nelson of Dames and Moore, Salt Lake City, UT assisted by Jamie Gardner, Alexis Lavine, Don Krier, and Claudia Lewis (LANL), using a Geometronix ES-1225 engineering seismograph with a 12-lb sledgehammer source. Refraction lines were oriented both parallel to trenches, and parallel to fault scarps. Eight lines were shot, six of which were reversed, ranging from 24 m long (2 m geophone spacing, depth resolution ca. 1-2 m) to 60 m long (5 m geophone spacing, depth resolution ca. 2-3 m). Subsurface interpretation was based on P-wave first arrival times. Interpreted seismic profiles are shown in Appendix 1.

2.4 Laboratory Methods

Radiocarbon Methods

Before submission to the analytical laboratory, each charcoal sample was air-dried, examined under a binocular microscope, and cleaned to remove dirt and roots. All samples were analyzed by the accelerator mass spectrometry (AMS) method, and were processed by Beta Analytic, Inc., of Miami, Florida. Sample pretreatment by Beta Analytic included standard hot acid (HCl) treatment to remove carbonates from the samples, followed by alkali (NaOH) treatment to remove secondary organic acids, followed by conversion to graphite (which constituted the actual accelerator target).

The radiocarbon analyses were calibrated to an absolute dendrochronological time scale using the computer program CALIB 3.0.3 developed by the Quaternary Isotope Laboratory of the University of Washington (Stuiver and Reimer, 1993). This calibration corrects for differences between radiocarbon years and calendar years imparted by variations in the ^{14}C production rate in the atmosphere, and incorporates uncertainties both in the measurements of the radiocarbon content and in the calibration curves. The calibration can incorporate an "error multiplier" to account for sources of laboratory

uncertainty that are not encompassed by the reported analytical plus-or-minus (Stuiver and Reimer, 1993), and, following other researchers, we have previously used an error multiplier of 2.0 in work at Los Alamos (e.g., Reneau et al., 1995). Use of 2-sigma (2 standard deviation) uncertainties and an error multiplier of 2 provides a conservative estimate of the laboratory uncertainty associated with each radiocarbon analysis, although other uncertainties still exist (as discussed above).

2.5 Acknowledgments

This study would not have been possible without the support and cooperation of LANL personnel, in particular Douglas E. Volkman, Jamie N. Gardner, and Alexis Lavine. Our trenching crew of L.C.A. Jones, T.E. Cooper, and Juan-Carlos Moya persevered through rain, fire and mud to produce some fine trench logs. Jamie N. Gardner and Alexis Lavine revised our logging over part of Trench 2 and much of Trench 4. Don Creer and Claudia Lewis assisted in sample collected and unit description. Eric McDonald described soils in our trenches and Glenn Berger analyzed luminescence samples. Trench reviewers William R. Lettis and Frank H. Swan provided many helpful observations during their field review. Our day-to-day trench safety was ensured by Mr. Will Hobbs (Johnson Controls, Inc.). We also thank the efficient crew from Parker Construction for their artful trench shoring, particularly Mr. Brad Parker.

Table 3. Summary Table of Radiocarbon Dates (all dates on charred material; see Appendix 2)

Trench	Sample No.	Unit	Material dated/weight	Lab. No.	Dating method/Pre treatment	C13/C12 ratio	C-14 Age	Calendar Age[1] (cal yr BP, flanked by 2-sigma limits)	Event Constraint
T2	98T2-1	2bBt2 b1	charcoal/NA	B-122084	AMS/acid-alkali-acid	-24.6 ‰	106% modern	N/A	no faulting
T4	98T4-2	4c2	charcoal/NA	B-122086	AMS/acid-alkali-acid	-23.0 ‰	30,910 +/- 180	N/A	Y4, maximum age
T4	98T4-3	4a1	charcoal/NA	B-122087	AMS/acid-alkali-acid	-22.9 ‰	29,570 +/- 150	N/A	Y4, maximum age
T4	98T4-4	5t1	charcoal/NA	B-122088	AMS/acid-alkali-acid	-25.7 ‰	43,660 +/- 750	N/A	Z4, far maximum age
T4	98T4-5	1Bw	Pinus charcoal, wood/NA	B-122649	AMS/acid-alkali-acid	-24.0 ‰	1420 +/- 50	736 (943) 1170	Z4, close minimum age
T4	98T4-6	1cBw	conifer charcoal/ 0.003 g	B-122650	AMS/acid-alkali-acid	-25.1 ‰	840 +/- 50	276 (471) 620	Z4, close minimum age
T4	98T4-7	3a1	conifer charcoal/ 0.013 g	B-122651	AMS/acid-alkali-acid	-24.9 ‰	17,940 +/- 100	N/A	Z4, maximum age
T5	98T5-1	9C	Pinus charcoal/ 0.031 g	B-122652	AMS/acid-alkali-acid	-24.0 ‰	400 +/- 50	N/A	Z5, minimum age
T6	98T6-1	2a	Pinus charcoal/ 0.016 g	B-122653	AMS/acid-alkali-acid	-24.0 ‰	2370 +/- 50	1738 (1972) 2269	Z6, close minimum age

[1] from CALIB 3.0, lab. error multiplier=2.

3. RESULTS

3.1 Geomorphology of the Intermediate-Age Alluvial Fan

The alluvial fan that hosts Trenches 1a, 1b, 2, and 3 lies 300 m south of Pajarito Canyon and is bisected by West Jemez Road (Fig. 2a). This location marks a major change in the strike of the Pajarito fault, which trends N-S south of the fan, but N 35° E north of the fan. Structural complexities associated with this change in strike (discussed later) are probably responsible for the small embayment in which the alluvial fan has formed.

The unnamed stream responsible for fan deposition trends due west from the fan, and heads on the Pajarito Plateau west of the PF zone. West of the PF, the stream is incised 20- 30 m into Bandelier Tuff on the upthrown fault block. This stream course may be controlled by a linear fault or fracture associated with the 35° bend in the PF.

The alluvial fan heads at an elevation of 7870 ft (2399 m) and slopes to the ESE at 6°- 7°. The fan extends at least 640 m in the downslope direction and about 500 m in the across- slope (approximately N-S) direction. The fan deposits may extend farther downslope, east of the LANL security fence, but that area was not mapped by Reneau (1996). The modern stream channel flows along the southern part of fan and is incised ca. 5 m into the fan. Two small discontinuous terraces are present along the modern channel, a young low terrace ca. 1 m above the channel (afy1 on Fig. 3) and a poorly- defined terrace about 2.5 m above the channel (afy2).

Reneau (1996) mapped this alluvial fan as a fan complex composed of old, intermediate, and young components (Fig. 2a). The oldest fan surface (Qfo?) occurs on the southern margin of the fan complex, south of the modern channel. Most of the fan surface is mapped as intermediate age (Qfi?). According to Reneau (1996), Qfi pre-dates the El Cajete pumice, but its "exact age range is uncertain" and the map unit contains "multiple distinct fan lobes in some areas". For example, on the Sept. 13, 1996 version of his map Reneau shows at least 8 distinct lobes on the alluvial fan, all labeled Qfi? About 20% of the fan surface is mapped as Qfy?, divided into at least 12 distinct lobes. Most Qfy? areas flank small incised drainages on the fan, particularly along the north margin.

The "type areas" for Qfi are south of Pajarito Canyon, between the two large water tanks and the Back Gate (intersection of West Jemez Road with NM Highway 4), where the El Cajete pumice covers the fan surface and overlies a buried soil. This relationship is well- exposed in soil pit WJR-7 on the east side of West Jemez Road, 0.8 mi north of the Back Gate (Reneau and McDonald, 1994, p. 82-90). At this location and east and west of the Back Gate, it is clear that Qfi predates the deposition of the El Cajete pumice, and has received no alluvial deposition subsequent to pumice deposition.

The relation of our alluvial fan to the El Cajete pumice is less clear, since Reneau (1996) does not map the pumice as a surface map unit on our fan. Soil pit WJR-4 (Reneau and McDonald, 1994, p. 94-96) is located on our fan near the local high point of West Jemez Road, and east of the road. That 2 m-deep pit exposed an 80 cm-thick "post-El Cajete soil" overlying a 1.2+ m-thick "pre-El Cajete soil", but there is no El Cajete pumice between the two soils. If the correlation of these two soils is correct, then the absence of

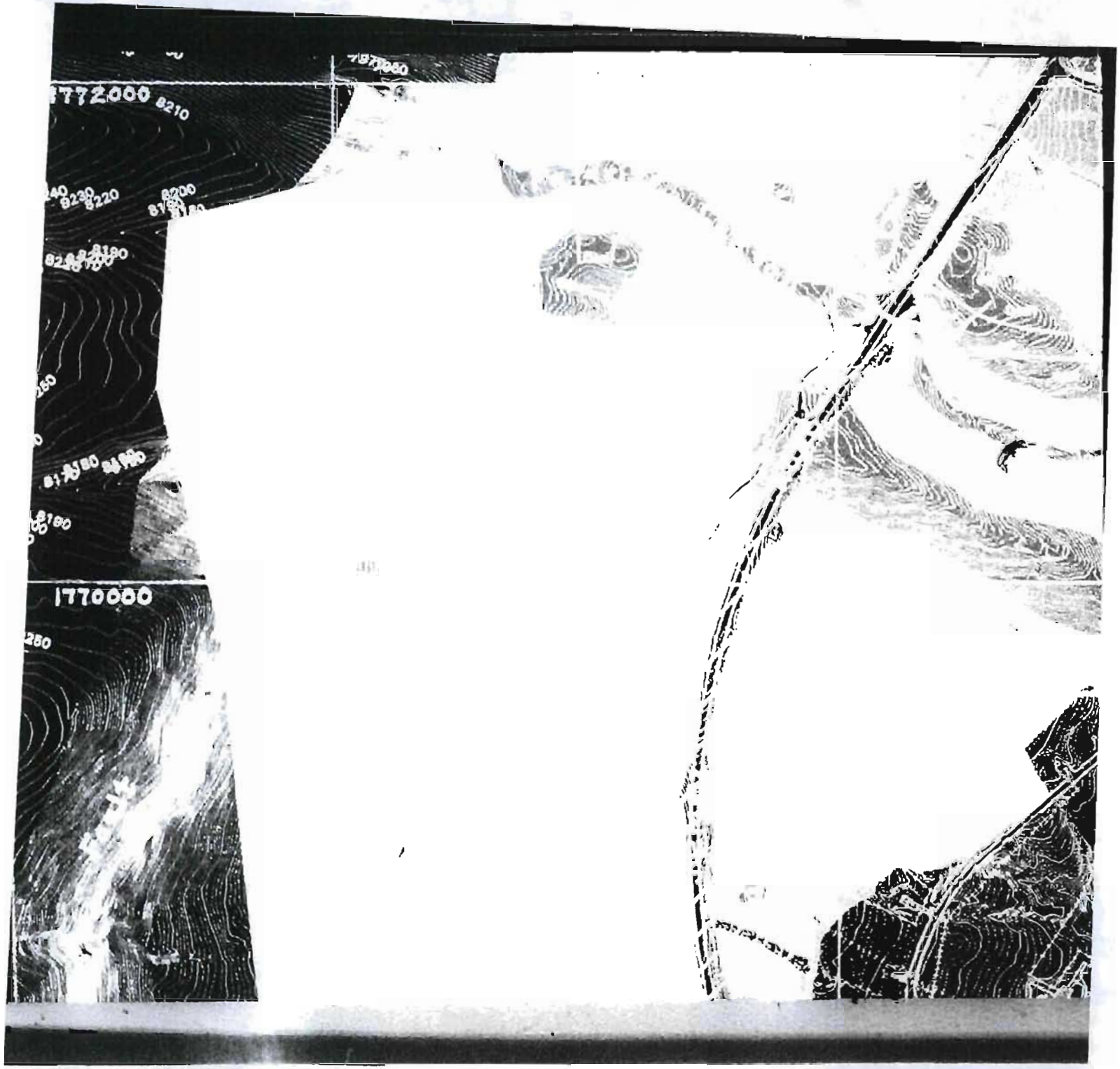
1772000
8210
8230
8220
8200
8180
1770000
8280

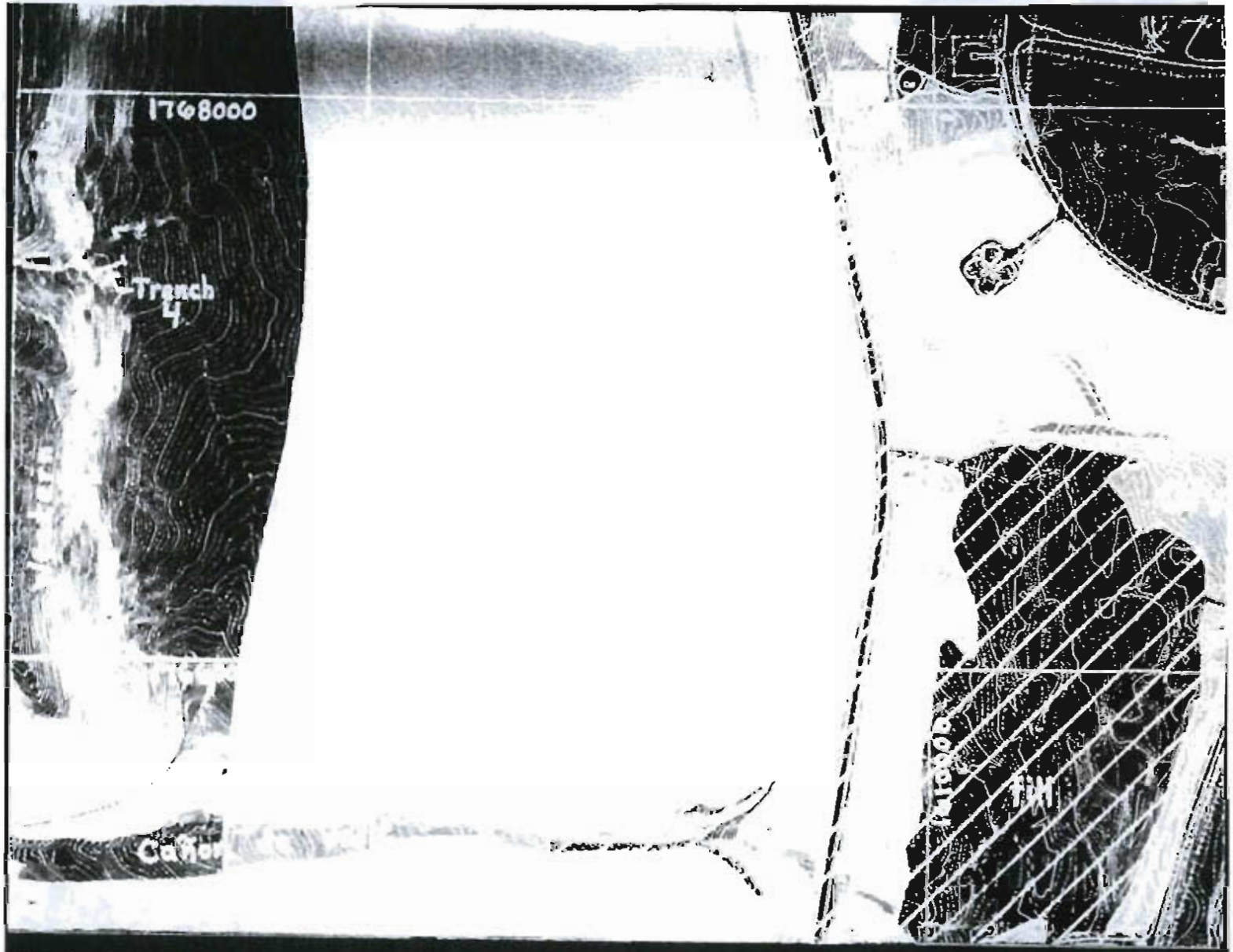

Fig. 2a. Reconnaissance geologic map of the main Pajarito fault scarp west of LANL, between Pajarito Canyon and Canon de Valle. From Reneau, 1996.

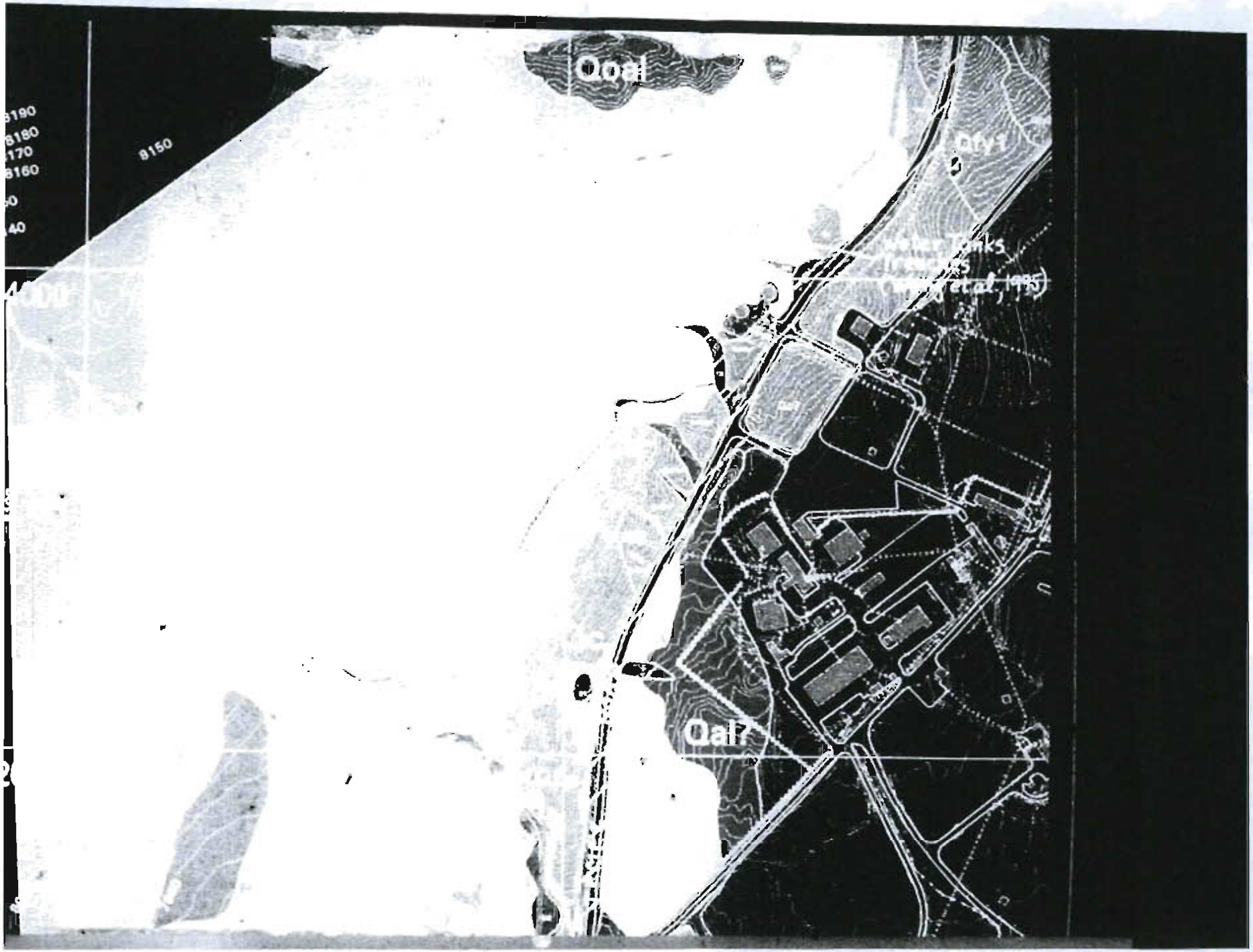
Qoal
Qfy1
Qal?
8190
8180
8170
8160
8150
40

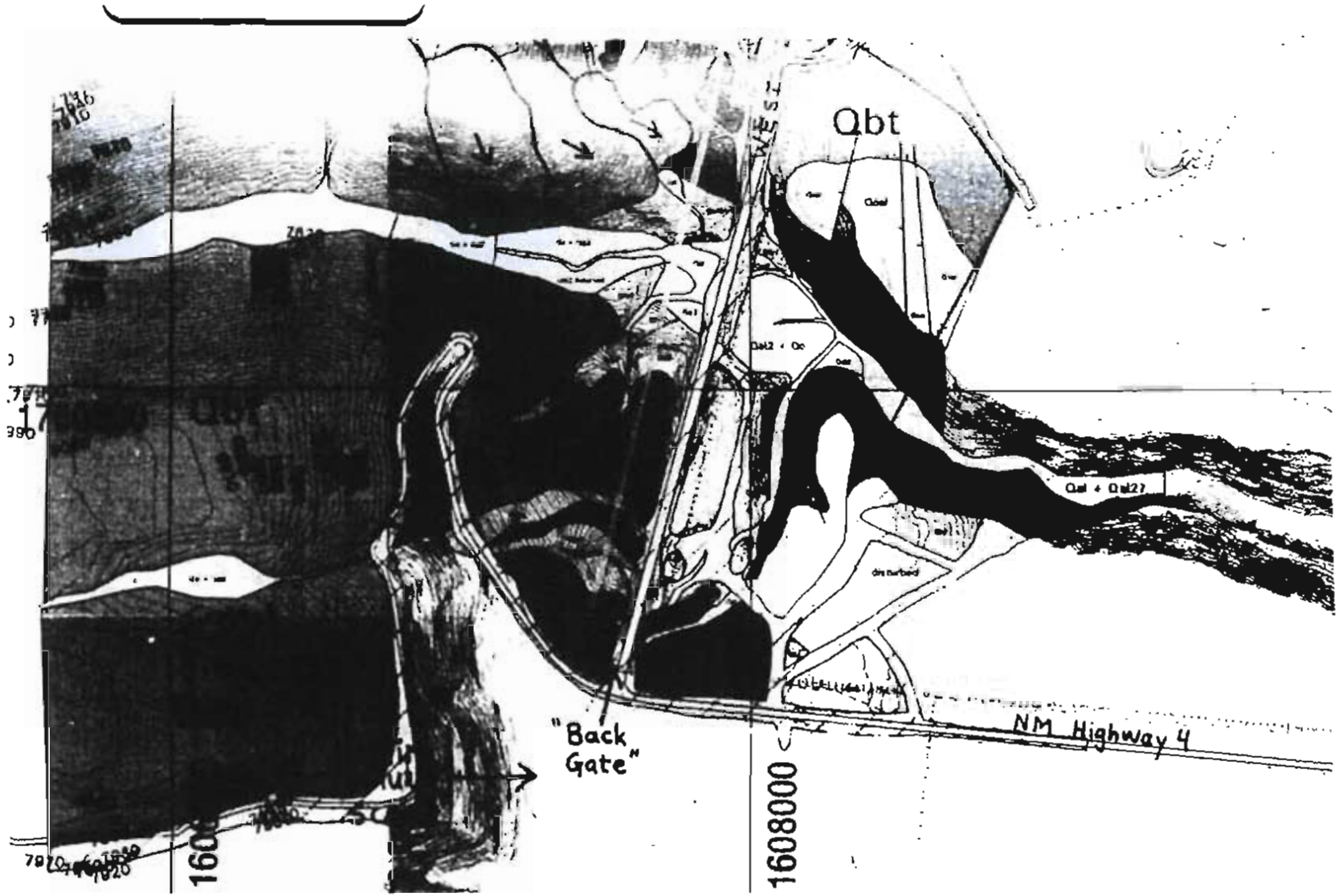

Fig. 2b. Reconnaissance geologic map of the main Pajarito fault scarp west of LANL, between the Water Tanks and NM Highway 4. From Reneau, 1996, except for landslide mapping (hachures and arrow symbols)..

20

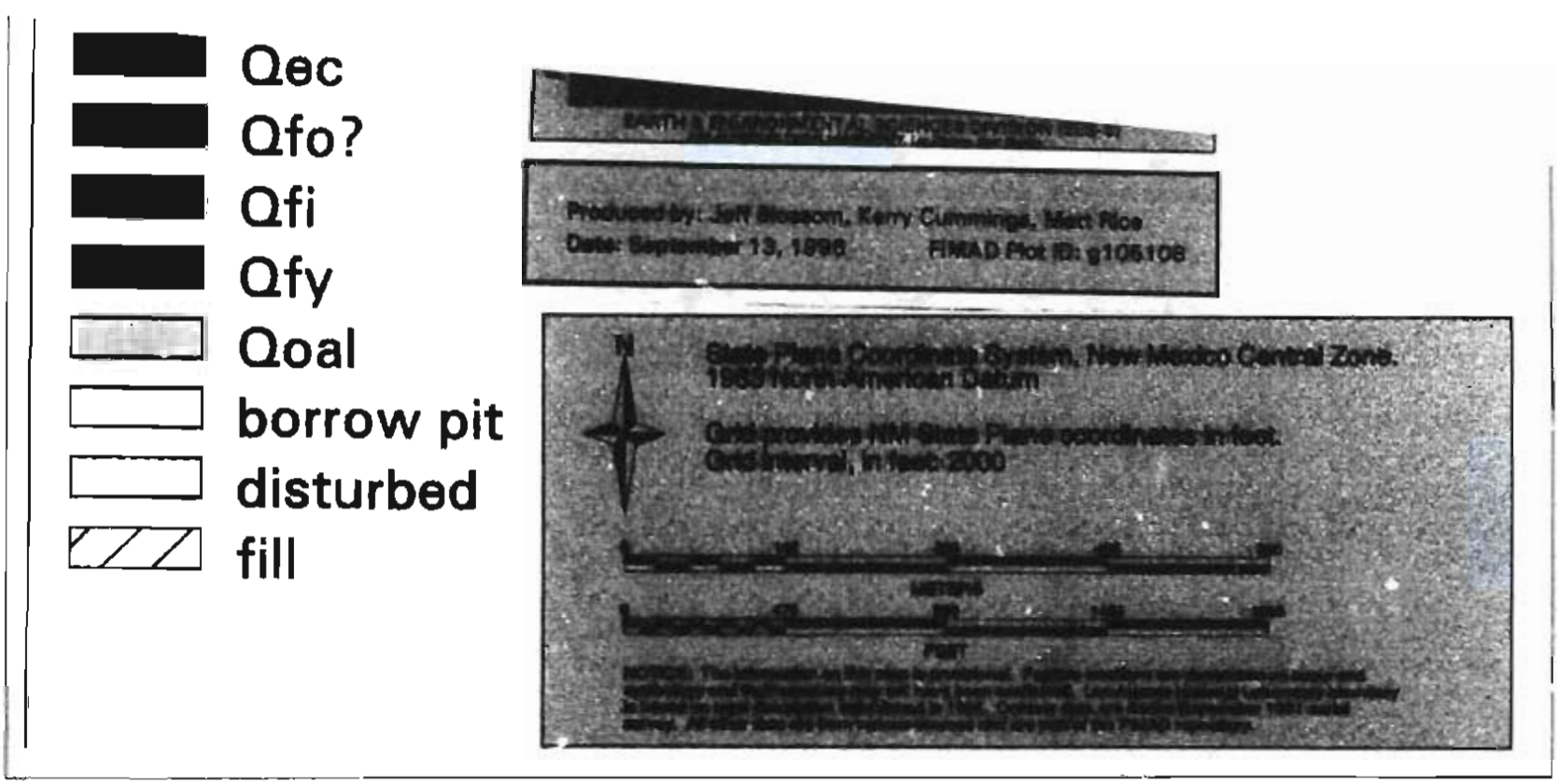

Fig. 2c. Explanation for reconnaissance geologic map of the main Pajarito fault scarp west of LANL. From Reneau, 1996. Map unit descriptions are in Appendix 3.

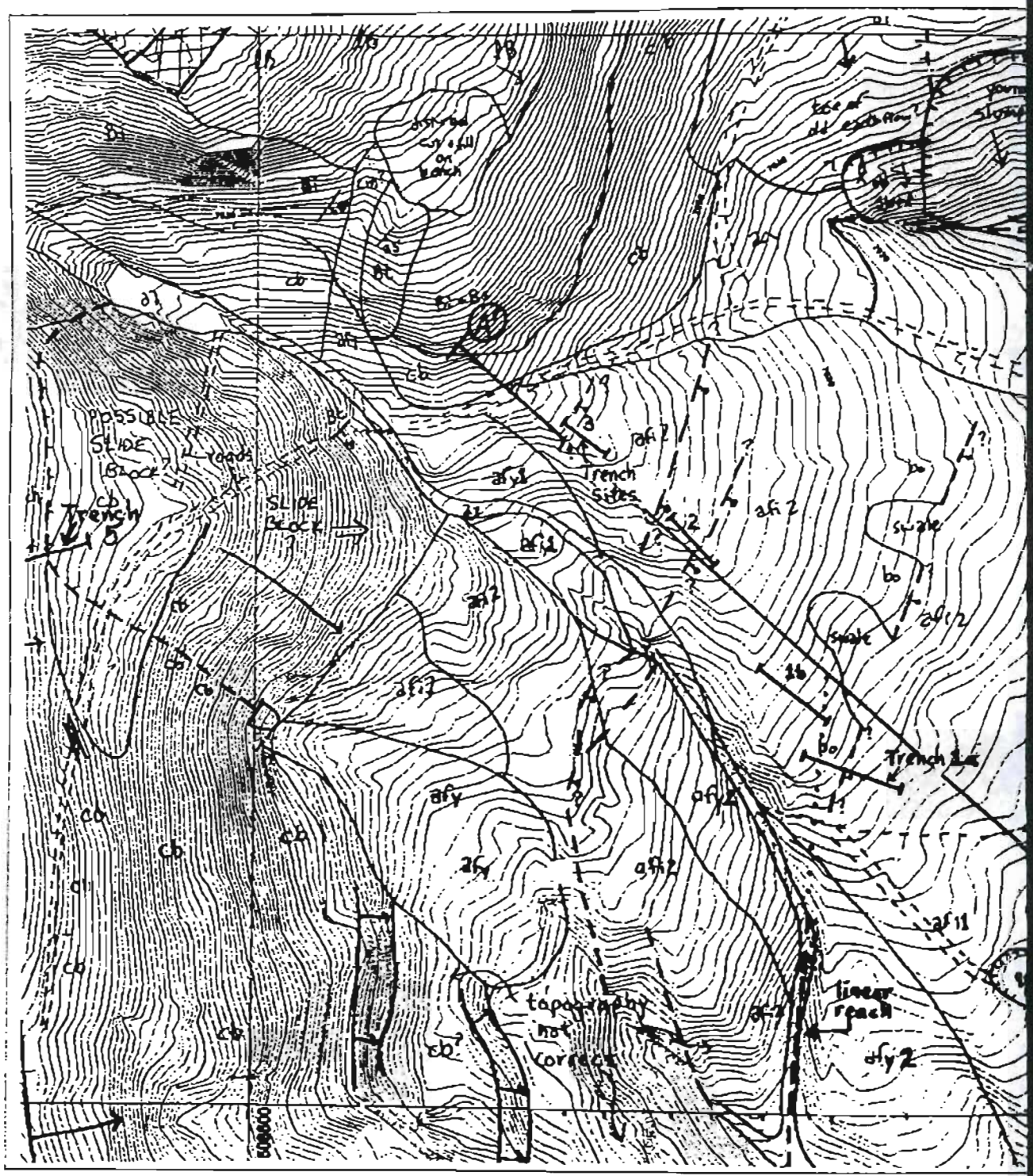

Fig. 3 . Geologic map of the intermediate-age alluvial fan and location of Trenches 1a, 1b, 2, and

EXPLANATION OF MAP UNITS

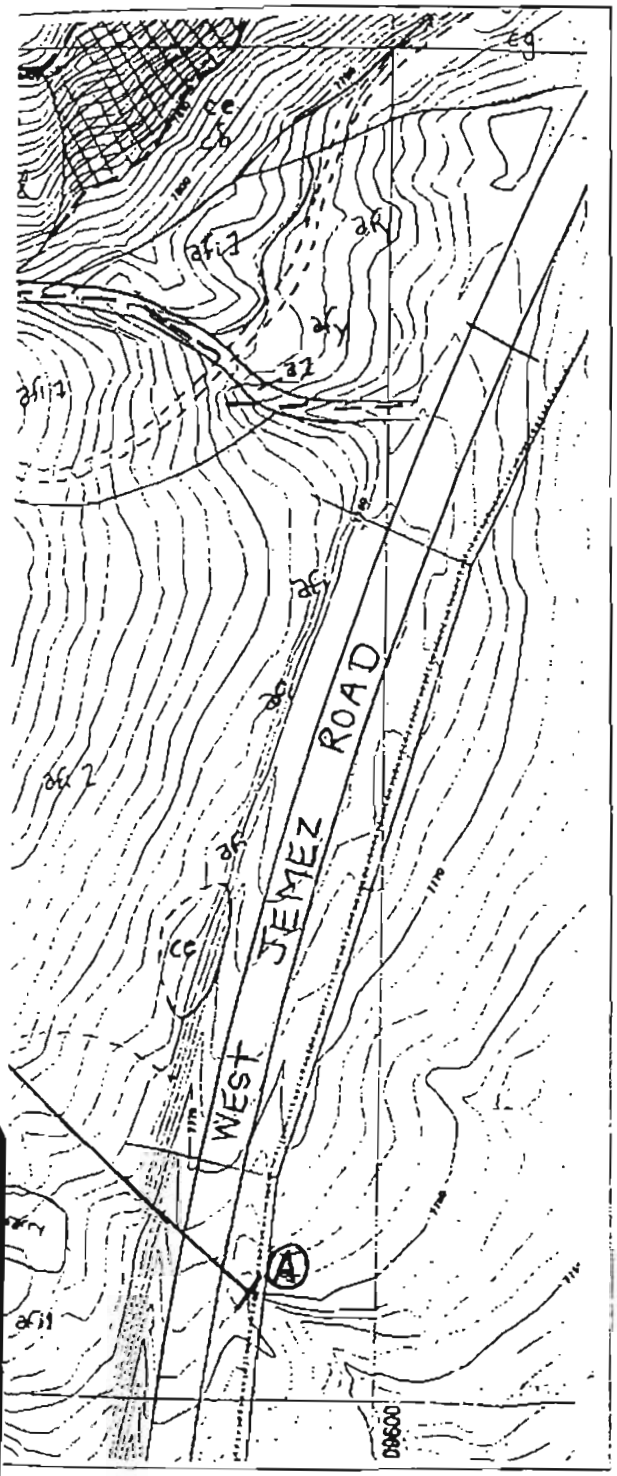

		Correlative Units of Reneau (1996)
	Holocene	
ay	modern channel alluvium	Qal
afy1	young alluvial fan	Qfy
afy2	young alluvial fan	Qfy
acy	young alluvium and colluvium	Qal2
	Holocene and Late Pleistocene	
cb	bouldery colluvium	Qc
	Late Pleistocene	
ce	colluvium composed mainly of El Cajete pumice	Qec
afi1	Intermediate-age alluvial fan	Qfi
afi2	Intermediate-age alluvial fan	Qfi
	Mid-Late Pleistocene	
lB	landslide composed of intact masses of Bandelier Tuff	Qbt
	Early Pleistocene	
Bs	Bandelier Tuff, slope-parallel slabs	Qbt
Bi	Bandelier Tuff, in-situ	Qbt

Symbols

topographic scarp

lineament with slight topographic relief

lineament with no topographic relief (dotted where obscure)

landslide head scarp (dashed where obscure)

direction of slide movement

200 ft
61 m

3. Part of Plate 6 in McCalpin, 1996. Contour interval = 2 ft.

pumice is just another example of its irregular distribution along the base of the Pajarito fault scarp. McCalpin (1997, Plate 6) mapped some pumice near the top of the west-side roadcut of West Jemez Road through the fan, and correlated it to the El Cajete pumice, but that correlation was not supported by any mineralogical or trace- element analysis. If that pumice is indeed the El Cajete, it implies that the oldest parts of the Qfi? fan are probably pre-El Cajete, but that other Qfi? lobes are post-El Cajete.

At the latitude of our alluvial fan the Pajarito fault is composed of four major east-facing scarps with numerous subsidiary shear and pull-apart zones. The scarp farthest west is informally named the Western Splay scarp, and it continues south to Canon de Valle as a distinct 25- 30 m-high east facing scarp, parallel to, but 500 m west of the crest of the main, 65-70 m-high scarp. Trench 4 (see Sect. 3.5) was excavated at the base of the Western Splay scarp. The main scarp of the Pajarito fault splits into two scarps directly south of the unnamed drainage that gave rise to our fan. The western splay of the main scarp trends N-S and is about 12 m high; Trench 5 was excavated across this splay (see Sect. 3.6). The splay continues northward across the unnamed drainage and maintains a similar height.

The eastern splay of the main scarp trends N 30° E and is 25 m high south of the unnamed drainage, but decreases in height northwards. South of Pajarito Canyon this deformation zone transforms from an east-facing scarp with a pull-apart trough at its head, to a 200 m-wide zone of NE-trending pull-apart troughs with < 5 m of net down-to-the-east displacement.

The easternmost fault scarp is poorly-expressed south of the alluvial fan, and the detailed topographic maps (2 ft contours) do not correctly portray the topography in this densely wooded region. For example, the apparent small (3-5 m-high) N-S-trending scarps are artifacts of computer interpolation of contour lines. However, the modern drainage channel of the fan contains a 60 m-long, linear incised reach that parallels the strike of the main fault scarp. Because this reach nearly parallels the contours of the fan, McCalpin (1997, Plate 6) inferred that it is structurally controlled.

North of the fan this easternmost fault scarp is well developed as a N 55° E-trending, east-facing, 15-20 m-high scarp. Farther to the north this scarp trends more northerly, and directly south of Pajarito Canyon this scarp was trenched by Woodward-Clyde Consultants in 1995 (Wong et al., 1995, their "Pajarito Canyon" trench).

The surface of the alluvial fan contains many small, irregular undulations that might be the result of either depositional or tectonic processes (Fig. 4). At four locations (Fig. 3) the surface undulations seem to define more-or-less continuous east-facing lineaments. These lineaments consist in part of mini-scarps. It was the presence of these vague topographic lineaments, and their parallelism with structures north and south of the fan, that prompted us to dig the four alluvial fan trenches.

The easternmost of the four lineaments appears to be a northward projection of the 60 m-long linear reach of the modern channel. In two places on the fan surface broad swales occur west of the lineament but are not as well developed east of it, as if the swales might be incised into an upthrown fault block. Between the swales, the fan surface west of the lineament exposes abundant boulders, whereas boulders are not observed east of the lineament. One explanation for this disparity is erosion of fines from the

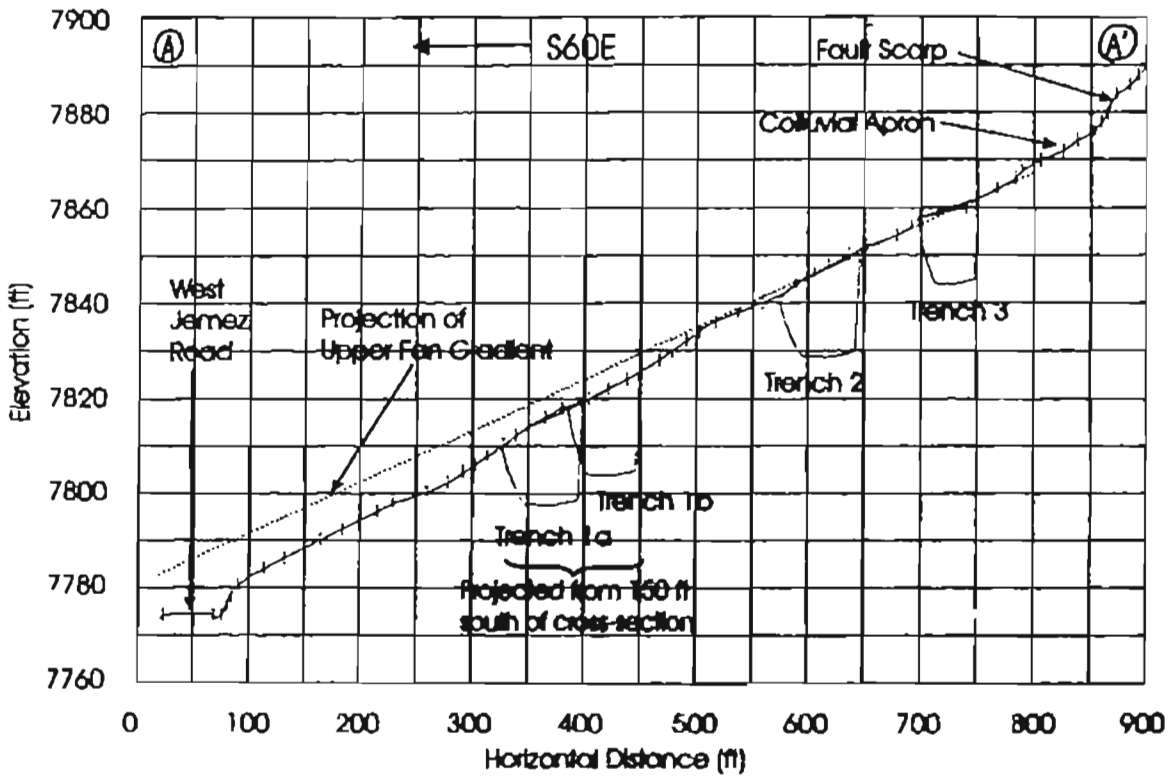

Fig. 4. Longitudinal topographic profile down the intermediate-age alluvial fan; elevation data are from 2 ft contour map of FIMAD. Trenches 2 and 3 are on line, Trenches 1a and 1b are projected from south of the line. The gradient of the upper fan is less than that of the lower fan. Vertical exaggeration= 5x.

upthrown block, which subsequently buried boulders on the downthrown block.

The other three lineaments farther west on the fan have an even more obscure geomorphic expression.

3.2 Trench 1a

3.2.1 Geomorphology:

Trenches 1a and 1b are located on the afi2 fan surface, across the northward projection of the linear, N-S-trending reach of the modern channel (Fig. 3). Due to the uncertainty of projecting the inferred structural trend, the Trench 1 originally suggested by McCalpin (1997) was replaced with two overlapping trenches. The farther downslope trench was Trench 1a (Fig. 5), which was 5 m deep and 25 m long, and intersected the structural projection near its head. Trench 1b was parallel to Trench 1a but shifted 5 m farther north, and overlapped the western 2 meters of Trench 1a, so that no north-trending structures could pass between the two trenches.

The northward projection of the linear channel reach climbs up onto the fan surface at a slight break in slope. This slope break coincides with the eastern end of a bouldery natural levee that is part of the afi2 fan. East of the slope break the fan surface is finer- grained and has a lower gradient. The slope break appears to mark the apex of a younger sub-fan (afi1 on Fig.3). This sub-fan was probably formed when stream flow jumped out of the modern channel at the 30° change in direction at the upstream end of the 60 m-long linear reach.

3.2.2 Stratigraphy:

Trench 1a exposes five parent materials, five soils, and nine soil horizons that can be mapped over the 25 m length of the trench (Fig. 6). The youngest parent material (unit 1) is a 0.5- 0.8 m-thick debris flow deposit, consisting of an abundant, pale brown, loose silt matrix surrounding angular clasts of tuff up to 25 cm in diameter. The color and friability of this deposit are similar to that of the uppermost Holocene colluvial units exposed in the seven trenches excavated across the Pajarito fault in 1997 (McCalpin, 1998).

Unconformably underlying unit 1 is a second debris flow deposit (unit 2), the matrix of which has been partly transformed to a moderately cohesive red clay by pedogenesis. Unit 2 contains angular tuff clasts up to 30 cm in diameter, and matrix comprises about 60% of deposit volume. Subjacent parent material 3 is a better-sorted, clast-supported gravel in which clasts are subrounded and imbricated upslope. The sedimentology of this unit, and the channeling of its lower contact into subjacent units, indicates this is a fluvial gravel transported by clear-water or hyperconcentrated flow. The red color and pedogenesis in Unit 3 is a continuation of that in Unit 2.

At the base of unit 3 is an erosional unconformity cut into older, denser, more cohesive deposits. The uppermost part of unit 4, which has been partly eroded, consists of a 10-15 cm-thick clast-free silt. This bed (unit 4EBb2 on Fig. 6) is probably an overbank deposit, although it could also have a loess component. More

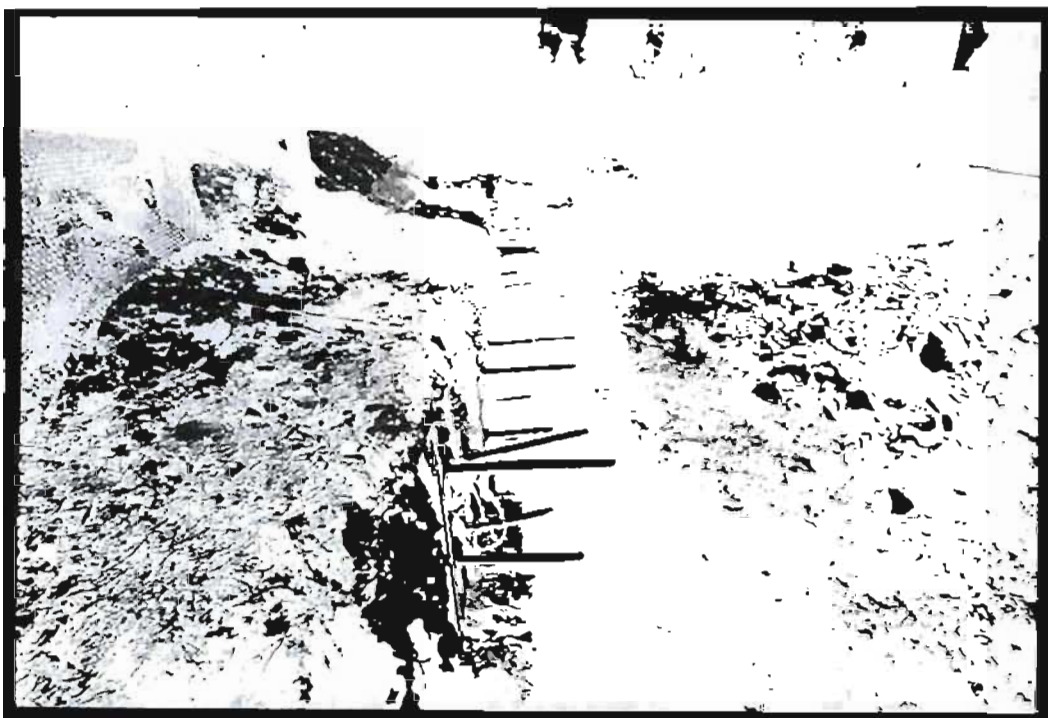

Fig. 5 Photographs of Trench 1a (a)- View east down the trench axis

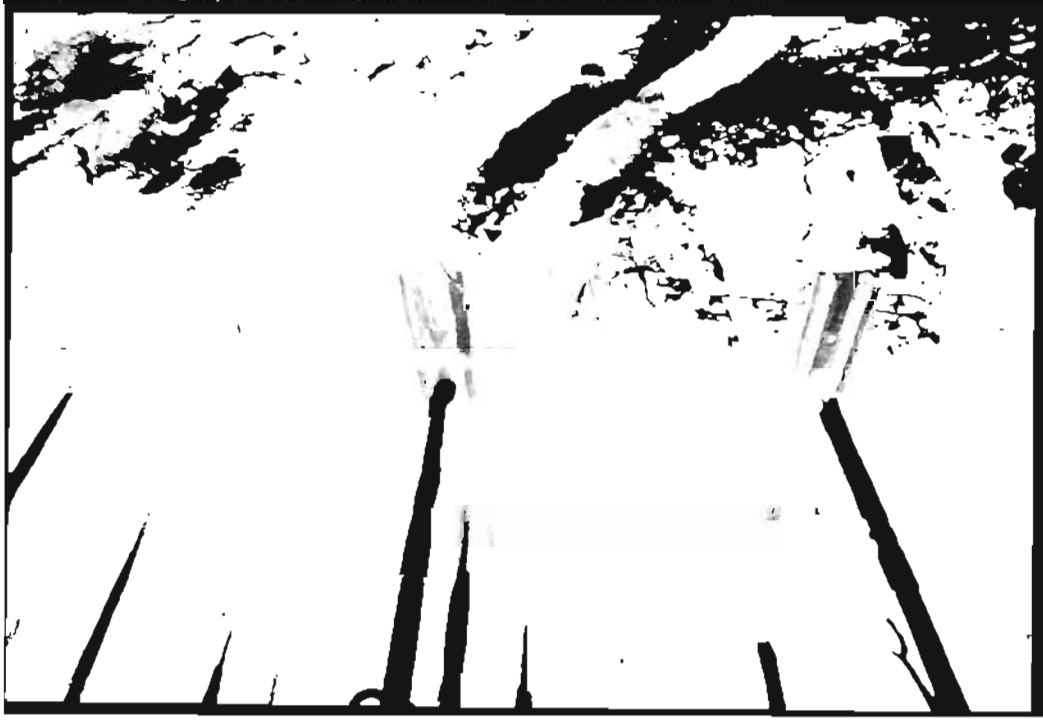

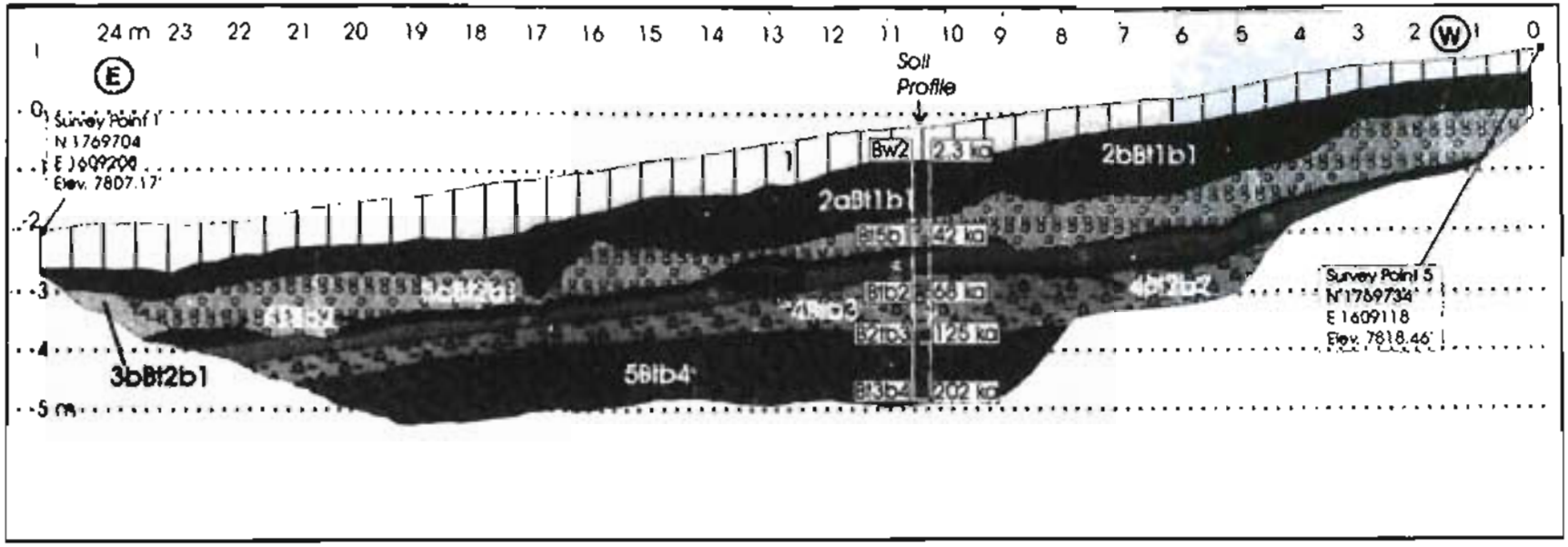

	Parent material	Soil
1	debris flow	*Surface soil (A and C horizons)*
2aBt1b1	red debris flow	*Buried soil 1; Bt Horizon developed on unit 2, debris flow*
2bBt1b1	tan debris flow	
3aBt2b1	red pebble and cobble gravel	*Buried soil 1; Bt Horizon developed on unit 3, fluvial gravel*
3bBt2b1	red debris flow	
4EBb2	clast-free silt	*Buried soil 2; EB horizon*
4Bt1b2	pink clay with cobbles	*Bt horizons developed on unit 4, debris flow*
4Bt2b2	red silty Bt with strong ped structure	

	Parent material	Soil
4Btb3	red-brown debris flow	*Buried soil 3; Bt horizon developed on unit 4, debris flow*
5Btb4	cohesive debris flow	*Buried soil 4; Bt horizon developed on unit 5, debris flow*

NOTES:

1. Trench excavated 11 June 1998.
2. Trench logged by J.R. McCalpin, L.C.A. Jones, T.E. Cooper, and J.-C. Moya, 12-16 June 1998
3. Soil profiles defined and described by E.D. McDonald and A.E. Levine. Soil horizon nomenclature modified from Soil Survey Staff (1990) and Birkeland (1984). Only selected horizons are shown for simplicity.
4. Survey points surveyed by J.N. Gardner and A. Levine, referenced to New Mexico State Plane Coordinates, Central Zone, based on NAD83 (in feet).

SCALE

0 2 4 meters

GEO-HAZ Consulting, Inc.

LOS ALAMOS NATIONAL LABORATORY

PAJARITO FAULT, 7 SCATTERED TRENCHES, SUMMER 1998

TRENCH 1a-South Wall

DATE JAN. 1999 | FIGURE 6

DWG. NO. C:\GEOHAZ\LANL\PAJARITO98\TRENCH1a.COR

importantly, the bed marks a paleo-ground surface that was exposed for some time before deposition of unit 3. The remainder of Unit 4 is debris flow beds, with an upper, cobble-rich unit (4Btb1) overlying a clast-poor, compact massive silty sand (4Bt2b2), which overlies a debris flow bed with subequal parts clasts and matrix (4Btb3). Unit 4 totals about 1-1.5 m thick. Rare, small reworked pebbles of pumice appear in subunit 4Btb2, and may be the El Cajete pumice.

The oldest parent material is unit 5, a very dense, matrix-supported debris flow deposit

3.2.3 Soils:

In addition to the weak surface soil there are four buried soils mapped in Trench 1a (Fig. 6). The surface soil is restricted to unit 1 and is composed of A and Bw horizons. A single buried soil (1) is developed in units 2 and 3, and it contains five textural B horizons (Appendix 3). Unit 4 contains buried soil 2, composed of an EB horizon developed in a clast-free silt (uppermost unit 4), and two subjacent textural B horizons developed in debris flow deposits. The lower 1/3 of unit 4 has increased Bt horizon development, indicating a third buried soil, and suggesting that the lower 1/3 of unit 4 represents an older debris flow event than the upper 2/3. Unit 5 contains a buried soil with three Bt horizons. In each of these buried soils, Bt horizon development is stronger in the upper part of the soil and weakens downward. Eric McDonald described a detailed soil profile at 10.6 m on the horizontal scale of the trench (10.6 mH) after we had logged the trench (Appendix 3).

The degree of soil development in Trench 1a can be compared to that of dated soils elsewhere on the Pajarito Plateau, as described by Reneau and McDonald (1994, Table 2-10). Using the Profile Development Index (PDI; Harden, 1982; Harden and Taylor, 1983) as a quantitative measure of soil development, the PDI value of 7.6 for the surface soil (Table 1) is similar to PDI= 7.4 for the soil on terrace Qt7 in Rendija Canyon, which is dated at 3 ka. Thus, unit 1 is late Holocene. The cumulative PDI values at the bases of buried soils 1 and 2 are 50.8 and 69.6, respectively. The latter value is very similar to the net PDI in the post- El Cajete soil exposed in soil pit WJR-5, which was dug into a Qfi fan about 2 km south of our alluvial fan. During the field review of the 1998 trenches in July, 1998, reviewer F. H. Swan collected some decomposed pumice pebbles from unit 4Bt1b2. Although it was not confirmed that this pumice was the El Cajete pumice, the cumulative PDI value at the base of buried soil 2 is essentially identical to that of a post-El Cajete soil at pit WJR-5 (Reneau and McDonald, 1994, p. 82-86, Table 2-10).

Buried soils 3 and 4 have cumulative PDI values of 102.9 and 140.8, respectively. According to the PDI chronofunction of McDonald (1999, p. 6), these PDIs suggest ages of 99-157 ka and 161-255 ka, respectively.

3.2.4 Structure:

There were no visible tectonic deformation structures in Trench 1a. Several unit contacts have sections that dip up to 45° (e.g., the unit 2a/3a contact), but at these locations subjacent contacts are subhorizontal, thus ruling out a tectonic deformation

origin. All of the contacts that dip more steeply than the ambient fan gradient (6°-7°) are interpreted as fluvial cut-and-fill contacts.

3.2.5 Geochronology:

No radiocarbon or luminescence samples were collected from Trench 1a, mainly because, in the absence of any deformation, a precise chronology of deposition was not required. Soil PDI values, plus rare pumice pebbles, suggest that unit 4Bt1b2 may be about the same age as the El Cajete pumice, i.e. 50-60 ka (Reneau et al., 1996). According to the latest PDI chronofunctions of Eric McDonald (McDonald, 1999)), the bases of buried soils 1, 2, 3, and 4 are dated at roughly 42, 68, 125, and 202 ka (Table 2).

3.3 Trench 1b

3.3.1 Geomorphology:

Trench 1b continues up fan from the western end of Trench 1a (Fig. 3), and approaches within about 5m of the edge of the steep fluvial cut slope that descends ca. 5 m down to the modern channel. All along this channel edge a subdued ridge of boulders indicates that a natural levee was deposited. The westernmost 4 m of the trench begins to ascend this levee from the afi2 surface (Fig. 7). Trench 1b is 22 m long and up to 4.5 m deep.

3.3.2 Stratigraphy:

Trench 1b contains debris flow and fluvial gravel deposits divisible into five major parent materials (Fig. 8), all of which correlate to similar-numbered parent materials in Trench 1a. However, units 2 and 3 are thicker in Trench 1b (2.5-3.8 m) than in Trench 1a (1-2 m). Because of this increased thickness, units 4 and 5 are encountered farther beneath the ground surface, and only the upper 0.4 m of unit 5 is exposed, compared to a 1.2 m thickness exposed in Trench 1a. Along with the increased thickness of units 2 and 3 there is more variability in sedimentology. Most of Unit 2 is debris flow deposits (unit 2a), but two lenses of gravels in the head of the trench appear to be fluvial gravel (units 2b, 2c). Likewise, most of unit 3 is a stratified fluvial gravel (unit 3a), but two matrix-rich lenses occur near the head of the trench (units 3b, 3c) that are probably small debris flow deposits. This sedimentologic variation probably results from the proximity of the head of the trench to the modern drainage channel of the fan, and the increased probability of encountering flood- and levee-related lenses.

The clast-free silt that capped unit 4 in Trench 1a is missing in Trench 1b, and indeed the upper two soil horizons of unit 4 are erosionally truncated in mid-trench. This truncation, along with the increased thickness of unit 3 gravels, suggests that fluvial erosion stripped off the clast-free silt prior to deposition of unit 3a. Aside from the differences just cited, the remainder of parent materials in Trench 1b (units 1, 4, and 5) are identical in sedimentology to equivalent units in Trench 1b.

Fig. 7. Photographs of Trench 1b. a. View to SE. Trench 1b in foreground. Trench 1a in background.

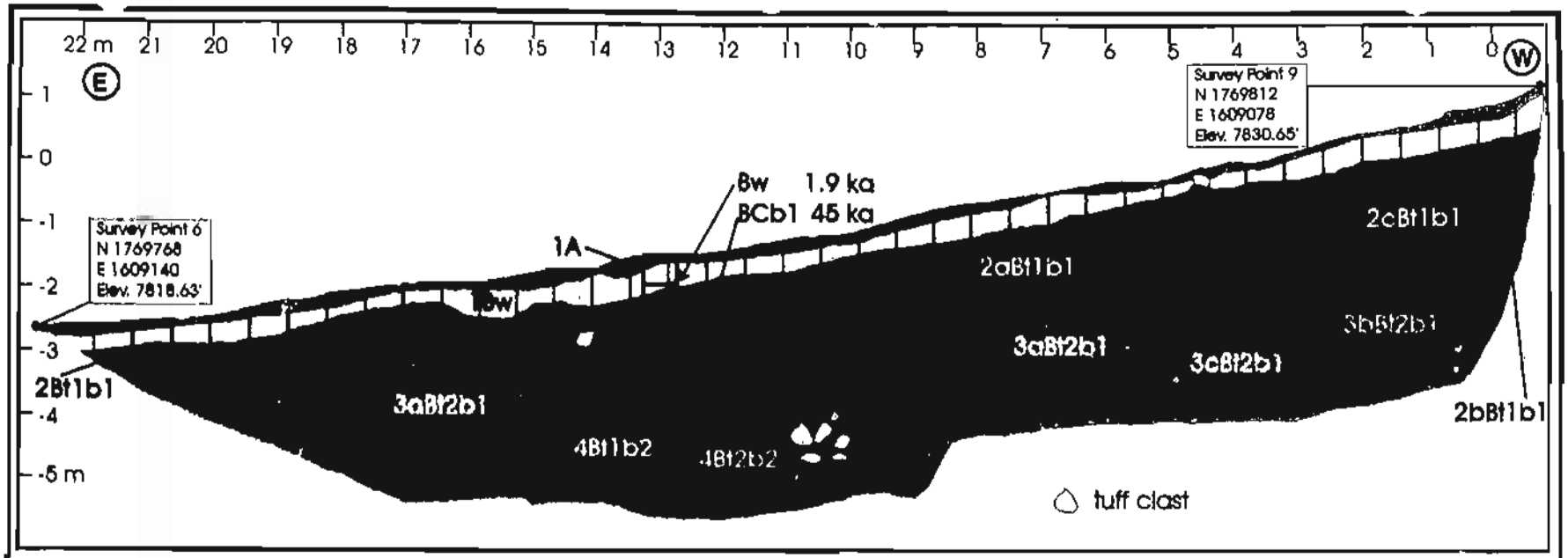

Parent material	Soil	
	Surface Soil	
1A	Holocene alluvium	A horizon
1Bw	Holocene alluvium	Bw horizon
	Buried Soil 1	
2Bt1b1	red debris flow, small clasts	Bt horizons
2aBt1b1	red debris flow, large clasts	Bt horizons
2bBt1b1	cobbles with clay matrix	Bt horizons
2cBt1b1	poorly stratified gravel	Bt horizons
3aBt2b1	red pebble and cobble gravel	Bt horizons
3bBt2b1	harder matrix than 3a, well-sorted small pebbles	Bt horizons
3cBt2b1	debris flow within red fluvial gravel	Bt horizons
3cBt2b1	silt bed	Bt horizons

Parent material	Soil	
	Buried Soil 2	
4Bt1b2	hard debris flow	Bt horizons developed on unit 4, debris flow
4Bt2b2	hard debris flow	Bt horizons developed on unit 4, debris flow

Parent material	Soil	
	Buried Soil 3	
4Btb3	hard debris flow	Bt horizon developed on unit 4, debris flow
	Buried Soil 4	
5Btb4	hard debris flow	Bt horizon developed on unit 5, debris flow

NOTES:

1. Trench excavated 11 June 1998.
2. Trench logged by J.P. McCalpin, L.C.A. Jones, T.E. Cooper, J.-C. Moya, and J.N. Gardner, 12-16 June 1998. Additions by J.N. Gardner and A. Lavine, July 16-17, 1998.
3. Soil profiles defined and described by E.V. McDonald and A.E. Lavine. Soil horizon nomenclature modified from Soil Survey Staff (1990) and Birkeland (1984). Only selected horizons are shown for simplicity.
4. Survey points surveyed by J.N. Gardner and A. Lavine, referenced to New Mexico State Plane Coordinates, Central Zone, based on NAD83 (in feet).

SCALE
0 2 4 meters

GEO-HAZ Consulting, Inc.

LOS ALAMOS NATIONAL LABORATORY

PAJARITO FAULT, 7 SCATTERED TRENCHES, SUMMER 1998

TRENCH 1b-South Wall

DATE	FIGURE 8
JAN. 1999	

DWG. NO. C:\GEOHAZ\USGS\PAJARITO\TRENCH1b.CDR

3.3.3 Soils:

The surface soil and four buried soils exposed in Trench 1b are similar in setting and development to the soils in Trench 1a. Eric McDonald described a detailed soil profile at 13mH and computed cumulative PDI values at the bases of the surface soil and buried soil 1. These PDI values, 6.8 and 52.9 respectively (Table 2), are essentially identical to PDI values from Trench 1a at the same stratigraphic level (7.6 and 50.8). Again, the PDI values suggest that units 2 and 3, and their soil (buried soil 1) post-date the El Cajete pumice, whereas the upper beds of unit 4 may be approximately coeval with the pumice.

3.3.4 Structure:

Trench 1b does not contain any tectonic deformation structures. The truncation of units 4Bt1b2 and 4Bt2b2 in mid-trench is ascribed to fluvial erosion, because underlying contacts are not deformed. Likewise, the lenticular and irregular contacts of sub units at the head of the trench, such as unit 3b, are attributed to erosional channeling in a fluvial sequence.

3.3.5 Geochronology:

No radiocarbon or luminescence samples were collected from Trench 1b. Soil PDI values, when applied to the PDI chronofunction, suggest approximate ages of 1.9 ka for unit 1 and 45 ka for the base of unit 3.

3.4 Trench 2

3.4.1 Geomorphology:

Trench 2 (Fig. 9) was excavated across a well-preserved east-facing mini-scarp (0-12 mH on the trench log; Figs. 3 and 10) that is fronted by an anomalously flat section of the fan (12- 20 mH on the log). The scarp face slopes up to 11° east (or 4° steeper than the average fan gradient), whereas the "flat" area slopes only 3°-4° east. However, this mini-scarp is best developed only within about 10 m of the edge of the incised modern channel. When traced northward across the afi2 surface the scarp disappears. Thus, prior to trenching we surmised that either: (1) the mini-scarp was an erosional or depositional feature, or (2) the scarp was tectonic, but had been eroded or buried in the center of the fan.

3.4.2 Stratigraphy:

Trench 2 exposes four major parent materials that are roughly equivalent to units 1-4 in Trenches 1a and 1b (Fig. 10). Unit 1 is a gravel, with clasts up to 30 cm, in a loose, "fluffy", very friable matrix of very pale tan-to-beige silt. The lack of stratification and the silty texture of the matrix suggest a debris flow origin, but the powdery nature of the pale silty matrix seems to contradict a water-laid origin. This unit has probably been subjected to some amount of downslope creep. Unit 1 is very similar in color and friability to the surface colluvium encountered in the 1997 trenches across larger scarps of the Pajarito fault zone.

Fig. 9. Photographs of Trench 2. (a) View southeast down trench axis.

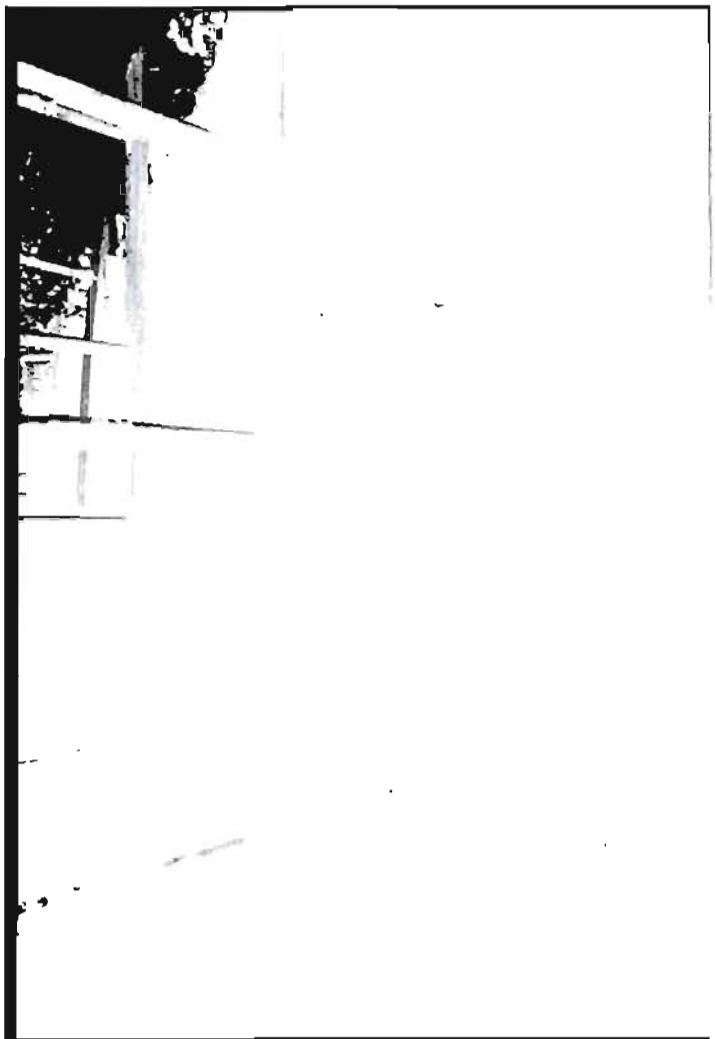

h wall from 9 mH to east end. level line at center is -3 mV. Un
pumice stringers is just above lower level line at ri

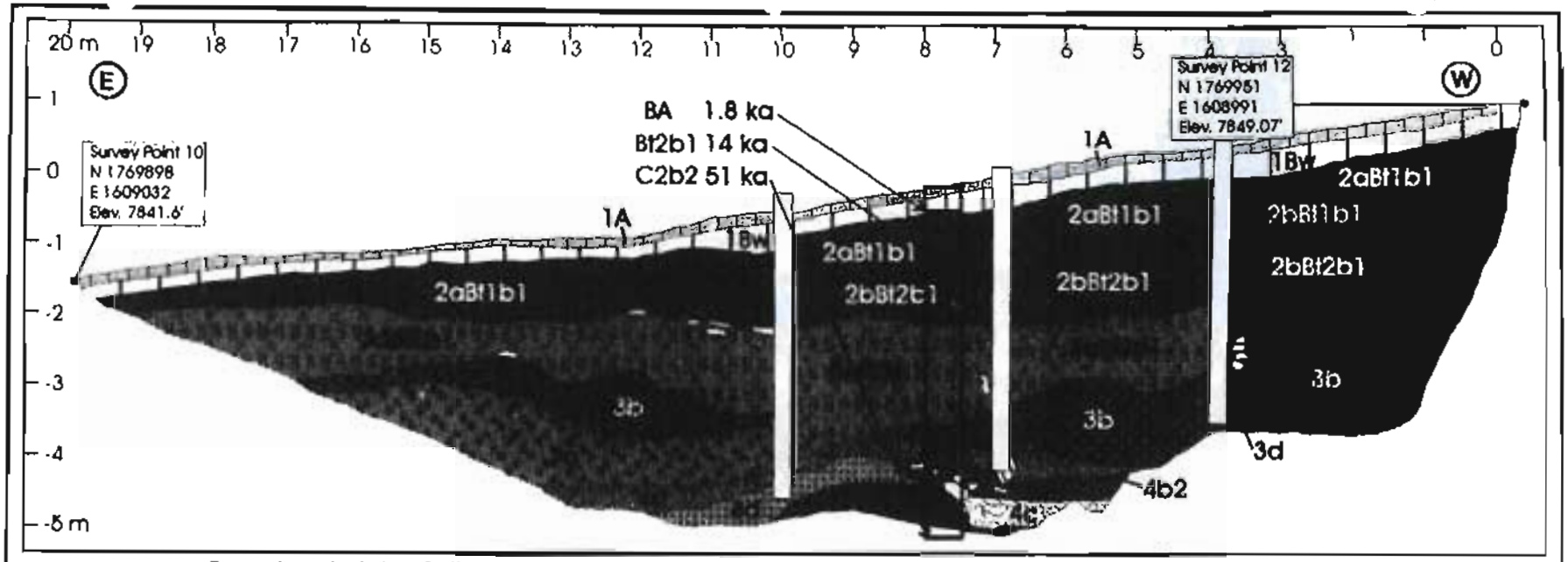

Parent material *Soil*

Surface Soil

1A	light tan silt with rare pebbles	A horizons
1Bw	light tan silt with rare pebbles	Bw horizon

Buried Soil 1

	Mainly debris flow	
2aBt1b1	sandy debris flow, small cobbles	Bt 1 horizons
2bBt1b1	fluvial gravel, matrix-poor	Bt 1 horizons
2bBt2b1	sandy debris flow, large cobbles	Bt 1 horizons
	Mainly fluvial gravel	
3aBt2b1	well sorted small pebble gravel	Bt 2 horizon
3b	subrounded fluvial cobble gravel	
3c	debris flow	

Buried Soil 2? (horizons partly eroded)

4a	sandy silt with pumice pebbles
4b1	chocolate brown hard silt with cobbles
4b2	lens of sand and pumice
4c	sandy channel gravel
4d	chocolate brown silt (mud flow)
4e	light brown massive silty sand

SCALE

0 2 4 meters

NOTES:

1. Trench excavated 11 June 1998.
2. Trench logged by J.N. Gardner, J.P. McCalpin, L.C.A. Jones, T.E. Cooper, and J.-C. Moya, 12-16 June 1998. Additions by J.N. Gardner and A. Levine, July 16-17, 1998.
3. Soil profiles defined and described by E.V. McDonald and A.E. Levine. Soil horizon nomenclature modified from Soil Survey Staff (1990) and Birkeland (1984). Only selected horizons are shown for simplicity.
4. Survey points surveyed by J.N. Gardner and A. Levine, referenced to New Mexico State Plane Coordinates, Central Zone, based on NAD83 (in feet).

GEO-HAZ Consulting, Inc.

LOS ALAMOS NATIONAL LABORATORY

PAJARITO FAULT, 7 SCATTERED TRENCHES, SUMMER 1998

TRENCH 2-South Wall

DATE Dec. 1998	FIGURE 10
DWG. NO. C:\GEOHAZ\USGS\PAJARITO\TRENCH2.CDR	

Unit 2 is composed of debris flow deposits with a sandy matrix stained red by B horizon pedogenesis. The upper part of unit 2 (unit 2a) is a pebbly debris flow that maintains an essentially constant thickness of 0.9 m beneath the ground surface, and is draped across a lens-shaped debris flow (unit 2bBt2b1) composed of large cobbles. Between these two subunits is a small fluvial gravel lens (2bBt1b1). The coincidence of the surface mini-scarp with the subsurface extent of the cobbly debris flow (subunit 2b) suggest that the scarp was created by depositional, rather than tectonic processes. For example, the contact of units 2 and 3 is essentially horizontal and unfaulted, so the present form of the mini-scarp cannot be attributed to either faulting or pre-unit 2 depositional processes. It appears that unit 2bBt2bi was deposited as a thick, viscous lobe of coarse debris atop the flat surface of unit 3 (fluvial gravels), and then later the debris flow of unit 2a buried this area, preserving the easterly slope of the top of unit 2bBt2b1.

Unit 3 is a fluvial gravel similar to those in Trenches 1a and 1b, but slightly thicker (1.8-2.4 m thick here). One of the three subunits (unit 3c) is a matrix-supported debris flow ca. 1 m thick, which toward the eastern end of the trench comprises about half the stratigraphic thickness of "fluvial" unit 3.

Unit 4 in this trench is more varied sedimentologically than in Trenches 1a and 1b, and contains a fluvial channel (units 4b2, 4c) and well-sorted fluvial sand deposits (units 4a, 4e), as well as matrix-supported clast-poor debris flows (units 4a, 4b1). However, unit 4 here is similar to unit 4 in Trenches 1a and 1b in that it represents an abrupt decrease in grain size, and increase in density and cohesiveness, compared to the overlying unit 3 fluvial gravels. The uppermost bed in unit 4 is a relatively well sorted sandy silt containing pockets and stringers of pumice pebbles. The near-constant thickness of this unit (0.25-0.35 m), its good sorting, and the presence of pumice pebbles much larger than the silt matrix suggests that this unit was deposited in quiet-water suspension conditions in a broad abandoned channel or slough. The larger pumice pebbles were probably partly buoyant and thus had a Stoke's settling velocity nearer to fine sand or silt than to normal pebbles. Abundant biotite phenocrysts indicate that the pumice is El Cajete.

Units 4b1, 4b2, and 4c are confined to a channel that is cut into 4d and 4e. In total, only two of the subunits of unit 4 here (4b1, 4d) are debris flows similar to those which make up the bulk of unit 4 in Trenches 1a and 1b. Thus, it is unclear if the unit 4 beds in Trench 2 are correlative with unit 4 debris flows in Trenches 1a and 1b, or whether the Trench 2 pumice and fluvial sand beds are younger units whose correlatives were removed by fluvial erosion along the unit 3/unit 4 contact at Trenches 1a and 1b.

3.4.3 Soils:

Trench 2 contains a surface soil (A, BA horizons) developed on unit 1, a buried soil 1 developed on units 2 and 3, and a possible buried soil 2 developed in unit 4. Because we did not observe significant signs of pedogenesis in the beds of unit 4, we did not include a buried soil 2 in our trench map units, but instead defined the map units strictly on lithology. In contrast, McDonald defined a buried soil 2 in our parent material unit 4. Aside from this difference, the horizonation of the surface soil and buried soil 1 is similar to that in Trenches 1a and 1b (Appendix 3). The PDI values of the surface soil (6.5) and the base of buried soil 2 (57.6) are similar to values from Trenches 1a and 1b (Table 2).

3.4.4 Structure:

All of the nonplanar contacts in Trench 2, with one exception, can be easily explained as erosional and depositional features in a dynamic fluvial environment. The one exception is the steep (>45°) contact between units 4d/4e and units 4b1/4c at the bottom center of the trench. The original trench floor was at the level of the 4b1/4c contact, and it was unclear if this >45° contact was a fault, or more likely, an erosional channel margin. Accordingly, we hand-dug the trench floor down an additional 0.7 m at this location. With the deeper exposure we could trace unit 4e beneath the eastern channel wall without offset or shearing. Therefore, we also interpret this steep contact as the margin of an erosional channel.

3.4.5 Geochronology:

The presence of reworked pods of biotite-bearing pumice, almost certainly El Cajete pumice, in unit 4a gives us the best chronological control in the four trenches on the alluvial fan. Although this reworked pumice clearly postdates the El Cajete eruptions by the some time span, the PDI-based age estimates for buried soils 1 and 2 in Trenches 1a- 2 (42-45 ka and 51-68 ka, respectively), which bracket the reworked pumice, also bracket the currently accepted age span of 50-60 ka for the El Cajete pumice. Thus, we infer that the pumice was eroded soon after deposition and redeposited on the alluvial fan within a few ka of the El Cajete eruption.

3.5 Trench 3

3.5.1 Geomorphology:

Trench 3 is located only 5-10 m from the apex of the alluvial fan (Figs. 3 and 11), and is 15 m long and up to 5 m deep. The alluvial fan surface in the eastern 2/3 of the trench (east of 5 mH) slopes east a ca. 5°, or somewhat less than the fan gradient at Trenches 1a, 1b, and 2. The ground surface west of 5 mH slopes at 9° east, and is evidently the toe of a colluvial apron shed from the 25 m-high fault scarp directly west of the trench.

3.5.2 Stratigraphy:

Trench 3 contains three major parent materials that broadly correlate with units 1, 2, and 3 in the other trenches (Fig. 12). Unit 1 is a cobble gravel with a pale beige, friable, silty matrix. West of 5 mH it contains thin, slabby clasts of tuff that are considerably larger and more angular than the other clasts. We infer that these slabs were deposited in Unit 1 by colluvial creep processes from the fault scarp directly west of the trench. In contrast, Unit 1 east of 5 mH is matrix-supported and resembles a debris flow deposit.

Unit 2 is a matrix-supported, pebbly and cobbly debris flow with a matrix stained red-to-orange by pedogenesis. Its sedimentology and thickness (0.7-1.6 m) are similar to that of Unit 2 in the other alluvial fan trenches.

Unit 3 comprises the remainder of the trench walls and is sufficiently thick (2.4-3.3 m) that unit 4 is not exposed in this 5 m-deep trench. Unit 3 in Trench 3 is not only 0.5-1 m thicker than unit 3 in the other trenches, it contains a higher proportion (>50%) of matrix-supported subunits than in other trenches. The uppermost subunit (3a) resembles

Fig. 11. Photographs of trench 8 (a) View northwest along trench axis, note fault scarp in distance

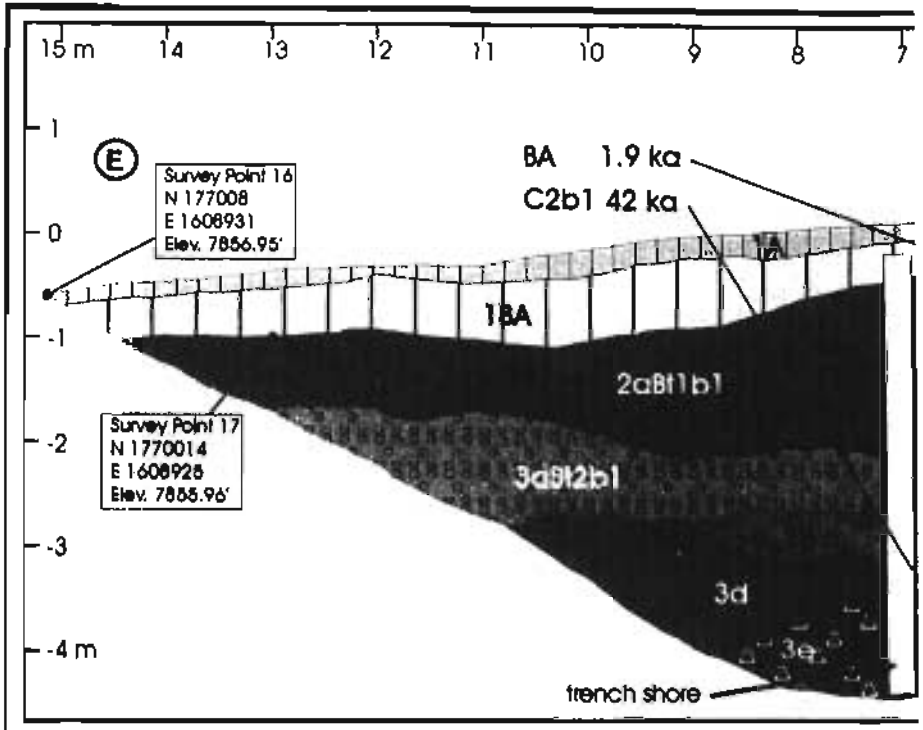

Parent material *Soil*

Surface Soil

1A	light tan silt with rare pebbles	A horizon
1BA	light tan silt with rare pebbles	BA horizon

Buried Soil 1

	Mainly debris flow	
2aBt1b1	sandy debris flow, small cobbles	Bt 1 horizons
2bBt1b1	fluvial gravel, matrix-poor	Bt 1 horizons
	Mainly fluvial gravel	
3aBt2b1	well sorted small pebble gravel	Bt 2 horizon
3b	gravel-rich debris flow, matrix support, large cobbles	
3c	lens of clast-supported gravel	
3d		
3e		

N

1. Trench excavated 11 Jur
2. Trench logged by J.N. G Jones, T.E. Cooper, and
3. Soil profiles defined and and A.E. Lavine. Soil hor from Soil Survey Staff (1 Only selected horizons a
4. Survey points surveyed Lavine, referenced to Ne Coordinates, Central Zo

the fluvial gravels of unit 3a in other trenches, but the lower matrix-supported subunits (3b, 3d, 3e) are apparently debris flows.

All three parent materials contain anomalous large, tabular slabs of Bandelier Tuff in the western 1/3 of the trench (only the largest of these rocks are portrayed on Fig.). These slabs probably indicate the downslope limit of colluviation coming from the fault scarp directly west of the trench.

3.5.3 Soils:

Trench 3 contains only two soils, the surface soil developed in unit 1, and buried soil 1 developed in units 2 and 3. The degree of soil development in these two soils, as represented by cumulative PDI, is virtually identical to that of similarly-numbered soils in the other trenches. The surface soil has a PDI of 6.7 (compared to PDI=7.6, 6.8, and 6.5 for the surface soil in Trenches 1a, 1b, and 2) and the base of buried soil 1 has a cumulative PDI of 50.9 (compared to PDI=50.8 and 52.9, for buried soil 1 in Trenches 1a and 1b).

3.5.4 Structure:

No faults or folds are exposed in Trench 3.

3.5.5 Geochronology:

The pumice-bearing beds of Unit 4 are not exposed in Trench 3, so age estimates rely only on soil PDI values. According to the PDI chronofunction of McDonald, the base of unit 1 is ca. 1.9 ka, and unit 3e is ca. 42 ka. This latter age is somewhat younger than that of the El Cajete pumice, and is consistent with our interpretation that pumice-bearing unit 4 is beneath the floor of Trench 3.

3.6 Overall Interpretation of the Alluvial Fan Trenches

The longitudinal topographic profile of the alluvial fan (Fig. 4) and the composite plot of all four trench logs (Fig. 13) show some geomorphic relations on the alluvial fan that have an indirect bearing on Quaternary faulting. First, the fan gradient apparently decreases toward the fan head (Fig. 4). This trend is opposite to that usually found on alluvial fans, and may indicate that the fan has been backtilted toward the Pajarito fault, along structures that presumably underlie the large fault scarp west of the fan. Second, older Pleistocene units (unit 4 and 5) are found closer to the ground surface farther downfan. This indicates that later Pleistocene units (units 2 and 3) are thinning downfan. Such thinning indicates that units 4 and 5 slope east even less steeply than does the ground surface, suggesting they may be more backtilted than younger units. Third, within units 2 and 3 debris flow facies become more abundant toward the head of the fan. For example, Unit 3 was initially defined as 100% well-sorted fluvial gravel in Trench 1a, and even in Trench 1b unit 3 contains only one small lens of matrix-supported gravel (unit 3c). In Trench 3, however, more than half the stratigraphic thickness of unit 3 is matrix-supported. This trend suggests that many debris flows that deposited material at the fan head did not extend farther down the fan to the sites of Trenches 1a and 1b.

(E)

Schematic Longitudinal Se

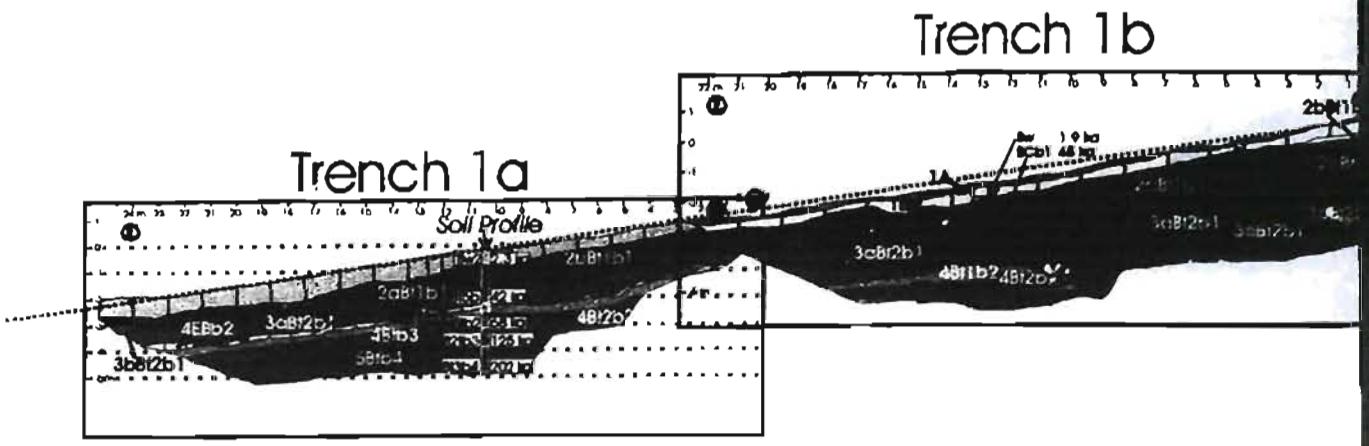

NOTES

1. Fan gradient decreases toward the fan head, whereas the reverse alluvial fans. This anomaly suggests that the fan has been tilted to the the large scarps of the Pajarito fault. NO FAULTS APPEAR IN THE TRENCH

2. Older Pleistocene units are found closer to the surface farther dowr indicating that later Pleistocene and Holocene units are thinning dowr

3.The downfan-thinning of younger units suggests that the underlying c even more back-tilted to the west than is the ground surface.

4. Within unit 3 (fluvial gravel, pink on logs) debris flow facies become abundant toward the fan head.

5. Lenses of reworked El Cajete pumice appear at the top of unit 4 ir where the upper part of unit 4 (horizons of buried soil 2) has been rem erosion. PDI-based age estimates for the top of unit 4 range from 42 l ka (T1b). Unit 4e in T2 (below the reworked pumice) is estimated to be AGES BRACKET THE EL CAJETE PUMICE, and are comparable to C-14 c from other locations.

ection of the Alluvial Fan

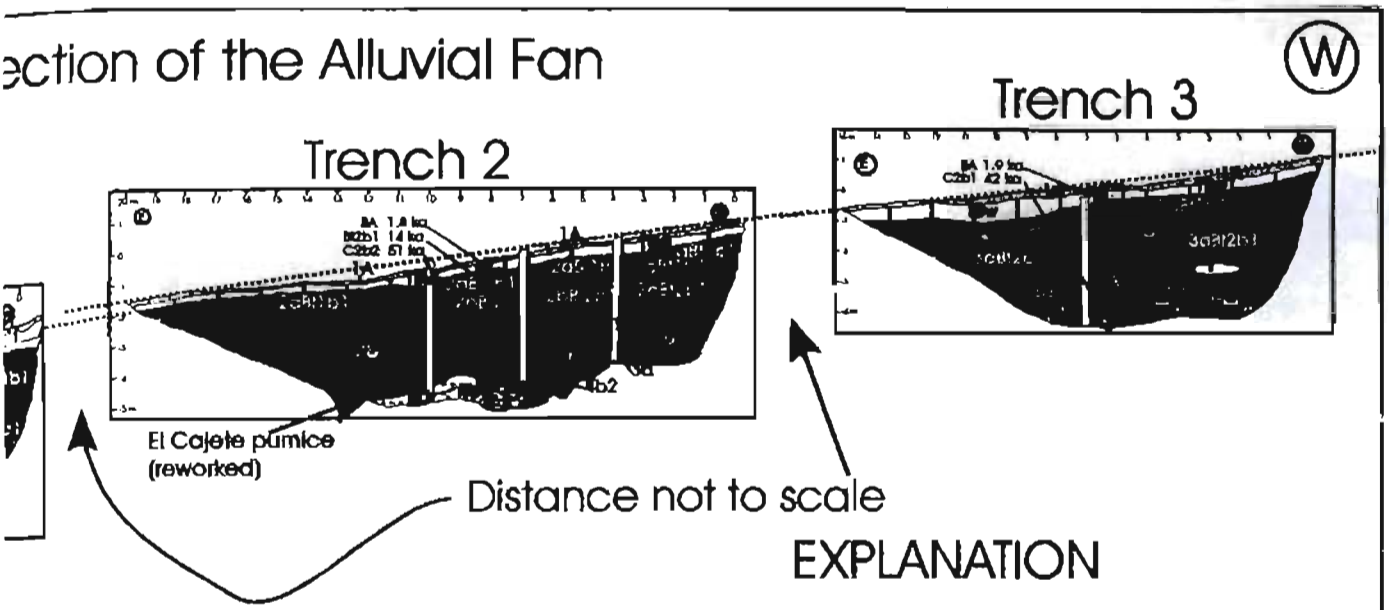

EXPLANATION

General colors

Holocene

Unit 1, tan silty colluvium — *Surface soil*

Late Pleistocene

Unit 2, loose debris flow — *Buried soil 1*

Unit 3, loose fluvial gravel — *Buried soil 1*

unconformity

Unit 4, hard debris flow — *Buried soil 2*

Unit 5, hard debris flow — *Buried soil 3*

ls true of most
west, toward
ES.

ıfan,
ıfan.

ıder units are

more

ı Trench 2,
ıoved by
ka (T1a) to 45
51 ka. THESE
ınd TL dates

GEO-HAZ Consulting, Inc.

LOS ALAMOS NATIONAL LABORATORY

PAJARITO FAULT, 7 SCATTERED TRENCHES, SUMMER 1998

TRENCHES 1a-3, South walls

DATE JAN. 1999	FIGURE 13
DWG. NO. C:\GEOHAZ\USGS\PAJARITO\FANSECT.CDR	

3.7 Trench 4

Trench 4 is located at the base of the Western Splay Scarp, roughly 650 m north of Canyon de Valle (Figs. 14, 15). The trench is 44 m long and up to 5 m deep (Fig. 16).

3.7.1 Geomorphology:

Trench 4 is located on a small alluvial fan built out from an unnamed creek that cuts through the Western Splay scarp (Figs. 2 and 14). This fan is approximately 250 m long in the downslope (east-west) direction, 275 m wide in the across-slope (north-south) direction, and descends from 8120 ft to 8050 ft elevation at an average gradient of 5°. The modern channel is incised 2.5-3.5 m into the fan head, with the depth of incision decreasing to 0.5 m at the fan toe.

McCalpin (1997, Plate 12) mapped fan surfaces of three ages here. The bulk of the fan is composed of a symmetrical cone sloping 6-7 degrees east, and was mapped as an intermediate-age fan (afi). This age designation was meant to indicate that the fan was probably not Holocene (in view of the amount of fan head incision), but not necessarily that the fan was pre El-Cajete in age. McCalpin (1997) did not dig any soil pits on this fan, nor did E. McDonald, and the fan is beyond the mapping limit of Reneau (1996), so no definite data existed on the fan age. The area adjacent to the incised modern channel is mapped as ay, and is certainly Holocene. On the eastern margin of the fan a lower-gradient extension of the fan is inferred to be older than afi, due to the greater local relief on the surface, and this area was mapped as afo? (old alluvial fan). This age designation is relative, but is presumed to be considerably older than the El Cajete pumice.

The geomorphic anomaly that initially attracted our interest, and led to Trench 4 being excavated here, is a small scarp and bench at the fan head. The scarp strikes N 20°-30° W or 20°-30° more westerly than the N-S-trending Western Splay scarp, and is about 4 m high. At the base of the small scarp is an 18 m-wide bench that slopes 3°-4° east, or 2°-3° less than the gradient of the afi fan farther east. Both the scarp and bench are covered with a dense grove of Gambel's oak, which is anomalous in the Pajarito fault zone, and typically indicates either local spring seepage or soils with an increased water-holding capacity. No boulders appear on the surface on the bench, although they appear suddenly on the eastern margin of the bench beneath a sharp, north-trending line of large conifer trees (mainly Douglas fir). This line of trees marks a linear break in the slope of the fan and in surface materials and vegetation type.

In the vicinity of the fan, the Western Splay scarp splits into a double scarp, with the higher (15-21 m-high) scarp on the west, and a smaller (6-9 m-high) scarp on the east. These two scarps are separated by a colluvium-covered bench that widens to 40 m wide north of the unnamed creek. The smaller eastern scarp projects beneath the fan head, and its projection coincides with the anomalous fanhead scarp and bench. Thus McCalpin (1997) inferred that the scarp on the fan may represent post-afi faulting, and the bench might be a graben that had been backfilled with alluvium and later slopewash. He suggested trenching this fan head because it is one of the few localities where landforms of suspected tectonic origin occur on an intermediate-age fan.

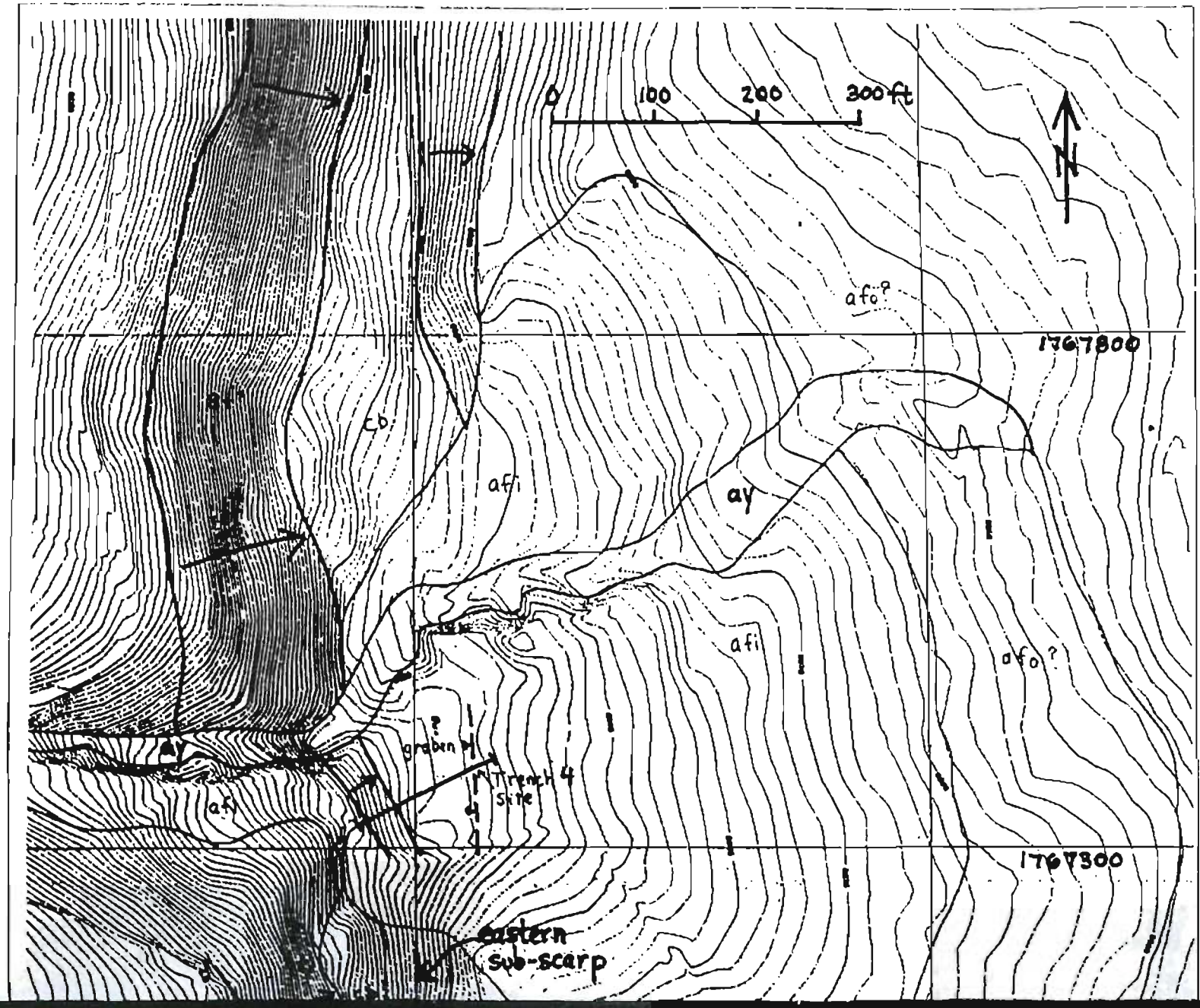
0
100
200
300 ft
N
afo?
1767800
afi
cb
afi
ay
afi
afo?
graben
Trench 4 Site
afi
1767300
eastern Sub-scarp

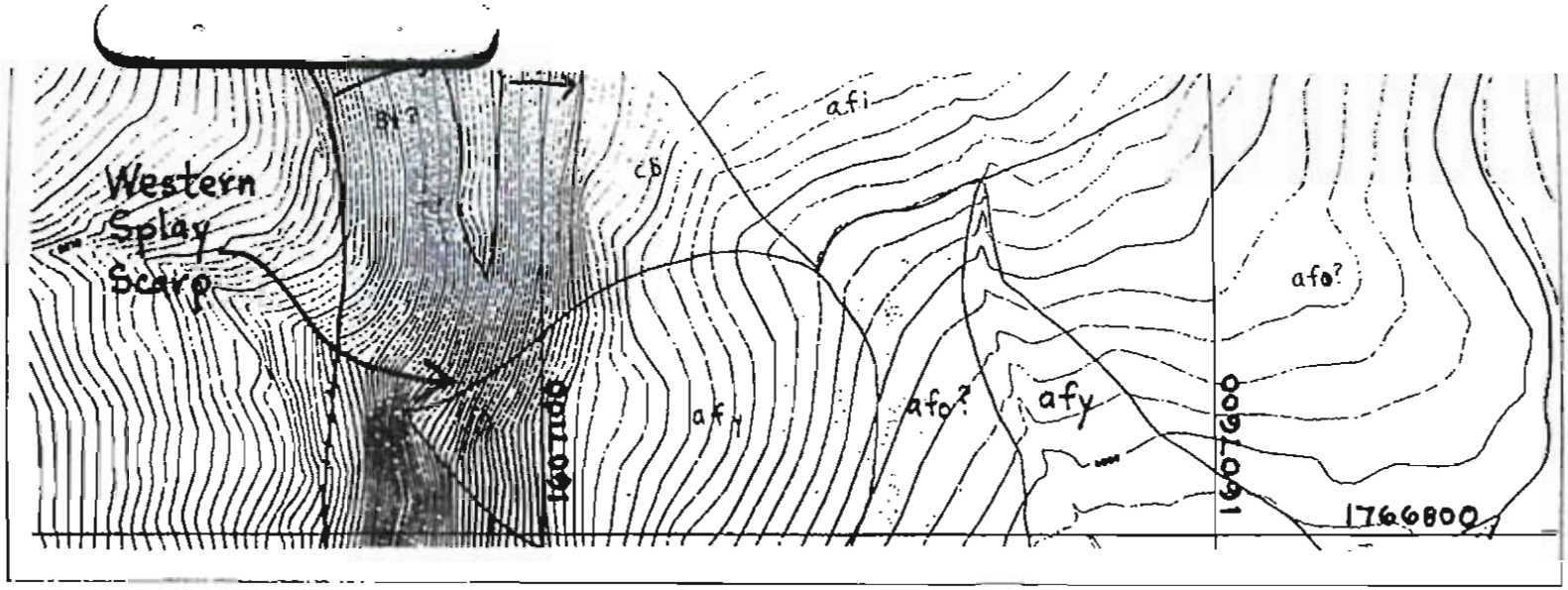

EXPLANATION OF MAP UNITS

Holocene

- ay — modern channel alluvium
- afy — young alluvial fan

Holocene and Late Pleistocene

- cb — bouldery colluvium

Mid-Late Pleistocene

- afi1 — intermediate-age alluvial fan

Early Pleistocene

- afo — Old alluvial fan
- Bt? — Bandelier Tuff, slope-parallel slabs

Symbols

- topographic scarp
- lineament with slight topographic relief
- lineament with no topographic relief (dotted where obscure)

Fig. 14 . Geologic map of the intermediate-age alluvial fan at the base of the Western Splay Scarp, and location of Trench 4. Part of Plate 12 in McCalpin, 1996. Contour interval= 2 ft.

Fig. 15. Photographs of Trench 4. (a)- Clearing trench footprint in the dense oak grove before excavation; view to southwest.

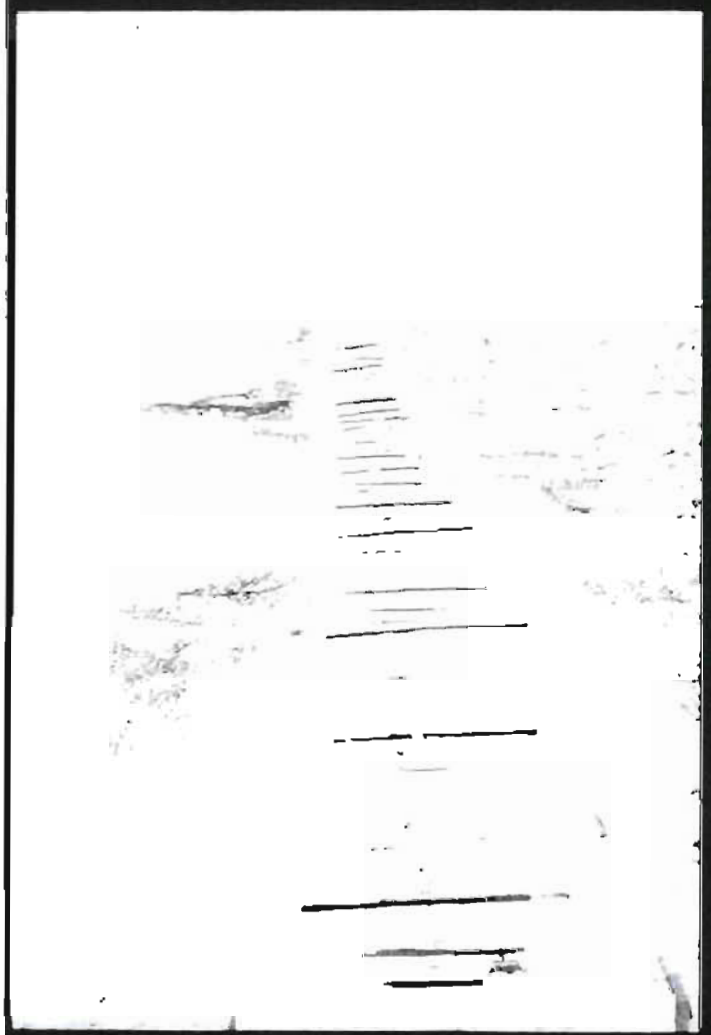

ew southwest (upslope) along trench axis.

3.7.2 Stratigraphy:

The stratigraphy exposed in Trench 4 is more complex than was anticipated and is not completelyy understood. We have subdivided the strata into three general groups that occupy the eastern, central, and western thirds of the trench wall. In the eastern 1/3 of the trench, subhorizontal alluvium and debris flows are termed the 'alluvial fan facies", and are subdivided into 4 major units (9 subunits). In the western 1/3 of the trench (i.e., that part underlying the upper scarp face), deposits of poorly-sorted colluvium with angular tuff clasts are termed the "colluvial/talus facies", subdivided into 4 major units (13 subunits). The central 1/3 of the trench is composed of a complexly deformed zone with deposits transitional between the alluvial fan and colluvial facies ("facies transition zone"). Our correlation of major units 2-5 between the alluvial fan and colluvial/talus facies relies on correlating beds in both sequences with those in the transition zone, and due to later deformation this correlation is somewhat tenuous.

Prior to trenching we anticipated that: 1) the Trench would expose alternating beds of debris flow and fluvial deposits, much like exposed in Trenches 1a-3, 2) that these beds would be offset by an east-dipping normal fault beneath the scarp, and 3) that finer-grained graben-fill beds would underlie the bench, and would terminate abruptly beneath the eastern bench margin against an antithetic normal fault. None of these assumptions turned out to be true.

The eastern half of the trench exposes a sequence of subhorizontal debris flow and fluvial gravel beds similar to that expected in an alluvial fan sequence. This sequence is labeled "alluvial fan facies" on Fig. 16 and all unit labels include the letter "a" for alluvial fan deposits. Only the uppermost of these beds (unit 2a) is clearly a matrix-supported debris flow, and it is the only bed in the sequence whose top slopes east at any significant degree. Subjacent beds are moderately well sorted and imbricated subrounded gravels, or sand beds that do not have debris-flow texture or sorting. The major beds in this fluvial sequence (3a4, 4a1, 4a2, 5a) are essentially horizontal, i.e. they do not slope 3°-4° east as does the bench, much less 6°-7° east as does most of the afi fan. From the lenticular shape of some units (3a1, 3a2, 3a3, 4a1, 4a3) the transport direction of these fluvial deposits was at a high angle to the strike of the trench. Such a southeasterly transport direction could be explained as a result of the normal radial mode of fan deposition, or as the result of southward flow down the axis of a north-south-trending structural sag. However, evidence for the latter is missing (see Sec. 3.7.4). The lowest unit in the alluvial fan section (unit 5a) is considerably finer- grained and denser than the overlying coarse fluvial gravels. In this regard unit 5a resembles unit 4 or 5 in Trenches 1a-2, which were cohesive debris flows distinctly older than the overlying looser fluvial gravels.

The beds at the head of the trench, beneath the upper scarp face, do not resemble either fluvial or debris flow deposits, but their exact origin is uncertain. The most striking aspect of these beds is their high content of angular slabs of tuff that share very similar orientations (Fig. 17). In some units (e.g., 1cBw, 2c2Bt) there are so many stones and so little matrix that the deposits resemble talus. In most deposits however, the angular slabs of tuff are "floating" in a hard, cohesive, oxidized matrix of sandy silt to silty sand.

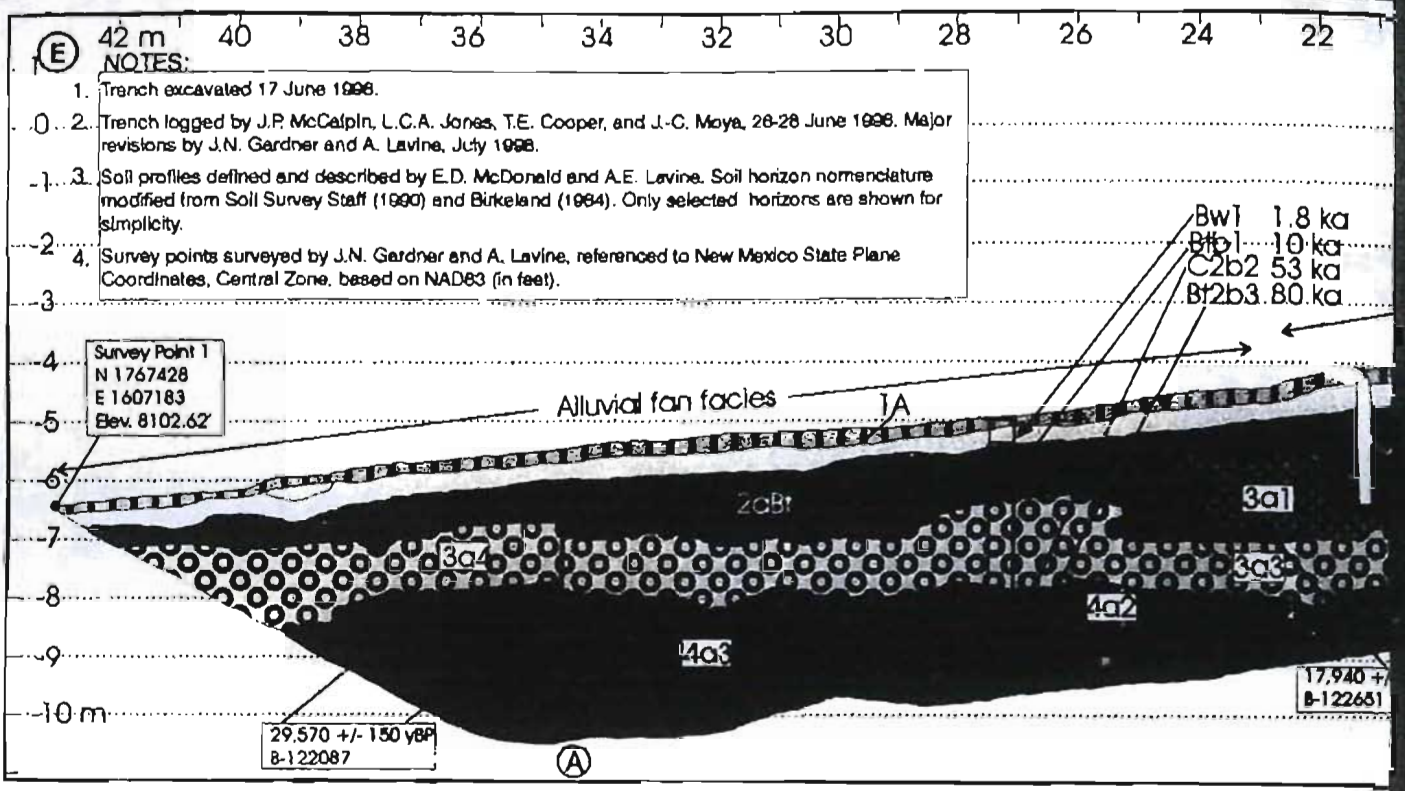

Parent material Soil

1A scarp colluvium *Surface soil (A horizon)*

1Bw scarp colluvium [1420 +/-

Alluvial fan facies ("a" parent materials)

	Parent material	Soil
2aBt	red debris flow	*Surface soil; Bt Horizon developed on unit 2, debris flow*
3a1	small pebble gravel	
3a2	medium sand	
3a3	lens of channel gravel	
3a4	fluvial large cobble gravel	[17,940 +/- 100 yBP]
4a1	fluvial silty sand	[29,570 +/- 150 yBP]
4a2	fluvial pebble gravel	
4a3	fluvial large cobble gravel	
5a	dense, hard fluvial sand & gravel	

Facies transition zone ("t" par

	Parent material	Soil
3tBt	colluvium	*Surface soil developed colluvium*
3t9	rounded pebble gravel and slabs in abundant matrix	
3t10	big angular slabs of tuff, random orientations	
4t1	mixture of angular tuff slabs and rounded gravels	
4t2	clast-free silt	
4t3	imbricated slabs of tuff, smaller than to west	
4t4	large angular slabs of tuff, imbricated to west	
5t1	gravelly sand with rounded small pebbles	[4
5t3	fluvial gravel	

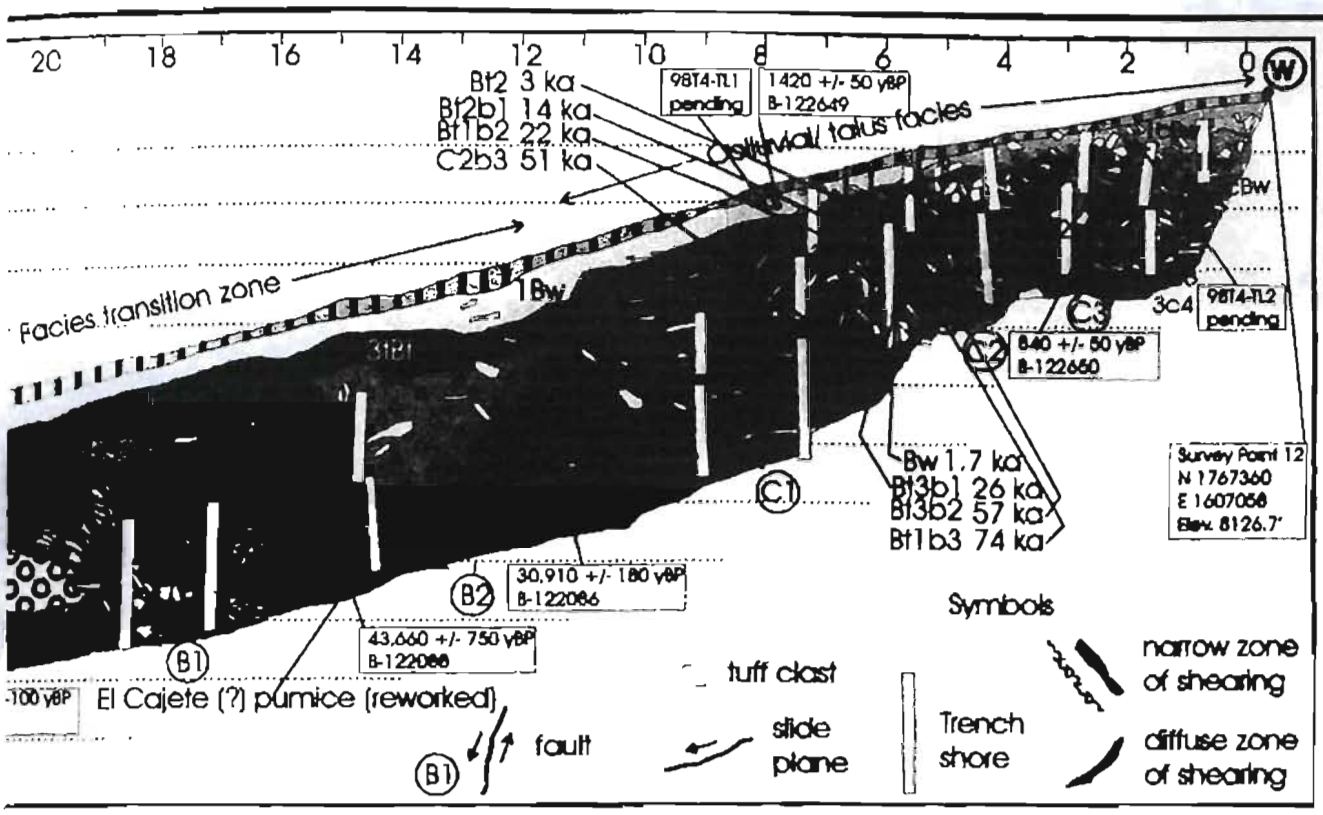

ivium Bw horizon → 1cBw loose white colluvium — *Surface soil; Bw Horizon developed on unit 1c, stony colluvium* [840 +/- 50 yBP]

ent materials)

Colluvial/ talus facies ("c" parent materials)

	Parent material	Soil
2c1Bw	loose white, light orange, and light pink sandy silt	*Surface soil; Bw Horizon developed on unit 2c1, sandy colluvium*
2c2Bt1	very stony colluvium, matrix-poor	*Buried soil 1; Bt Horizon developed on unit 2c2, very stony colluvium*
3cBw	pebble-rich sandy silty mixture	*Surface soil; Bw Horizon developed on unit 3, pebbly colluvium*
3c1	white to pale orange very fine sandy stony colluvium	
3c2	medium orange Bt soil with abundant slabs of tuff	
3c3	dark orange, clast-free silty sand	
3c4	reddish-brown pebbly sand	
3c5	white to tan silty fine sand with some pebbles	
4c1	dark orange, clast-free silty sand	
4c2	reddish-brown pebbly sand [30,910 +/- 180 yBP]	
4c3	white to tan silty fine sand with some pebbles	
5c1	reddish-brown pebbly sand	
5c2	white to tan silty fine sand with some pebbles of El Cajete pumice	

: Bt Horizon on unit 3,

angular

3,660 +/- 750 yBP]

GEO-HAZ Consulting, Inc.

LOS ALAMOS NATIONAL LABORATORY
PAJARITO FAULT: 7 SCATTERED TRENCHES, SUMMER 1998

TRENCH 4-South Wall

DATE March 1999	FIGURE 16
DWG. NO. F:\GEOHAZ\LANL\PAJARITO98\TRENCH4.CDR	

Fig. 17. Photograph of steeply-dipping tuff slabs at the head of Trench 4.

However, even where tuff slabs comprise only 10-20% of the deposit by volume, slab long axes share a consistent orientation.

A clue to the origin of this clast fabric comes from units 3c2, 3c3, and 3c4. Unit 3c3 is a clast-free silty sand that is recognizable as a distinct bed in this generally homogenous and chaotic "colluvial" sequence. Although the bed has been folded, clast long axes in the units above and below unit 3c3 parallel its upper and lower contacts. Thus the original long-axis orientation of slabby clasts was probably parallel to depositional contacts, rather than having a steep initial imbrication. Strong, slope-parallel clast fabric is typical of colluvial deposits, as is the occurrence of angular thin rock slabs that would not likely survive fluvial transport. Thus, deposits 1c, 2c, and 3c beneath the upper scarp face are interpreted as colluvial deposits shed from the 15-21 m-high western scarp of the Western Splay scarp.

Subjacent units 4c and 5c are more thinly bedded, better sorted, and resemble the fluvial beds of unit 4 in Trench 2 on the intermediate-age fan farther north. Unit 5c2 contains lenses and pockets of a biotite-bearing pumice correlated to the El Cajete.

Between the alluvial fan facies (24-44 mH) and the colluvial/talus facies (0-12 mH) is a 12 m-wide zone of transition deposits (facies transition zone). The exact correlation of these transition beds with beds to the east and west is complicated by the subsequent deformation that affected deposits in the middle and upper trench. Generally, deposits in the facies transition zone are coarser-grained than beds in the colluvial/talus facies, but less well sorted and stratified than beds in the alluvial fan facies. The thickest unit in the transition zone, unit 3t10, is a chaotic collection of large (up to 1 m in length) angular slabs of tuff with random orientations. The second-thickest unit, unit 4t4, contains similar slabs with a consistent long-axis dip to the west. Comparison of these units suggests that unit 3t10 may have originally possessed a consistent fabric like unit 4t4, but that fabric was destroyed by internal deformation.

Independent evidence for internal deformation in the transition zone is the bimodal nature of units 3t9 and 4t2, both of which contain a subequal mixture of subround pebbles and cobbles mixed with angular slabs of tuff. This physical mixture of clasts from alluvial and colluvial sources is unusual in a single bed, and argues that two adjacent beds of dissimilar content were physically mixed. A third line of evidence for deformation is the anomalous west dip of units 4t2, 4t3, and 4t4 (discussed later).

The lowest beds in the transition sequence (unit 5t) are well sorted and stratified fluvial sands and gravels. Although these beds are subhorizontal and appear relatively undeformed, they may contain subhorizontal shear zones.

Our preliminary stratigraphic correlation between the alluvial, transition, and colluvial facies zones rests on three observations. First, the basal units in all three zones (unit 5) are considerably denser and more matrix-rich than overlying units. This difference in density suggests that units 5c, 5t, and 5a are all approximately the same age. Second, in each zone there is an apparent unconformity between units that we term 4 and 5. In the alluvial fan facies this is an erosional unconformity, in the transition facies it is a strong angular unconformity (perhaps coincident with a slump plane), and in the colluvial facies it is a weak angular unconformity. Third, units in the upper part of unit 4 in the alluvial fan facies (4a1) and in the colluvial/talus facies (4c2) have nearly identical radiocarbon ages (29,570

+/- 150 vs. 30,910 +/- 180 C-14 yr **BP**, respectively). Based on these observations, we correlate the dense basal units (unit 5) and the overlying well-bedded fluvial units (unit 4) among the three facies sequences in the trench. Correlation of units 2 and 3 across the length of the trench is based only on their relative position above unit 4 and below unit 1 within each section. Unit 1 can be physically traced along the entire trench wall.

3.7.3 Soils:

Eric McDonald measured detailed soil profiles at 5.4 mH, 6.5 mH, and 27.2 mH (Fig. 16, Table 2, and Appendix 3). The profile at 5.4 mH extends through soil horizons that dip ca. 45° west on the west limb of an anticline, whereas the profile at 6.5 mH is approximately centered on the crest of the anticline. McDonald's surface soil coincides with our surface soil and is restricted to unit 1. His buried soil 1 is developed in our units 2c2Bt and 3c1, both of which lie above and are younger than our unit 3c2. His buried soils 2 comprises our map unit 3c2, whereas his buried soil 3 includes our units 3c3 and 3c4.

PDI values from the surface soil are 6.3-9.1, or similar to PDI values from the surface soils in Trenches 1a-2. This similarity is expected, because all surface soils share the pale tan, very friable silt matrix. The PDIs for buried soils 1, 2, and 3 on the crest of the anticline (24.7, 33.7, 57.2) tend to be about 20 less than PDIs of equivalent soils on the west flank of the fold (36.9, 61.7, 73.3; Table 2). This difference is partly due to the thinning of the soil column on the crest of the anticline, and to the existence of the additional fissure fill (unit 3c1) on the flank of the fold.

The soil profile in the alluvial fan facies defines a surface soil coincident with our parent material 1a, and three buried soils approximately coincident with units 2a, 3a+4a, and 5a. The surface soil carries a PDI of 6.6, emphasizing that parent material 1 and its soil are essentially identical over the entire length of the trench. Buried soils 1 (unit 2a; cumulative PDI= 19.9), 2 (units 3a+4a; cum. PDI=61.7), and 3 (unit 5a; cum. PDI=77.0) have cumulative PDIs comparable to buried soils 1, 2, and 3 in the colluvial/talus facies, although the soils cannot be physically traced through the facies transition zone. Readers should note that we did not define any soil horizons within units 3, 4, or 5 when defining our trench mapping units. Age estimates based on PDI values are cited in Sec. 3.7.5.

3.7.4 Structure:

Trench 4 contains three distinct deformation zones, but the origin and relations among them are not clear. The westernmost deformation zone (zone C) underlies the upper scarp face and is essentially coincident with the colluvial/talus facies defined previously. Units 3c2, 3c3, and 3c4 are clearly folded into an anticline-syncline pair with an amplitude of 2 m and a wavelength of 4-5 m. On the limbs of the fold, slab long axes dip as steeply as 45°. The even steeper slab orientations in units 1c, 2c, and 3c2 west of 5 mH are inferred to also result from folding, although no discrete folds are mapped here. Instead, a diffuse east-dipping shear zone (C3) disrupts unit 3c2, and a 1 m-wide fissure fill (unit 3c1) occurs on the west limb of the anticline. Unit 3c3 at the floor of the trench is interrupted by several "fingers" of overlying colluvium penetrating downward along fissures or shears, as if the unit was stretched horizontally into boudinage. The eastern limb of the anticline is

faulted down-to-the-east by a narrow subvertical shear zone, but this shear causes less vertical offset of subjacent unit 4 than of units 3c3 and 3c4 on the fold limb.

In summary, the deformation of the colluvial/talus facies include features of east-west compression (the fold pair), east-west extension (the fissure fill unit 3c1 and diffuse shear zone), and vertical displacement (vertical shear at 8 mH). The fold pair appears to be the oldest feature, since the vertical shear cuts the fold, and the fissure fill overlies the western fold limb. Interestingly, units 4 and 5 are not affected by the folding, which suggest that the fold is decoupled from the lower units, either within the lower part of unit 3c5, or at the 3c5/4c1 contact.

The second major deformation zone ((B) is coincident with the facies transition zone. This zone appears to be a rotational slump, the headscarp of which truncates the folds in unit 3c, and the toe of which is thrust over the subhorizontal gravels of the alluvial-fan facies. Although the headscarp and toe failure planes can be closely defined by abrupt juxtaposition of dissimilar lithologies, and by truncation of bedding, the central part of the failure plane is harder to identify because it parallels bedding. We have inferred one strand of the central slide plane at the base of unit 4t4, because all units above are tilted 7-8 degrees to the west as expected for rotational movement. However, units 5t and 5c in the transitional and colluvial sections do not correlate, in texture or cohesion, to the loose fluvial gravels of units 3a and 4a at the same elevation east of the slump. The higher elevation of unit 5t in the transition zone compared to 5a east of it implies that unit 5t1 is also caught up in the slumping. The lateral truncation of unit 5c2 (which contains the El Cajete pumice) can also be explained if subsidiary slump planes penetrate unit 5t1. However, during our initial logging units 5t1 and 5c1 were mapped as a single unit unbroken by shearing. Thus, the dashed failure plane through unit 5t1 is justified more on geometric grounds than by field observations of shearing.

It is unclear if the lowest unit in the transition zone (5t3) is also slumped, despite the abrupt contact of overlying unit 4t4 with unit 3a3 and 4a2 along the toe thrust. Two possibilities exist: (1) the detachment slump plane is at the top of unit 5t3, so it is in-situ, or (2) the slump plane lies beneath unit 5t3. At this time we cannot prefer one hypothesis over the other.

The third deformation zone (A) is composed of a single, subvertical, down-to-the-west (antithetic) normal fault at 35 mH. This fault displaces units 3a4 through 5a by 20-30 cm, but does not offset the top of buried soil 1 (unit 2aBt). Although this antithetic fault is in the same location as the antithetic fault inferred by McCalpin from surface geomorphology (1997, Plate 12; also Fig. 14 of this report), it does not juxtapose fine-grained graben fill against coarser fan deposits. The net vertical displacement is <25% of the thickness of a typical bed in the fluvial section, and no additional beds occur on the downthrown side of the fault that do not also exist on the upthrown side. There is a slight suggestion that beds east of this fault dip eastward parallel to the rest of the fan, whereas beds west of the fault (i.e., beneath the surface bench) are more horizontal.

3.7.5 Geochronology:

Age control comes from three sources: (1) presence of pumice, (2) soil PDI values, and (3) radiocarbon and luminescence ages. A biotite-bearing pumice is contained in unit

5c2. According to J.N. Gardner (personal communication, Sept. 24, 1998) this pumice contains "components that look like they might be El Cajete-related, but they are trace compared to Bandelier-like components". If this is the El Cajete pumice, it implies an age of 50-60 ka for unit 5c2.

Soil PDI values suggest an age of ca. 80 ka for unit 5a in the alluvial section (Appendix 3) or an age-depth trend of 19 ka/m of stratigraphic thickness. Thus, the entire well-stratified packages of beds in the lower and middle trench appear younger than 80 ka.

PDI-based ages in the colluvial section are older at a given depth below the surface than in the alluvial fan facies, but they contradict the C-14 age of 30,910 from unit 4c2. The truncated soil profile on the anticline crest predicts an age of 22 ka for the top of unit 3c3, whereas the profile on the fold limb predicts an age of 57 ka for this same horizon. The latter age defines an overall age-depth trend of 27 ka/m, or 43% older ages at similar stratigraphic levels compared to the alluvial and transition facies. This fact, and the fact that unit 3c3 overlies the El Cajete (?) pumice with a probable age of 50-60 ka, casts doubt on the validity of the 57 ka age estimate from PDI.

Five radiocarbon ages can be used to calibrate the PDI-based age estimates. In the alluvial fan facies, unit 3a1 dates at 17,940±100 C-14 yr BP, and unit 4a1 dates at 29,570±150 C-14 yr BP. This latter date is from a stratigraphic level similar to the base of unit 4a2, dated by PDI at 53 ka. Thus, the PDI age for this stratigraphic level is 79% older than its radiocarbon age. This discrepancy could be explained if the dated organic material in unit 4a1 was younger than its host deposit, but field observations did not suggest the organics were intruded. The other, more likely, possibility is that PDI overestimates deposit age in this section.

In the facies transition zone unit 5t1 dates at 43,660±750 C-14 yr BP. This sample was only 30 cm higher than the lenses of reworked pumice in unit 5c2. If the pumice is El Cajete (50-60 ka), then a date of 44 ka from slightly higher in the stratigraphic section is reasonable. However, unit 5c2 is also truncated in this vicinity, and there may be a slump failure plane within unit 5t1 between the radiocarbon date and the pumice. Unit 4c2, another well-stratified unit in the colluvial facies that overlies the pumice-bearing unit, dates at 30,910 +/- 180 yr BP. Given its stratigraphic position above both the pumice and the 43,660 year date, this age of 30 ka is considered reliable.

Finally, in the colluvial/talus facies unit 1Bw dates at 1420±50 C-14 yr BP and 1cBw dates at 840 +/- 50 yr BP. PDI-based age estimates for the base of unit 1Bw are 1.7 ka (at 5.6 mH) and 1.8 ka (at 27.2 mH), so an age of 1420 yr BP ka slightly above the base is reasonable. The even younger C-14 age of unit 1cBw can be interpreted in two ways: (1) unit 1cBw is even younger than unit 1Bw, despite the way the contact between these two units is drawn (at 5 mH), or (2) the dated charcoal was intrusive and unit 1cBw is older than 840 yr BP.

3.7.6 Paleoseismic Interpretation:

Fault Zone A

Along fault A the contact between units 2aBt and 3a4 is offset, but not the top of unit 2aBt. The base of the parent material 2a debris flow may be tectonically offset, or the debris flow may be draped over a small scarp in the top of unit 3a4. Thus we know with

certainty that unit 3a4 is offset, the base of unit 2a may be offset, the top of unit 2a is not offset, and the top of buried soil 1 is definitely not offset. This brackets offset on this small antithetic fault between about 10 ka (estimated age of inception of soil formation for buried soil 1) and 29.5 ka (age of unit 4a1, which is slightly older than faulted unit 3a4).

Fault Zone B

At the head of the facies transition zone, soil 3tBt is apparently truncated at the headscarp of the rotational slump, but it is actually the parent material unit 3 colluvium that is truncated. The Bt horizon continues westward into unit 3c2. Thus, displacement on this structure postdates deposition of parent material 3t9, and predates formation of buried soil 1 [variously dated by PDI at 10 ka (27.2 mH), 14 ka (6.5 mH; possibly a stripped soil section), and 26 ka (5.4 mH; inherited PDI components may cause an age overestimate here)]. If our correlation of strata between the alluvial fan facies and transition facies is valid, then the base of unit 3 is younger than 29 ka (the age of unit 4a1), and the middle of unit 3 (unit 3a1) is ca. 18 ka. Therefore the upper part of unit 3 truncated by the slump headscarp must be younger than 18 ka, yet it carries a soil that probably took 10-14 ka to develop; this relationship appears to bracket faulting between about 10 ka and 18 ka..

The timing of movement on fault zone A (10-29.5 ka) is sufficiently similar to the timing of slump movement on zone B (10-18 ka) that the two movements may be contemporaneous. This temporal coincidence raises the question of what caused the rotational slump. One nontectonic explanation is that alluvial fan channels running north-south had undercut the base of the colluvial slope, and caused the slump at the alluvial-colluvial facies transition. Although this scenario is plausible, the relatively small channel deposits of units 3a1-3a3 would have to be responsible for this undercutting, since they are clearly overthrust by the slump toe and are thus the last alluvial deposits to predate slumping. In addition, the best-defined slump failure plane descends to the same stratigraphic level as the base of unit 3a3, and this is the expected geometry of a slump caused by basal undercutting.

A second, related explanation is that fluvial undercutting had created an east-facing slope at the facies transitions zone, but this slope did not fail by slumping until the earthquake that created the fault offset at 35 mH. This faulting event is bracketed between about 10-18 ka.

In his technical review of this report, Dr. W.R. Lettis suggested an alternative interpretation of Fault Zone B. He suspects that Fault Zone B, especially fault B1, is an antithetic fault to the main fault zone. However, a "main fault zone" is nowhere exposed in the trench, so the possible antithetic role of Fault Zone B cannot be confirmed. Dr. Lettis also points out that fault B1, as drawn on Fig. 16, extends beneath the bottom of the trench, and thus either: (1) implies a deeper slump than proposed by the author, one that would have to involve all strata in the facies transition zoner, or (2) is a likely canidiate for a tectonic (antithetic) fault. If both faults B1 and B2 penetrate the floor of the trench, it is possible to interpret Fault Zone B as a graben or giant fissure, in which the coarse rubble of units 3 and 4 accumulated as fissure fill, and were later rotated by differential movement on the bounding faults. We do not favor this interpretation because we could not trace fault B2 to the floor of the trench. Under the scenario above it would be the more

significant of the two bounding faults, and its obscure expression as it approached the trench floor argue against significant vertical displacement. However, we do admit that, in the base of a mainly tensional fissure, one would not expect large vertical displacements on the bounding "faults". However, at that location one would expect fissure fill units with subvertical fabric, and instead we observe well-stratified units 5t1 and 5t3 at this position.

Fault Zone C

The deformation exposed at the head of Trench 4 affects all units except 1A and 1Bw, the latter dated at 1.4-1.8 ka by C-14 and PDI. At least three episodes of deformation are indicated. The oldest episode of deformation resulted in folding of units 3c2-3c5 and (inferred) rotation of their clasts from a slope-parallel attitude to their present steep dips. The second episode of deformation dismembered unit 3c3 and opened the fissure into which unit 3c1 was deposited. A third episode of penetrative deformation apppears to be required by the steep dips of clasts in units 2cBt and 1cBw. (However, it is possible that soil horizons 1cBw, 2c2Bt, 2c1Bw and 3cBw could be in fact developed on the same parent material, one that was internally deformed during initial folding). In other words, at the head of the trench we may be observing young soils developed on old deformed parent materials which were brought up to the surface by folding and then erosionally truncated. In this scenario only two deformation episodes are required, an older episode to fold and internally deform unit 3, and a younger episode of faulting and fissuring. However, the C-14 age of 840 +/- 50 yr BP from unit 1cBw suggests that (if the charcoal is not intrusive) the deposit itself is not old. Thus, a key question here (as well as in other trenches) is whether radiocarbon dates dates the parent material, or younger soils developed on that parent material.

This distinction between old parent materials and possibly younger soils emphasizes a general danger in using soil PDI values to estimate deposit ages beneath fault scarps. PDI values only tell us the amount of soil development time, not the age of the parent material on which the soils are developed. In a dominantly depositional environment such as an alluvial fan, where deposits are laid down quickly and then soil development proceeds on them before the next eposiode of deposition, soil PDI ages can closely approximate deposit age. This approximation works because total geologic time is composed only of deposition time (negligible) and soil development time. In contrast, it is clear that folded deposits at the head of Trench 4 have suffered some erosional truncation, particularly unit 3c2 atop the anticline. In this case, geologic time is composed of deposition time, folding time, erosion time, and soil development time. Soil PDI values only permit estimation of the last component.

Given the distinctions outlined above, the parent materials containing the abnormally steep clast fabrics (units 1cBw and subjacent units) are either older than unit 1Bw dated at 1420 C-14 yr BP (if the contact between units 1Bw and 1cBw is correctly mapped), or about 840 +/- 50 yr BP (if the dated charcoal in 1cBw is not intrusive). Either of these dates indicates very young deformation. The physical stratigraphy indicates that unit 1Bw is a slope colluvium that pinches out near the crest of the scarp, and that unit 1cBw is an older (perhaps considerably older), deformed (?) unit that underlies unit 1Bw. Thus, the 840 yr age from beneath the 1420 yr age suggests that the sampled 840 yr-old charcoal is

younger than its host deposit. The 840 yr-old charcoal was derived from a bulk sample of soft, pale silty matrix that was dug out from the interstices between the angular tuff slabs. No charcoal was visible in the trench wall, but small pieces were retrieved from the bulk sample by Paleo Research Labs (see Appendix 2, sample 98T4-6). The dated sample was a composite of six pieces of conifer charcoal that totalled 0.003 g weight. The vegetation at the site today is Gambel's oak, but conifers are present directly upslope. In summary, we do not have sufficient information on sample context to state that the six pieces of charcoal were all definitely intrusive.

In order to locate the source of the fold deformation, J.N. Gardner and I examined the face of the larger western sub-scarp upslope from Trench 4 for signs of landsliding. We believed that the most reasonable mechanism for the folds in the colluvial/talus facies was local compression at the toe of a landslide that must lie upslope of the trench. However, despite our examination of 1:1200-scale aerial photographs and field checking, we could not locate any evidence of recent landsliding. Instead, the scarp face exposed numerous subvertical, thin slabs and flakes of in-situ (?) tuff, bounded by subvertical fractures oriented east-west, or down the fall line of the scarp. The consistency of slab orientation on the scarp face is similar to that found in the colluivial slabs at the head of Trench 4, but the two orientations have strikes perpendicular to each other. At present we are uncertain how these steeply-dipping tuff slabs on the scarp face were created, or whether their subvertical attitude has anything but a coincidental similarity to that of colluvial slabs exposed in the trench. The bedrock slabs most resemble in-situ tuff slabs found in transverse structure zones on the main Pajarito fault scarp by McCalpin (1997, 33-39), but those slabs were restricted to narrow zones, in contrast to the widespread steep slabs upslope from Trench 4.

The episode of extensional deformation at the trench head can be indirectly dated by soil PDI. Horizon Bt2b1 at 6.5 mH covers the crack fill of unit 3c1 and must post-date the crack, and dates at ca. 14 ka. Horizon Bt3b1 at 5.4 mH carries an older PDI age (26 ka), but this horizon is developed on the crack fill, and the crack fill parent material is unit 3 which already carried a soil before crack formation. Thus, I believe that the PDI age of 26 ka for unit 3c1 overestimates its age, because that unit is composed of "recycled" pieces of preexisting Bt horizons from either side of the fissure. If the crack fill formed before 14 ka, and well after 26 ka, then its time range overlaps the time range of antithetic faulting and rotational slumping farther downslope in the trench (10-18 ka). Thus, it is possible that all the extensional deformation in the trench occurred at the same time, ca. 10-18 ka.

Displacement

Due to the varied and distributed nature of this extensional deformation, it is not possible to calculate a net tectonic displacement during the event(s) between 10 and 18 ka. The antithetic vertical displacement of 20-30 cm on Fault A appears to be attributable to a single displacement episode, since displacement does not increase downward. In the colluvial/talus facies only subvertical shear C1 at 8 mH has appreciable vertical displacement, 25-30 cm down-to-the-east. Thus, the vertical displacement on the only subvertical shear zones at either end of the trench essentially cancels out.

A second way to estimate fault displacement is to assume that a buried normal fault zone exists beneath the rotational slump, and is responsible for the vertical separation between unit 5c in the colluvial facies, and correlative unit 5a in the alluvial facies. The top of unit 5c is ca. 2.5 m higher than the top of unit 5a. This discrepancy of age-vs-depth across the facies transition zone is confirmed by radiocarbon dates, which indicate an age of 44 ka at -6.85 mV in the transition zone, compared to an age of 29.6 ka at -8.15 mV in the alluvial facies section. This age-vs-depth discrepancy can be explained either by thrusting the colluvial section east over the alluvial section along a reverse fault coincident with the toe of the rotational slump, or by postulating a buried vertical fault beneath the slump, the expression of which is totally obscured by bedding-plane slip at the bottom of the slump. Both of these scenarios have weaknesses. The thrust model is not compatible with the evidence for a period of late extension near the toe and head of the trench, but it is compatible with the east-west compressional (?) folding of units 3c2-3c5. However, if the 2.5 m vertical separation was caused by thrusting, then it is attributable to the episode of compressional deformation, and this episode is more likely related to landsliding west of the trench than tectonic faulting. This scenario also assumes that the toe of the later slump is coincident with the earlier thrust fault.

The hypothesis of a buried vertical fault beneath the slump is more compatible with the style of faulting seen in the other 1997 and 1998 trenches, but unfortunately no evidence for such a structure was observed in the trench wall. However, if we merely back-rotate the slump to its original orientation (about 15° counter-clockwise on the log) the 2.5 m of vertical separation on the top of unit 5 still remains. Thus, the vertical separation between units 5a and 5t cannot be explained by eastward slumping, and if real, requires either: (1) a pre-slumping vertical displacement of some type in the center of the trench, or (2) slump movement vectors that are not parallel to the plane of the trench wall. The former explanation lends support to Dr. Lettis's interpretation of Fault Zone B as a graben structure.

3.8 Trench 5

Trench 5 is located approximately 150 m due west and 30 m upslope of Trenches 2 and 3, across the western sub-scarp of the main Pajarito fault scarp (Fig. 18). The trench is 36 m long, up to 6 m deep, and trends approximately east-west.

3.8.1 Geomorphology:

At this location the main displacement on the Pajarito fault is expressed as a 40-m-high scarp that lies west and south of the intermediate-age alluvial fan described in Secs. 3.1-3.6 (Fig. 18). About 120 m south of the fan-head drainage, this main scarp splits into a 12 m-high, north trending western sub-scarp, and a 25 m-high, northeast-trending, eastern sub-scarp. The 30 m-wide, gently sloping bench that separates these sub-scarps is labeled as a "possible slide block" by McCalpin (1997, Plate 6), partly because the eastern sub-scarp below the bench bulges out eastward in a suspicious manner. However, that bulge can also be interpreted as a result of a change in scarp strike from north to northeast.

South of Trench 5, the 40 m-high main scarp has a peculiar shallow, north-trending topographic sag just above (west of) the scarp crest. In part this sag is integrated into a south-flowing swale at the head of the scarp, but in places the sag has up to 0.5 m of topographic closure. McCalpin (1997, Plate 6) inferred that a down-to-the-east normal fault underlay this sag. However, based on the results of the 1997 trenching campaign, this type of landform more likely overlies a tensional pull-apart fissure, and is related more to eastward toppling than to dip-slip faulting.

A similar zone of eastward toppling exists on the north bank of the fan-head drainage, where drainage has incised through the main scarp. The face of the eastern sub-scarp north of the incised drainage is composed of slabs of tuff, the tops of which parallel the ground surface. Typically it is impossible to distinguish whether these surface-parallel slabs represent loose blocks of tuff sliding down the scarp face, or toppled megablocks of east-dipping tuff. In the latter case the scarp face is essentially a dip slope on east-dipping tuff (see McCalpin, 1997, 1998 for a more detailed discussion of fault zone structure types). A good exposure on the north bank shows a ridge of tuff at the scarp head, in which tuff beds dip 35 degrees east. Directly west of this ridge is a strike gully with no bedrock exposures, and directly west of the gully tuff dips at 8 degrees east. It thus appears that the gully has developed in a tension fissure created by 27 degrees of eastward toppling of the eastern sub-scarp. Farther north along strike a zone of fractures occurs where the tension fissure would project. The point of this discussion is to show that the style of faulting associated with the main scarp here is complex and contains elements of toppling as well as dip-slip faulting.

The main reason this site was selected for trenching was the smooth topographic profile presented by the western sub-scarp. Elsewhere on the Pajarito fault, scarps as high

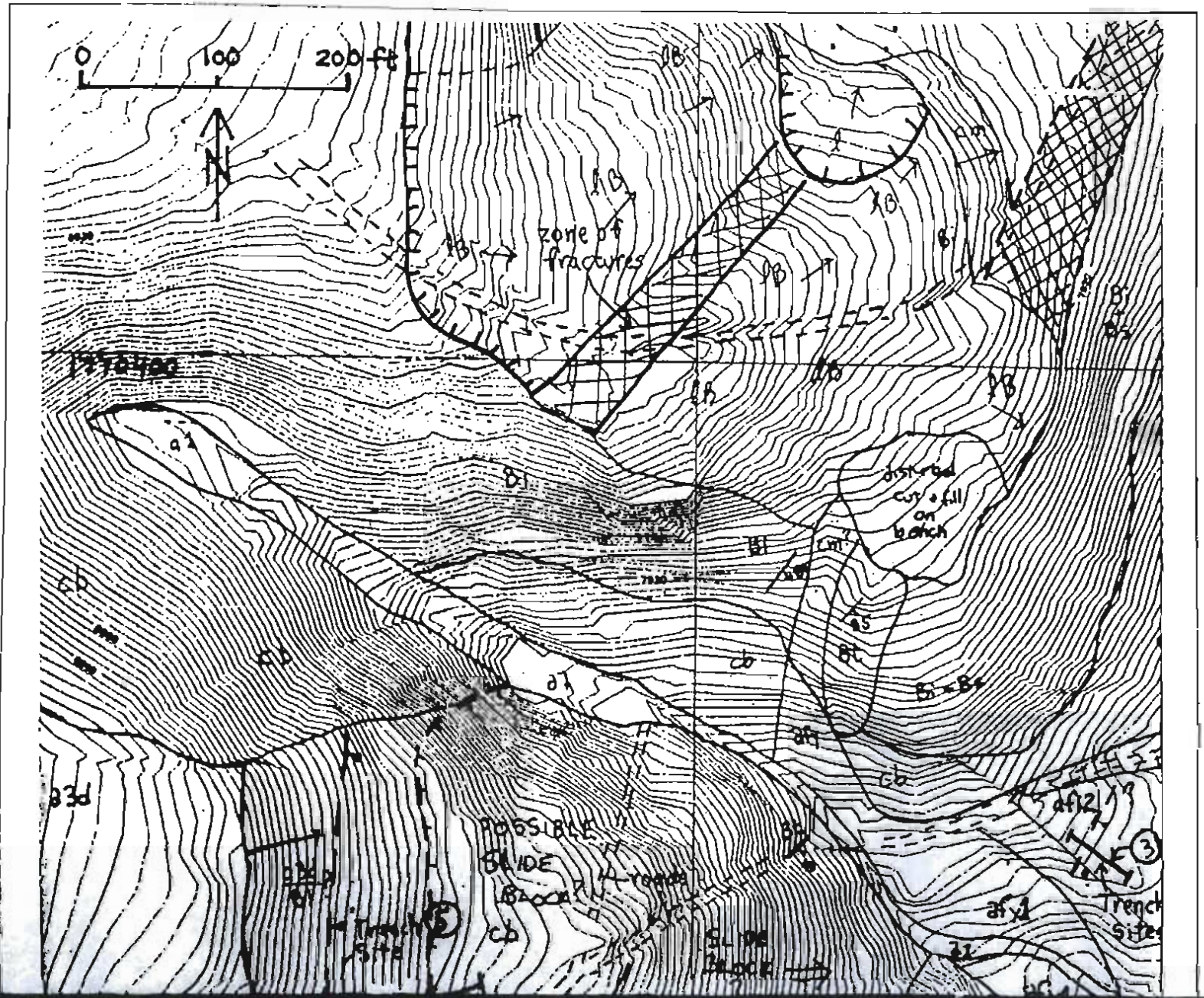
0
100
200 ft
N
zone of fractures
disturbed cut & fill on bench
POSSIBLE SLIDE BLOCK
SLIDE BLOCK
Trench Site
Trench Site

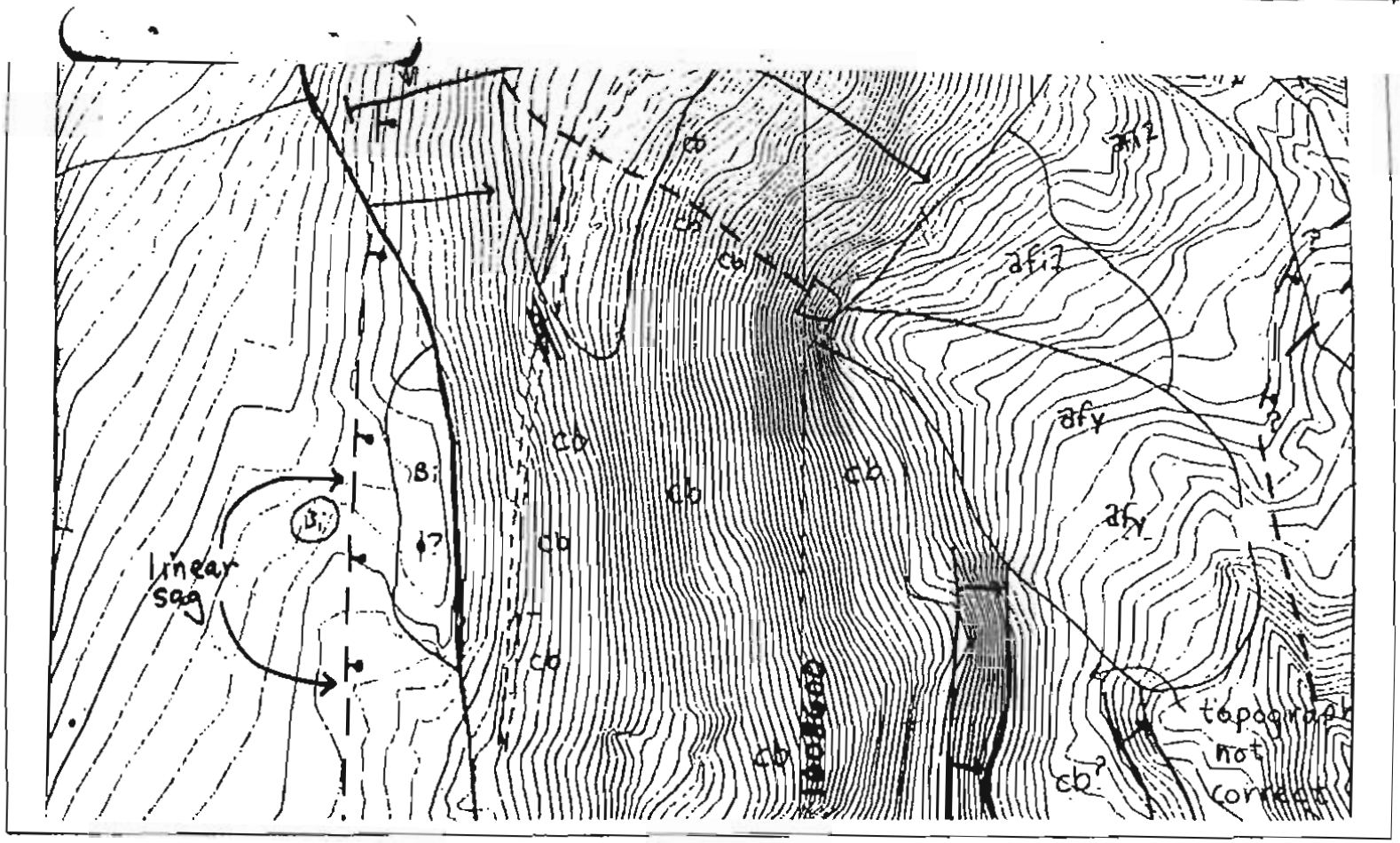

Fig. 18 . Geologic map of the main Pajarito fault scarp west of the Intermediate-age alluvial fan, the head of which (and Trench 3) is at far right center. Trench 5 is located on the western sub-scarp at left center. Part of Plate 6 in McCalpin, 1997. Contour interval= 2 ft. For explanation of map units, see Figs. 3 and 14.

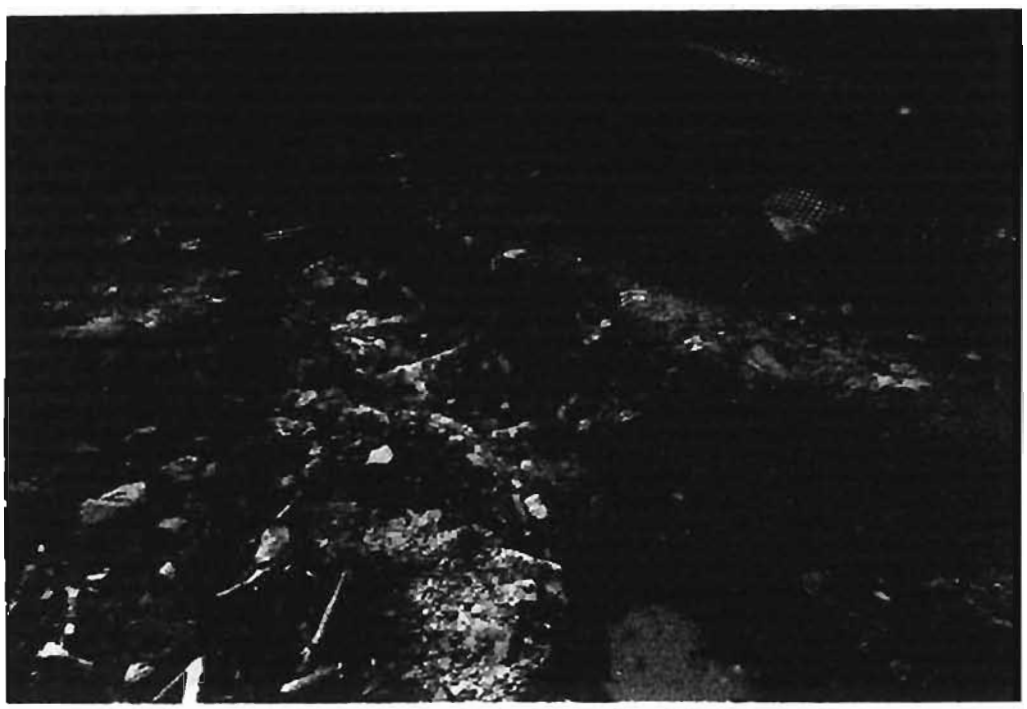

Fig. 19. Photographs of Trench 5. (a)- View east down the trench axis, from the upslope end of the middle fault block (at center). The upper pocket is out of photo to the lower right, the lower pocket is at upper left.

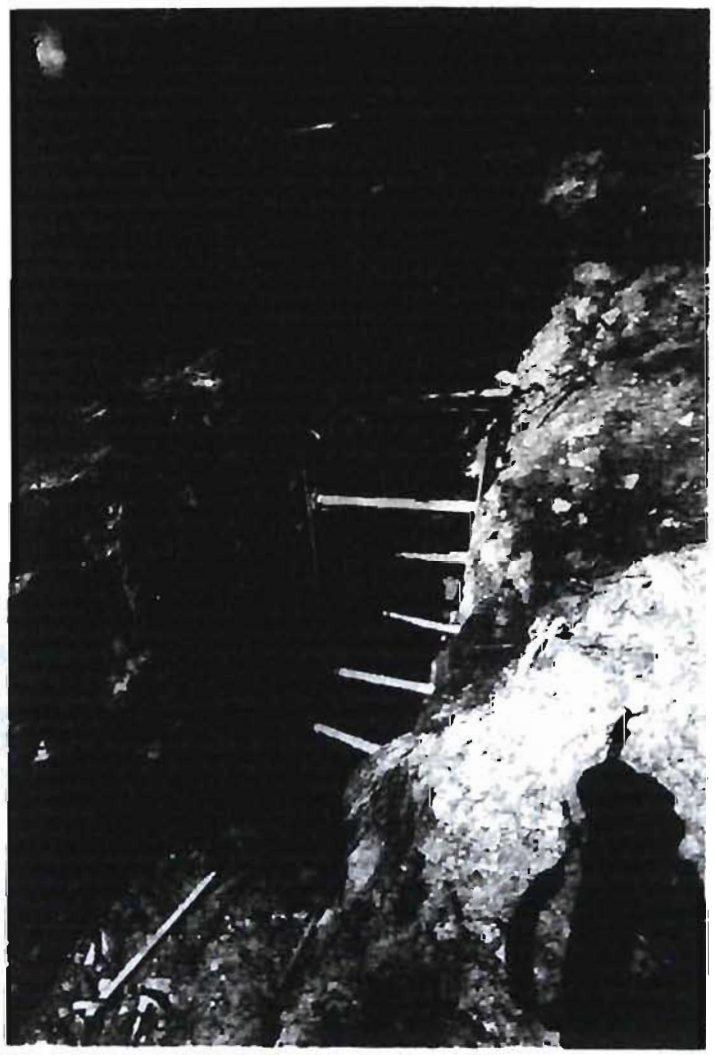

(b)- The upper pocket, view to west.

as 12 m typically expose either in-situ (i.e., gently east-dipping) tuff or surface-parallel slabs of tuff, on a planar upper scarp face that is distinctly steeper than the colluvial apron. The contact between the steeper upper scarp face underlain by tuff and the lower scarp face underlain by colluvium is sharp. In contrast, the western sub-scarp here does not show such a distinction. No in-situ tuff or even large tuff slabs appear on the upper scarp face. Instead of having an asymmetrical profile, this sub-scarp has a symmetrical profile, similar to profiles of fault scarps that displace unconsolidated Quaternary deposits. In addition, McCalpin (1997, Plate 6) mapped the upthrown block surface as being covered by old dacite-bearing alluvial gravels. Based on the gravel cover and symmetry of the scarp profile, we inferred that this scarp may have displaced an old gravel strath terrace cut onto Bandelier Tuff. If this was the case, then there was opportunity for: (1) preserving equivalent gravel deposits on both sides of the fault, which would aid in the geometric reconstruction of faulting, and (2) creating and preserving colluvial wedges derived from gravel on the upthrown block. In contrast, most of the trenches excavated in 1997 did not contain distinct scarp-derived colluvial wedges, because there were no thick unconsolidated deposits on the upthrown block to act as a source. It was hoped that a sequence of scarp-derived colluvial wedges would provide a basis for interpreting the paleoseismic chronology in the trench, that would be less ambiguous than one based on the type of fissure-fill stratigraphy typical of the 1997 trenches.

3.8.2 Stratigraphy:

The stratigraphy exposed in trench 5 will be discussed in two sections, because unconsolidated deposits occur mainly in two deep "pockets" in the trench (Fig. 19). Within each pocket units are numbered from 1 (youngest) to 9 (oldest), with "l" denoting units in the lower trench pocket and "u" denoting units in the middle trench and upper pocket. Units 1-3 are age-correlative across the entire trench, whereas units 4-9 constitute local age sequences within each pocket that cannot be physically correlated with each other (Fig. 20).

Lower Trench Units

The lower trench pocket is at least 6 m deep (Fig. 21). No in-situ tuff was exposed at the bottom of the trench, although shattered and brecciated tuff is exposed in the "rat hole" at the base of the south wall. The oldest deposits exposed (unit 9l) are a red gravelly sand with thin beds of small pebble gravel. Overlying this unit is unit 8l, which comprises 60% of the total stratigraphic thickness. Unit 8l is a massive, unstratified, hard silty sand containing <1% small angular clasts, none of which exceed 2-3 cm in diameter. This unit can be subdivided into subunits 8la (hard silt) and 8lb (light tan silt with angular clasts of soft tuff) in the eastern part of the pocket, but over most of the trench wall this 3.5 m-thick unit cannot be subdivided. Unlike unit 9l, unit 8l displays no evidence of stratification and no buried soils that would permit subdivision of the unit. The depositional environment of such a thick, homogeneous, clast-free but unstratified deposit is difficult to envision. The unit cannot represent slope colluvium, because all modern slope colluvium contains abundant large angular tuff clasts. On the other hand, sag pond deposits laid down by fluvial or lacustrine deposition might be this fine-grained,

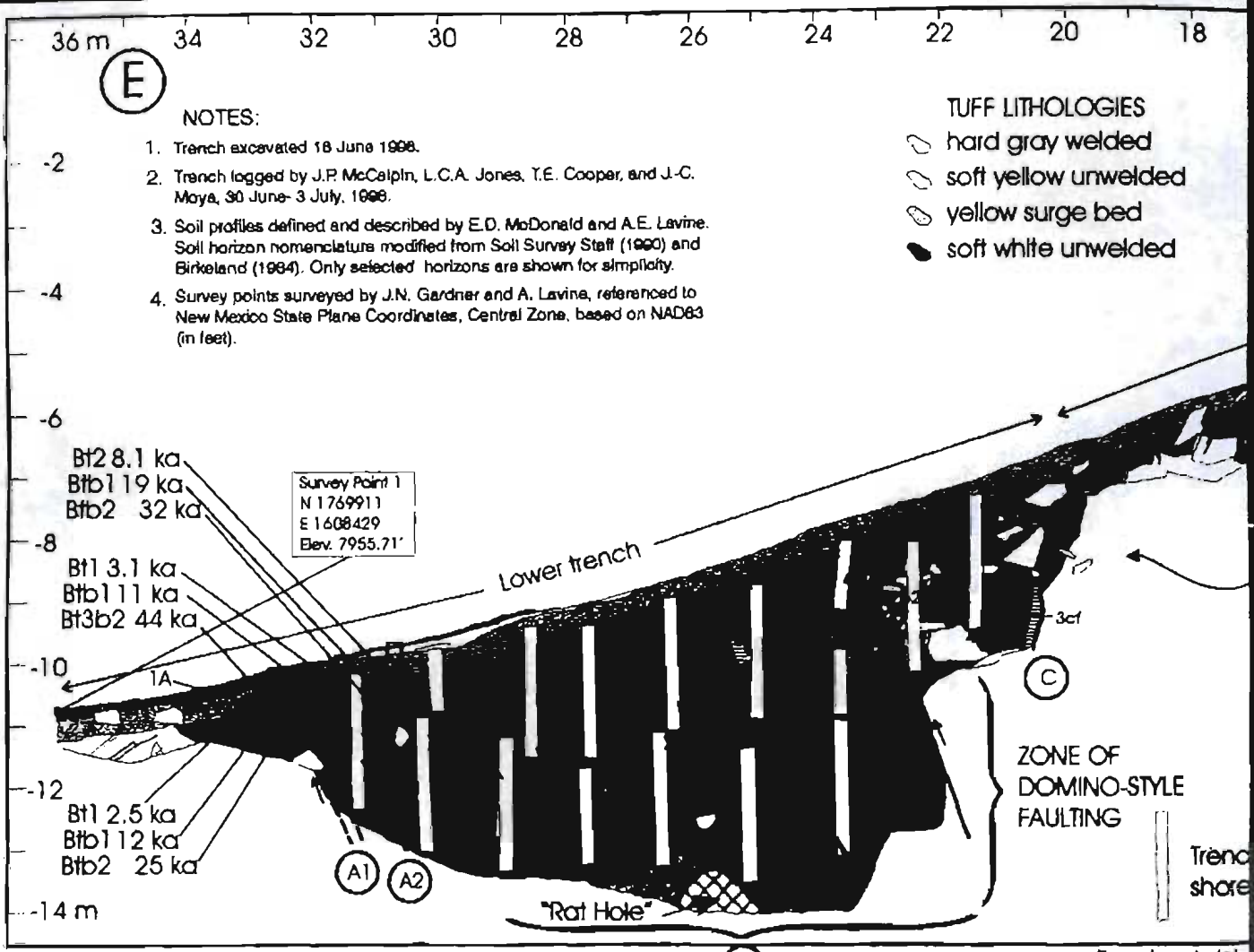
36 m
34
32
30
28
26
24
22
20
18
E
NOTES:
1. Trench excavated 18 June 1998.
2. Trench logged by J.P. McCalpin, L.C.A. Jones, T.E. Cooper, and J.-C. Maya, 30 June- 3 July, 1998.
3. Soil profiles defined and described by E.D. McDonald and A.E. Lavine. Soil horizon nomenclature modified from Soil Survey Staff (1990) and Birkeland (1984). Only selected horizons are shown for simplicity.
4. Survey points surveyed by J.N. Gardner and A. Lavine, referenced to New Mexico State Plane Coordinates, Central Zone, based on NAD83 (in feet).
TUFF LITHOLOGIES
hard gray welded
soft yellow unwelded
yellow surge bed
soft white unwelded
-2
-4
-6
-8
-10
-12
-14 m
Bt2 8.1 ka
Btb1 19 ka
Btb2 32 ka
Bt1 3.1 ka
Btb1 11 ka
Bt3b2 44 ka
Bt1 2.5 ka
Btb1 12 ka
Btb2 25 ka
Survey Point 1
N 1769911
E 1608429
Elev. 7955.71'
Lower trench
1A
3cf
C
ZONE OF DOMINO-STYLE FAULTING
A1
A2
"Rat Hole"
B
Parent material
1A scarp colluvium
Surface soil (A horizon)
1AC scarp colluvium
Lower trench units ("1" parent materials)
Parent material
Soil
3la8tb1 silty sandy distal colluvium
Buried soil 1: Bt Horizon developed on unit 3la, sandy colluvium
3lb8tb1 stony scarp-derived colluvium
Buried soil 1: Bt Horizon developed on unit 3lb, stony colluvium
4lb8tb2 stony scarp-derived colluvium
Buried soil 2: Bt Horizon developed on unit 4l, stony colluvium
4l8Cb2 stony scarp-derived colluvium
Buried soil 2: BC Horizon developed on unit 4l, stony colluvium
5l8t1b2 silty sandy distal colluvium
5l8t2b2 silty sandy distal colluvium
Buried soil 2: Bt Horizon developed on unit 5l, sandy colluvium
5l8Cb2 silty sandy distal colluvium
Buried soil 2: BC Horizon developed on unit 5l, sandy colluvium
6l well-sorted sand ("beach sand")
7l fluvial small pebble gravel
6-8l8tb2 sandy distal colluvium
FILL IN LOWER FISSURE
6-8l sandy distal colluvium
8l slightly gravelly sand, hard, massive
8lo hard silt
8tb light tan silt with angular clasts of soft tuff
9l red pebble gravel w/sandy matrix

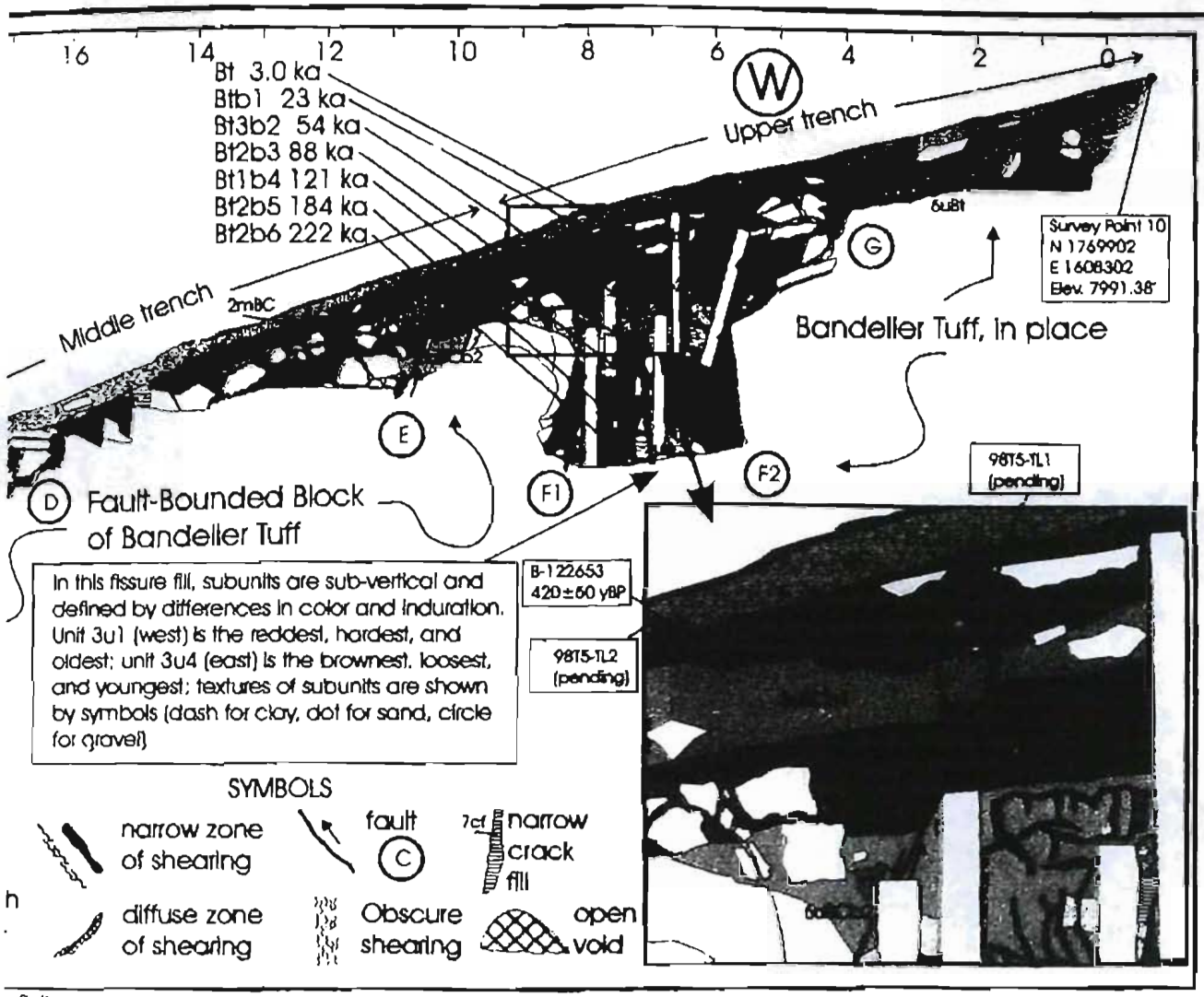

Soil

Horizon → loose white colluvium

1C — Surface soil: Bw Horizon developed on unit 1c, stony colluvium

Middle and Upper trench units ("m" and "u" parent materials)

Parent material		Soil
m3C	sandy colluvium	Surface soil: Bt Horizon developed on units 2m and 2u colluvium
mBtb1	stony colluvium	Buried soil 1: Bt Horizon developed on unit 3m, stony colluvium
mBt1b3	stony colluvium	
mBt2b4	stony colluvium	
mBCc1	stony colluvium	
uBtb2	stony colluvium	Buried soil 2: Bt Horizon developed on unit 6u, stony colluvium
uBt1b2	stony colluvium	
uBt2b2	stony colluvium	
uBCb2	stony colluvium	
6uBt	brown clay	

7u4	FILL IN UPPER FISSURE
7u3	fissure fill, composed mainly of silty sand with embedded fractured clasts of soft tuff (several lithologies); heavy soil development has transformed the finer beds to red silty clay
7u2	
7u1	

GEO-HAZ Consulting, Inc.

LOS ALAMOS NATIONAL LABORATORY

PAJARITO FAULT, 7 SCATTERED TRENCHES, SUMMER 1998

TRENCH 5-South Wall

DATE March 1999	FIGURE 20
DWG. NO. F:\GEOHAZ\LANL\PJ\LABITO98\TRENCHS.CDR	

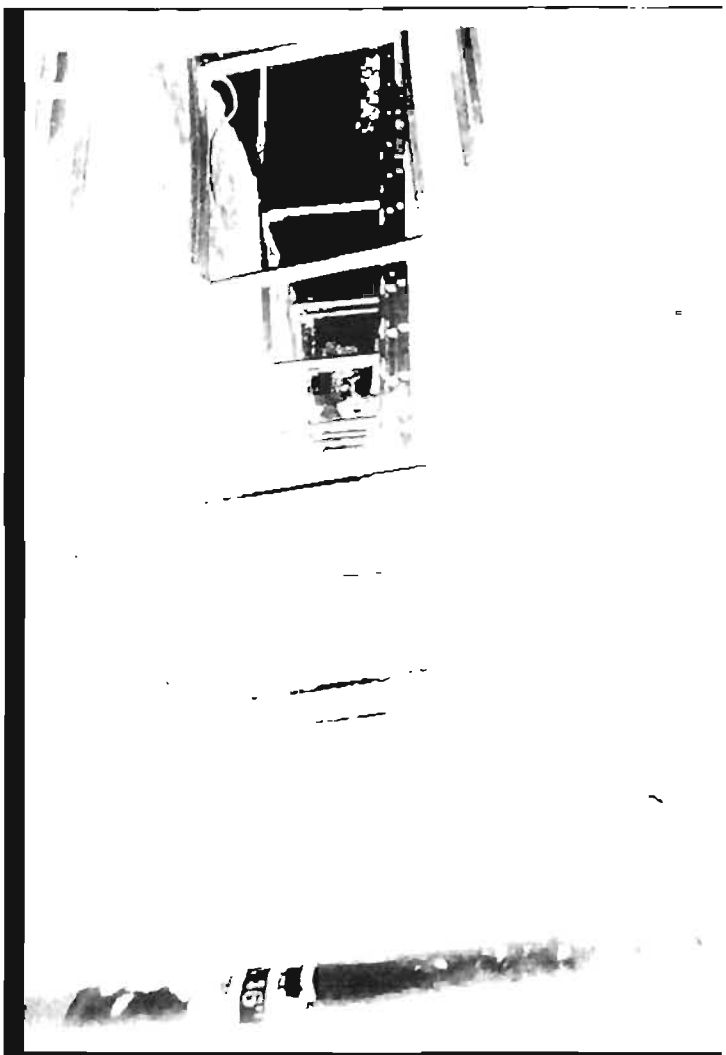

ograph of the lower pocket and its fine-grained fissure fill. View
a at the base of the left (south) trench wall is the void space te

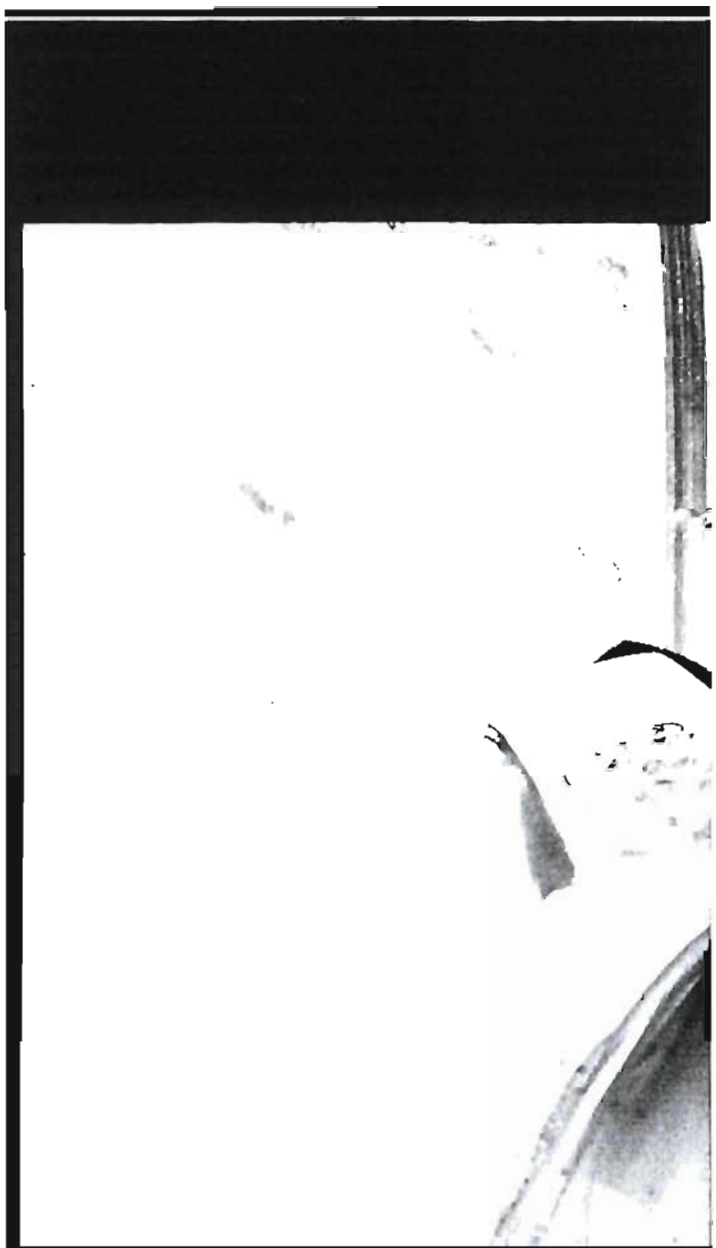

ograph of Trench 5. (a)- Unit 6l (the "beach sand") showing th
ng and the small conjugate normal faults. Finger is pointing to
een units 6l (to the left) and 7l (to the right).

but should exhibit some stratification or other evidence for hiatuses in sedimentation. Unit 8l does resemble the deposits in 1997 Trench 6 across the crestal tension fissure directly south of Ski Hill Road (McCalpin, 1998, p. 74-83). However, the massive deposits in the tension fissure carried four buried soils that permitted estimation of their orientation and displacement across domino-style faults. No such soils can be recognized in the 1998 Trench 5.

Most of unit 8l is overlain by a 30 cm-thick red small pebble (pea) gravel (unit 7l). Overlying this gravel is a 0.8-1.5 m-thick, well stratified, well sorted sand (unit 6l), informally termed the "beach sand" by the logging team. Individual beds in unit 6l are 0.5-2 cm thick and range in texture from fine sand to very coarse sand (Fig. 22a). The good sorting and bedding suggest that this deposit is a fluvial infill of a topographic depression. At the eastern end of the lower pocket, deposits caught up in the normal fault zone share characteristics of parent materials 6l, 7l, and 8l, and have been mixed by faulting and overprinted near the surface with Bt soil horizon development. Rather than try to subdivide this zone in detail, we merely map it as unit 6-8l.

On the western end of the lower pocket unit 6l appears to be partly overlain by, and to partly grade into, a massive, unstratified silty sand (unit 5l). Within 2 m of the steep bedrock headwall of the pocket, there are sufficient large tuff clasts that the deposit resembles a proximal (debris-facies) colluvial wedge (unit 4l). Due to structural complications (discussed later) we are not confident that these two facies of colluvium (unit 5l, wash-facies colluvium, versus unit 4l, debris-facies colluvium) are coeval, so we have assigned them different unit numbers, rather than just assigning them different letters as is done for other subunits. Given the domino-style of faulting prevalent in the lower pocket, unit 5l could be separated from unit 4l by a domino fault, in which case unit 5l could be stratigraphically below unit 4l.

Unit 3l includes a wash-facies colluvium (unit 3la, silty sand texture) and a debris-facies component (unit 3lb, stony texture) that cover the entire pocket, and unconformably overlie the strong soil developed on units 4l-6l. The increased thickness of unit 3lb against the headwall of the lower pocket and its high content of tuff slabs with east-dipping fabric, indicates it is a proximal colluvial wedge derived from a free face at ca. 20 mH. Upslope of 20 mH the soil developed on unit 3l (buried soil 1) continues in an attenuated section of stony colluvium, the upper part of which may be coeval with unit 3lb, but the lower part of which could be considerably older. Thus, this thinner colluvium is mapped as unit 3-5m.

The uppermost parent material in the lower pocket is unit 1l, a stony, loose colluvium with a pale beige to white, very friable, silty matrix. This colluvial unit is similar in appearance to the youngest unit of slope colluvium encountered in all of the 1997 trenches, and is probably mid-late Holocene.

Middle and Upper trench units:

The middle third of the trench (8-20 mH) is only 0.8-1.4 m deep, because at that depth intact Bandelier Tuff was encountered. Four units are defined in this attenuated section of stony scarp colluvium. The youngest unit is a continuation of unit 1, the Holocene colluvium which mantles the entire scarp. Below unit 1 between 10 and 15 mH

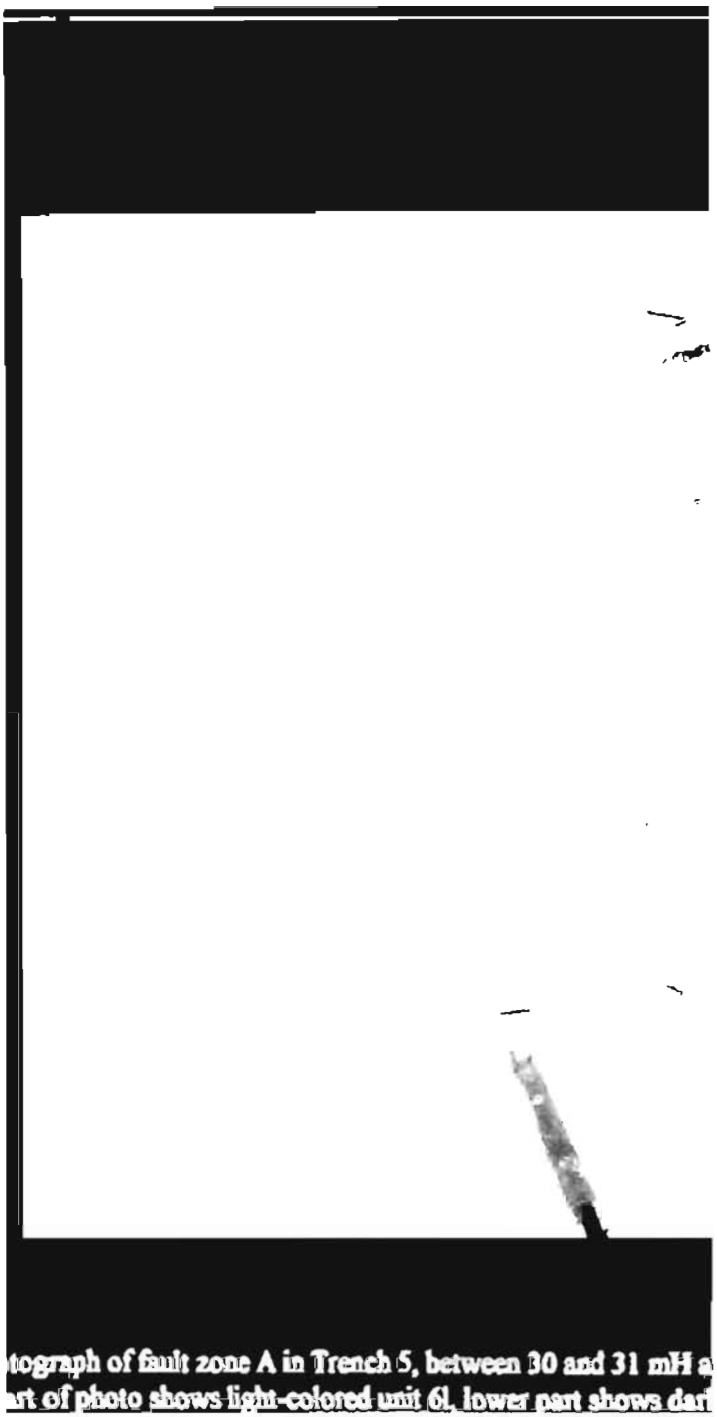

tograph of fault zone A in Trench 5, between 30 and 31 mH a
rt of photo shows light-colored unit 6l, lower part shows dar

is a 20 cm-thick lens of sandy colluvium (unit 2mBC) that has no correlatives farther east of west. This deposit clearly overlies unit 3/buried soil 1, yet it carries a pre-Holocene degree of soil development. The coincidence of this unit with the downthrown block of fault E suggests that the lens filled a topographic swale soon after fault-related warping of parent material 3m.

Unit 3m/3u extends to the trench head with a relatively uniform thickness of 30-80 cm, and is most easily recognized because it carries buried soil 1. However, correlation of parent material units based on the soils they carry invites errors of miscorrelation, In this instance, it is possible that the unit mapped as 3-5mBtb1, in the thinnest part of the mid-trench stratigraphic section, actually contains little if any parent material as young as unit 3 elsewhere. For example, the upslope (free face) contact with colluvial wedge unit 3lbBtb1 appears to cut unit 3-5mBtb1, indicating that parent material 3-5m is older than parent material 3l.

In a similar manner, parent materials 6m/6l are mainly defined by the presence of the strong red clayey buried soil 2. Parent material 6m/6l contains abundant large angular tuff clasts embedded in a sticky dense matrix of red clay. Where unit 6 is >1m thick its buried soil 2 has multiple Bt horizons, the development of which decreases in strength downward. In thinner sections, the red clay matrix shows no vertical change in structure or color, and above the contact with in-situ tuff the clay fills fissures <1 cm thick. The lack of sand or silt in the clay, and its ubiquitous appearance in and out of small fissures, suggest that the clay may have accumulated atop the bedrock contact because it could not translocate any deeper.

Unit 7u is encountered only in a 3 m-wide >4.2 m-deep tension fissure (the "upper pocket") near the head of the trench. Differentiation of subunits in this fissure fill was complicated by faulting and soil formation. However, deposit hardness and secondary clay content decreases from west to east, and the best-preserved faults and fissure fills are on the east margin of the pocket, so we infer that the fissure fill subunits became younger toward the east. In addition, different parts of the fissure fill contain distinctive types of tuff clasts. The floor of the trench and steep sidewalls of the "pockets" are composed of a hard, gray, welded tuff. In contrast, clasts of soft yellow unwelded tuff typify subunits 7u2 and 7u3, whereas clasts of soft white unwelded tuff occur in unit 7u1 and pieces of a coarse-sandy textural, yellow surge bed occur in subunit 7u4. Thus, it appears that the four subunits of 7u are subvertical fissure fills that get younger eastward.

3.8.3 Soils

Trench 5 exposes a weak surface soil and two stronger buried soils. The horizon of maximum development in the surface soil is a weak Bt horizon. PDI of the surface soil ranges from 8.2-9.3-17.3 at the toe of the trench, and 9.1 at the head. By comparison, surface soils at other trenches have PDI= 6.3-9.1. Thus, with the exception of the soil profile at 30.7 mH (PDI= 17.3), the development of this soil is very similar to that of mid-late Holocene surface soils elsewhere.

Buried soil 1 is developed along the entire trench in parent material 3, and is composed of an orange Bt horizon 30-35 cm thick. Cumulative PDI at the base of this soil is 21.2-

30.5 at the trench toe, and 34.8 at the head, the latter value reflecting a thickened solum, over the upper fissure.

Buried soil 2 is mapped along the entire length of the trench. However, that portion between 14 and 20 mH, in the thinnest section of colluvium, may result more from the presence of shallow bedrock impeding downward translocation of clay rather than normal pedogenic processes. The character of buried soil 2 varies markedly along the trench wall, due to complex patterns of faulting-induced erosion and deposition. In the lower pocket, the easternmost section of the soil is developed on a thinned section of distal colluvium/fine slopewash (unit 6-8l) on the upthrown block of fault zone A. This section of colluvium has probably undergone repeated periods of deposition, soil formation, uplift, partial erosion, renewed deposition, and more soil formation. Due to the thinned nature of the stratigraphic section, successive soils tend to "weld" onto lower soils, such as buried soil 1 now welded onto buried soil 2 above fault zone A.

The amount of geologic time represented by the deposition of 5 m of units 6l, 7l, 8l, and 9l in the lower pocket is thus represented east of the fault by only 0.6 m of colluvium. This thin section of colluvium probably contains some components of soil development coeval with deposition of unit 6l-9l, as well as soil development coeval with that of buried soil 2 over the lower pocket. However, due to pervasive welding of soils in the 60 cm-thick zone, separate soils can no longer be distinguished. A similar soil/geomorphic relation across a fault was described by McCalpin (1998, p. 74-83). In addition, erosion has probably periodically stripped off part of the parent materials and their soils on the upthrown block.

Over the eastern 3/4 of the lower pocket, buried soil 2 is composed of an anomalously thin (5-10 cm) but strongly developed red clayey Bt horizon, with sharp upper and lower contacts. This peculiar combination of strong development but small thickness suggests that this Bt horizon has been erosionally truncated. Soil truncation is expected on the upward-protruding corners of domino fault blocks, and admittedly the entire stratigraphy beneath 6Bt1b2 has been deformed by domino faulting. However, we observe no lateral thickening and thinning of this Bt horizon as one might expect on the tops of a series of west-dipping domino fault blocks. Because the Bt horizon is everywhere developed on the "beach sand" of unit 6l, it appears that the tops of the fault blocks were deeply eroded prior to or during the formation of buried soil 2. Following development of buried soil 2, more stripping occurred.

Traced farther west, buried soil 2 passes from unit 6l to units 4l and 5l, at the same time gaining thickness and the distinction of multiple Bt and BC horizons. The thickness increase is probably due to down-to-the-west domino faulting and the creation of additional tectonic "space" west of 24 mH. In contrast, east of 24 mH the same soil was uplifted and truncated by erosion. Individual soil horizons (Bt1b2, Bt2b2, BCb2) are mapped as extending across the facies contact between units 4l and 5l with no interruption. This geometry indicates that either: (1) units 4l and 5l are coeval, or (2) unit 4l might be a younger deposit tectonically downdropped against unit 5l, but buried soil 2 is younger than the downdropping episode. Buried soil 2 is clearly truncated by faulting at fault C.

In the middle portion of the trench buried soil 2 is mapped as developed on parent material 6, but in fact this thin colluvial parent material may include deposits and components of soil formation older than unit 6, as does unit 6-8Btb2 east of the lower pocket. In the upper part of the trench buried soil 2 is clearly developed on a colluvial parent material that is younger than the older three fissure fill subunits (7u1-7u3), but is maybe partly coeval with the youngest subunit (7u4). Although the parent material is numbered 6u, it may be younger than unit 6l, perhaps more coeval with unit 4l and 5l.

McDonald (1999) measured a detailed soil profile at 7.4 mH in the upper pocket and identified the same surface soil and buried soil 1 that we use as map units. His buried soil 2 only includes the Bt horizons of our buried soil 2, and he includes our horizon 6uBCb2 in his buried soil 3. In the lower half of the upper pocket McDonald defines three more buried soils (b4, b5, and b6) all of which are in our fissure fill subunit 7u3. There is certainly subhorizontal stratigraphy within subunit 7u3 but it is unclear whether that stratigraphy represents: (1) multiple blocks of material that fell into the fissure; (2) a single stratified block that fell into the fissure; or (3) strata that were deposited in the fissure as subhorizontal clastic layers by fluvial or colluvial processes. Regardless of the origin of the parent materials, we could not define soil horizons below buried soil 2 well enough to use them as map units in the upper pocket.

At the very head of the trench pockets of massive brown and red clay underlie buried soil 1 and overlie in-situ tuff. Based on clay content and color these clay pockets are assigned to buried soil 2, but they may include clay components of older soils and clay accumulated atop the bedrock contact.

3.8.4 Structure

Seven faults or fault zones are identified in Trench 5. The easternmost **fault zone (A)** bounds the eastern margin of the lower pocket and is a zone up to 1.2 m wide that contains discrete faults as well as zones of diffuse and obscure shearing. The eastern boundary fault (A1) juxtaposes hard gray welded Bandelier Tuff on the upthrown block against old silty fissure fill deposits (unit 6-8l) on the downthrown block. Cumulative vertical displacement of tuff across this fault is greater than 1 m, and probably greater than 2.5 m, because no in-situ tuff was exposed at the base of the lower pocket. The eastern margin of fault zone A juxtaposes unit 6-8l against unit 6l. No faults or shears are traceable into unit 3, so movement on fault zone A predates unit 3.

The fine-grained fissure-fill deposits of the lower pocket are extensively disrupted by a series of master west-dipping normal faults spaced roughly 0.5-1 m apart (**fault zone B**). These master faults define domino-shaped blocks that have rotated counterclockwise (as viewed to the south); a similar style of deformation was exposed in the crestal tension fissure south of Ski Hill Road (Trench 6 of McCalpin, 1998, p.76). Vertical displacement on the master faults ranges from 10-80 cm, in most cases being down-to-the-west, but in some cases down-to-the-east.

On some faults (e.g., the second one west of the "Rat Hole"), the net displacement on the unit 8l/9l contact is greater than that on the overlying unit 7l/8l contact; this difference in displacement could be explained by recurrent fault movement. However, other faults display more confusing geometries, such as the fault that intersects the top of the "Rat

Hole". This fault displaces the unit 8l/9l contact down to the west, in the expected manner of a domino fault, but farther updip it displaces the unit 7l/8l contact in the opposite direction! Part of this reversal in displacement could be explained by the fault branching upward, such that it accomplishes a net down-to-the-west offset of unit 7l across a graben-like zone 1 m wide (between 27-28 mH).

Within the domino blocks defined by the master normal faults are smaller-displacement normal faults, spaced 5-15 cm apart (Figs. 22a, 22b). These faults can be traced only in well-stratified unit 6l, and are not visible in unit 8l, although they are undoubtedly present. These smaller faults typically dip either west, parallel to the 50-60 degree west dip of the master faults, or 70-80 degrees east, forming a conjugate set of normal faults. The line bisecting the subhorizontal axis of this conjugate set dips 10° east, which we take as the approximate attitude of the least principal stress axis and thus the direction of local extension. The small-displacement faults typically are marked by a thin smear of clay in the otherwise clay-poor unit 6l. On the trench log we do not portray all these minor faults.

The westernmost master normal fault juxtaposes fissure fill (unit 8l) against an overlying, west-dipping wall of hard gray welded tuff. Although this fault is labeled as a reverse fault on the log (dictated by bedrock being up on the hanging wall), it must also have elements of a tensional pull-apart. All of the master faults in fault zone B are truncated at the base of unit 3l, so movement predates deposition of unit 3.

The upper bedrock headwall of the lower pocket is defined by a steep east-dipping normal fault that places hard gray welded Bandelier Tuff against scarp-derived colluvial wedges 3l and 4lb (**fault zone C**). This fault zone consists of: (1) a narrow crack fill (unit 3cf) that separates in-situ tuff from the older unit 4l colluvial wedge; and (2) a zone of sheared tuff along the western margin of the younger unit 3lb colluvial wedge. The unit 3cf crack fill is clearly younger than unit 4l, because buried soil 2 does not cross the crack fill. We thus interpret that the older colluvial wedge (unit 4l) has been faulted subsequent to its deposition, whereas the younger wedge (unit 3lb) has not. The shear zone in tuff at the western margin of unit 3lb is a zone of smeared red clay from soil horizon 4lBtb2. We infer that the contact between this smeared clay and the younger colluvial wedge (unit 3lb) is a depositional contact, because we observed no shear fabric in unit 3lb near this contact. Additionally, the top of the unit 3lb colluvial wedge is presently at a higher elevation than in-situ tuff bedrock to the west. It is unlikely that this would be true if there had been a normal faulting event subsequent to the deposition of the younger colluvial wedge. Thus, we believe that unit 3lb was deposited following the latest fault movement on fault zone C. This movement must predate unit 3l, as well as buried soil 1, but post-date buried soil 2.

The middle part of the trench contains numerous abrupt vertical steeps in the top of Bandelier Tuff, some of which coincide with obscure shear zones in the overlying colluvium (**fault zone D**). Typically the vague traces of shearing (oriented clasts, open void spaces) can be seen in unit 6m but not be traced into unit 3m, where they are probably obscured by the development of buried soil 1. Therefore, these small steps probably represent minor faults that have experienced small (cm-scale) vertical displacements over a long period of time, the latest of which predates the formation of buried soil 1.

The upper part of the trench is dominated by the 3-m-wide fissure termed the upper pocket. This fissure is bounded on the east and west by overhanging walls of hard gray welded tuff (Fig. 19b). The fissure fill deposits adjacent to the tuff walls were examined for shear fabric, but none could be found. Instead, at least on the eastern margin it was clear that fissures had opened at the tuff/fissure fill contact, and that the fissure enlarged mainly by east-west extension. Within the fissure itself, the fill is a chaotic mixture of loose clasts, intact stratigraphic blocks with various attitudes, all deformed by a network of steeply east-dipping, anastomosing faults. These faults (not all of which are portrayed on the log) could only be observed if the trench wall was scraped or planed with a sharp metal edge (we typically used the tangs of a claw hammer). However, this scraping technique sufficiently smeared the wall that soil horizons and stratigraphic units could not be distinguished. Therefore, after scraping the wall to map the faults and fractures, we "plucked" the wall with the clay hammers to reveal stratigraphic and soil contacts. Sometimes a given part of the trench wall would be scraped and plucked multiple times until the pattern of strata and faults that resolved began to make geometric sense.

In the vicinity of the upper pocket there are three discrete normal faults that displace either buried soil 2 (**faults E and F1**) or buried soil 1 (**fault G**). Fault E clearly offsets the top of buried soil 2 by 15 cm down-to-the-east. The fault is dashed in the lower part of buried soil 1 (horizon 3uBCb1) and does not appear to displace the 3uBtb1/3uBCb1 horizon contact. However, the anomalous lens-shaped deposit of unit 2mBC appears almost exactly where this fault would project upward, suggesting that the top of buried soil 1 was downwarped ca. 10 cm.

Fault F1 bifurcates and displaces the top of buried soil 2 about 20 cm on two strands, down-to-the-east. Like fault E, the strands of fault F1 seem to penetrate into the lower part of unit 3u, but cannot be traced to the top of buried soil 1. Finally, fault G can be traced vaguely into the lower part of unit 3 (horizon 3BCb1), but does not displace the top of buried soil 1. Thus, all three of these small faults appear to displace the lower part of parent material 3, but do not significantly displace horizons of buried soil 1 developed on unit 3. Only fault E has an indirect suggestion of displacement after the formation of buried soil 1, and that interpretation rests on unit 2mBC filling a small tectonically-created swale, which is uncertain.

3.8.5 Geochronology

Chronologic control comes from one radiocarbon date, two TL dates, and four detailed soil profiles with PDI values. Unfortunately, no El Cajete pumice was observed in the trench.

The sole radiocarbon date yielded an age of 420±50 yBP for the base of unit 1. This date is younger than the 1.4 ka C-14 date from uppermost colluvium in Trench 4, and is considerably younger than PDI-based age estimates of 1.7-3.0 ka from other trenches. The dated charcoal sample was small (0.031 g) and may have been intrusive to the deposit. Soil PDI values (Table 2) suggest that the surface soil represents 2.5-3.1 ka of development time, except at 30.7 m where the inferred age is 8.1 ka. These ages are similar to PDI-based ages from the other trenches.

The PDI-based age of the base of buried soil 1 ranges from 11-19 ka in the lower pocket, to 23 ka in the upper pocket. Despite the 2x range in estimated ages, we believe that buried soil 1 is the same soil all across the trench because we can physically trace it. The base of buried soil 2 yields estimated ages of 25-44 ka in the lower pocket, and 54 ka in the upper pocket. As previously discussed, we feel that buried soil 2 in the lower pocket has been erosionally truncated, so PDI ages there would be minimum estimates. If the PDI of 59.5 and estimated age of 54 ka from the upper pocket are more representative, it appears that buried soil 2 has similar development to the post El-Cajete soil of Reneau and McDonald (1994, Table 2-10).

The PDI-based age estimates for buried soils 3-6 in the upper pocket (88-222 ka) are harder to interpret, because those soils cannot be mapped laterally within the pocket. Taken at face value, they suggest that the fissure began opening at least 222 ka because sediments of that age are preserved at the bottom of the fissure.

3.8.6 Paleoseismic Reconstruction

3.8.6.1 The Most Recent Event

The most recent faulting event on faults E, F1, and G disrupts the lower part of parent material 3, but not the horizon boundaries of buried soil 1. Thus, the faulting is somewhat younger than the deposition of parent material 3, but older than the burial of buried soil 1 by unit 1. The former date is approximated by the inception of buried soil 1 development at 11-23 ka, while the latter date is approximated by the inception of surface soil development at 2.5-3.0 ka.

The total displacement during this event is difficult to measure on the top of buried soil 2, but that displacement may result from both the most recent and penultimate events. However, the only firm evidence for differential displacement of buried soil 1 and buried soil 2 is the 10-15 cm thickness of unit 2mBC (which can only be indirectly attributed to warping), and the 15 cm displacement of buried soil 2 on fault E. These two values are sufficiently similar that one could argue that buried soil 2 has only been displaced by a single event, with 15 cm of displacement on fault E, 20 cm of displacement on fault F1, and negligible displacement (cracking?) on fault G.

3.8.6.2 The Penultimate Event

In the lower pocket buried soil 2 (age 25-42 ka by PDI; Table 2) is truncated at fault C, and it is overlain by unit 3lb upon which buried soil 1 (age 11-19 ka by PDI) is developed. Thus faulting is crudely bracketed between ca. 11-19 ka and 25-42 ka. The faulting event here predates the deposition of the colluvial wedge (unit 3lb). Thus, if parent material 3lb is correlative with parent material 3u, then this faulting event must be older than the event that faulted unit 3u, because this (PE) event predates unit 3lb, whereas the MRE post-dates unit 3u. However, both the PE and MRE post-date buried soil 2 in their respective parts of the trench. Given this close stratigraphic coincidence, we must consider the possibility that the PE and MRE as defined could be the same event. This coincidence could be explained if: (1) unit 3u was slightly older than unit 3lb; and (2) the dashed parts of faults E, F1, and G in unit 3 are post-faulting cracks rather than true

faults. This latter hypothesis would explain why horizons of buried soil 1 are not offset across the dashed lines.

The displacement on fault C during this event must be at least 1.1 m, which is the vertical extent of the red clay from buried soil 2 that was smeared along the fault zone. The 1.4 m maximum thickness of colluvial wedge unit 3lb implies at least a 1.4 m-high free face along fault C, while the "rule of thumb" that free face height= 2x colluvial thickness would imply an initial free face height of 2.8 m. The latter is a good maximum estimate of displacement in this event.

3.8.6.3 Earlier Events

The latest movement on the domino faults of fault zone B predates buried soil 2, and may have created the tectonic space into which the older colluvial wedge (unit 4l) accumulated. From soil PDI we can estimate that buried soil 2 began forming ca. 54 ka, so this movement must predate that age.

In the preceeding discussion I have assumed that the displacement events observed in the trench resulted from tectonic surface rupture. However, the downslope end of the trench does rest upon a topographic bench that I labelled in 1996 (Fig. 18) a "possible slide block". My present interpretation is that the topographic bench is a structural block bounded by deeply-penetrating normal faults, rather than a block back-rotated by relatively shallow slumping (i.e., slumping on a failure plane that "daylights" near the base of the present 40-m-high scarp). This interpretation is based on the linearity of the landforms bounding the bench, and their continuation north of the deeply-incised gully, far north of the reasonable limits of a shallow slump. However, given the height and steepness of the 40-m-high scarp downslope of Trench 5, and the extensional nature of domino-style faulting, it is possible that some or all of the extensional faulting observed in Trench 5 represents eastward toppling. Such toppling could be caused by either meteorologic triggers, shaking from earthquakes on the Pajarito fault, or shaking from more distant earthquakes. There is no rigorous way to test whether the observed near-surface normal faulting was caused by tectonic surface rupture as opposed to toppling, based on a shallow trench exposure such as Trench 5. Such a test would require tracing faults and their offsets to a depth of at least 40 m, to see if the extensional component of faulting died out at a elevation equal to that of the scarp base (as should occur for toppling), or whether it stayed constant. However, I do not know of any geophysical techniques that could trace offsets in the Bandelier Tuff to that depth. Thus, my preferred interpretation is that most of the vertical displacement observed in Trench 5 represents tectonic surface rupture, but it may include a lesser component (mainly of east-west extension) due to toppling.

3.9 Trench 6

Trench 6 is located approximately 260 m northwest of the abandoned guard building at the intersection of West Jemez Road and NM Highway 4 (also known as the "Back Gate", see Fig. 2b). The trench is 13m long and up to 3.5 m deep.

3.9.1 Geomorphology:

The Pajarito fault at the latitude of NM Highway 4 is composed of a single, 60 m-high north-trending fault scarp (Fig. 23). The portion of this scarp north of Highway 4 was mapped by McCalpin (1997, Plate 1) at a scale of 1:1200. The lower part of the scarp NW of the Back Gate is composed of Bandelier Tuff dipping 5°-10° east. This tuff is onlapped by an apron of bouldery colluvium and alluvial fans. Most of the fan surface (unit afi in Fig. 23) stands 2.5-6 m above the incised drainages, and is entirely mantled by El Cajete pumice (ce in Fig. 23) east and west of the Back Gate. Modern alluvium (unit a1 in Fig. 23) exists in the incised drainages.

North of Pajarito Canyon the large scarps of the Pajarito fault have a normal fault zone at the base of the topographic scarp, termed the basal fault zone by McCalpin (1997). Normally this fault zone is not well exposed, due to the minimal incision of local drainages into the colluvial apron. However, upslope of Trench 6 the roadside drainage along Highway 4 is diverted into a swale that trends directly down the scarp face. The augmented highway runoff in this swale has eroded all the loose colluvium and regolith off the tuff between the highway and 7650 ft elevation, making a broad channel roughly 30 cm deep. At 7650 ft the bottom of the swale drops 3 m vertically in a series of vertical steps; this area must be a series of waterfalls during runoff events.

The vertical steps of tuff in the waterfall area are planar and trend N10E and dip 60° E, and span a horizontal distance of ca. 5 m. East of the vertical steps tuff is no longer exposed in the bottom of the incised gullies, despite their depth of over 6 m. Thus, the planar nature of the steps, their coincidence with the tuff/fan contact, and the absence of tuff exposures to the east suggest that the steps represent the basal fault zone at this latitude.

North of the waterfall the lower scarp face is composed of two 3-5 m-high parallel steep scarplets in intact Bandelier Tuff, separated by a 30 m-wide bench covered by slabby colluvium. This colluvium contains abundant large slabs of tuff that dip 35°-55° E and may represent a fissure fill or toppled block (termed megablock colluvium by McCalpin, 1997; cm on Fig. 24).

Trench 6 was excavated directly south of the waterfall area, and was meant to intersect the basal fault zone at the bedrock/alluvial fan contact. This trench was hoped to reveal whether the El Cajete pumice had been faulted on the basal fault zone.

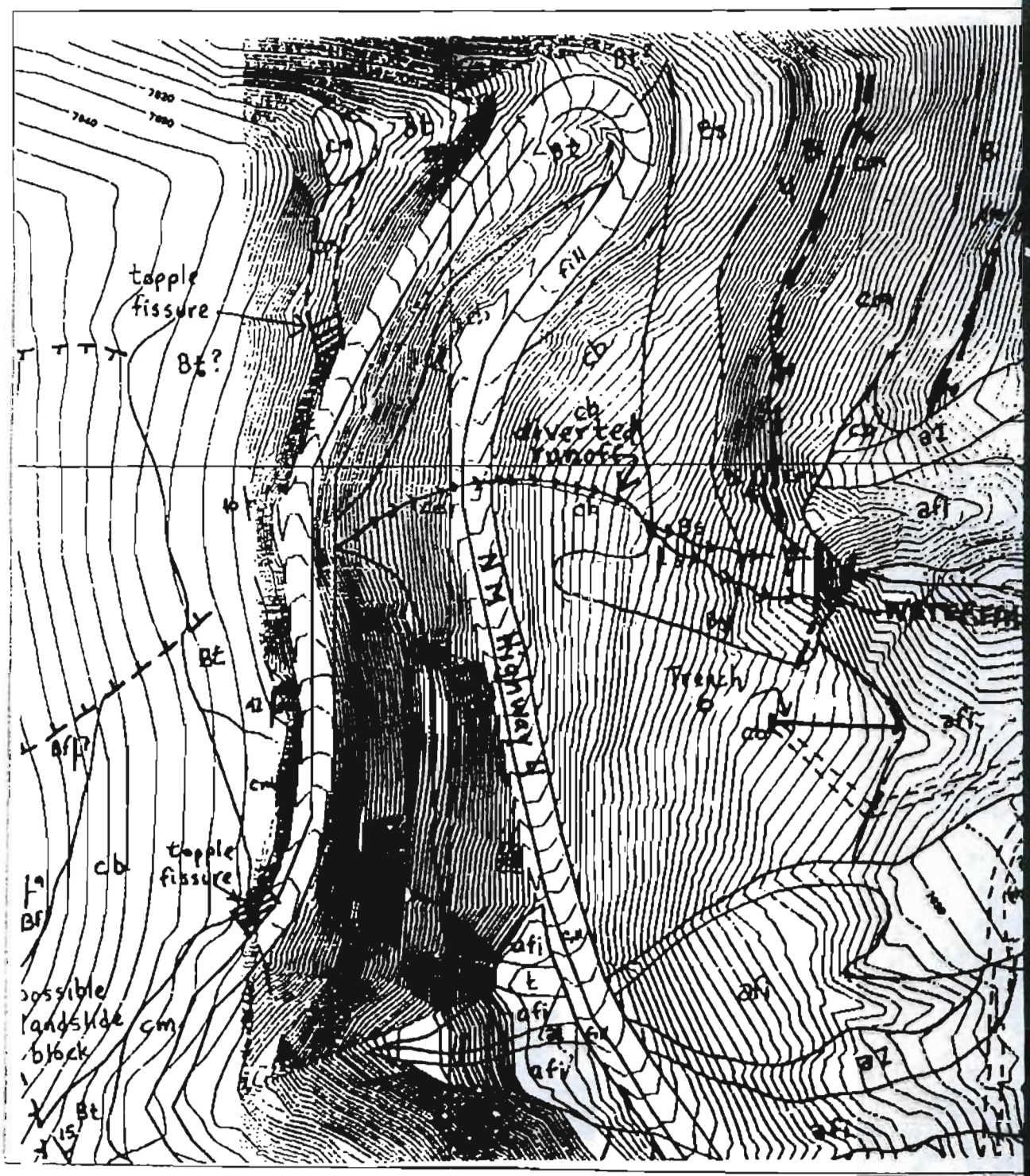

Fig. 23. Geologic map of the main Pajarito fault scarp where NM Highway 4 ascends the scarp. Tren
From McCalpin (1997, Plate 1). Contour interval = 2 ft on eastern 3/4 of the map, 10 ft elsewhere..

EXPLANATION OF MAP UNITS

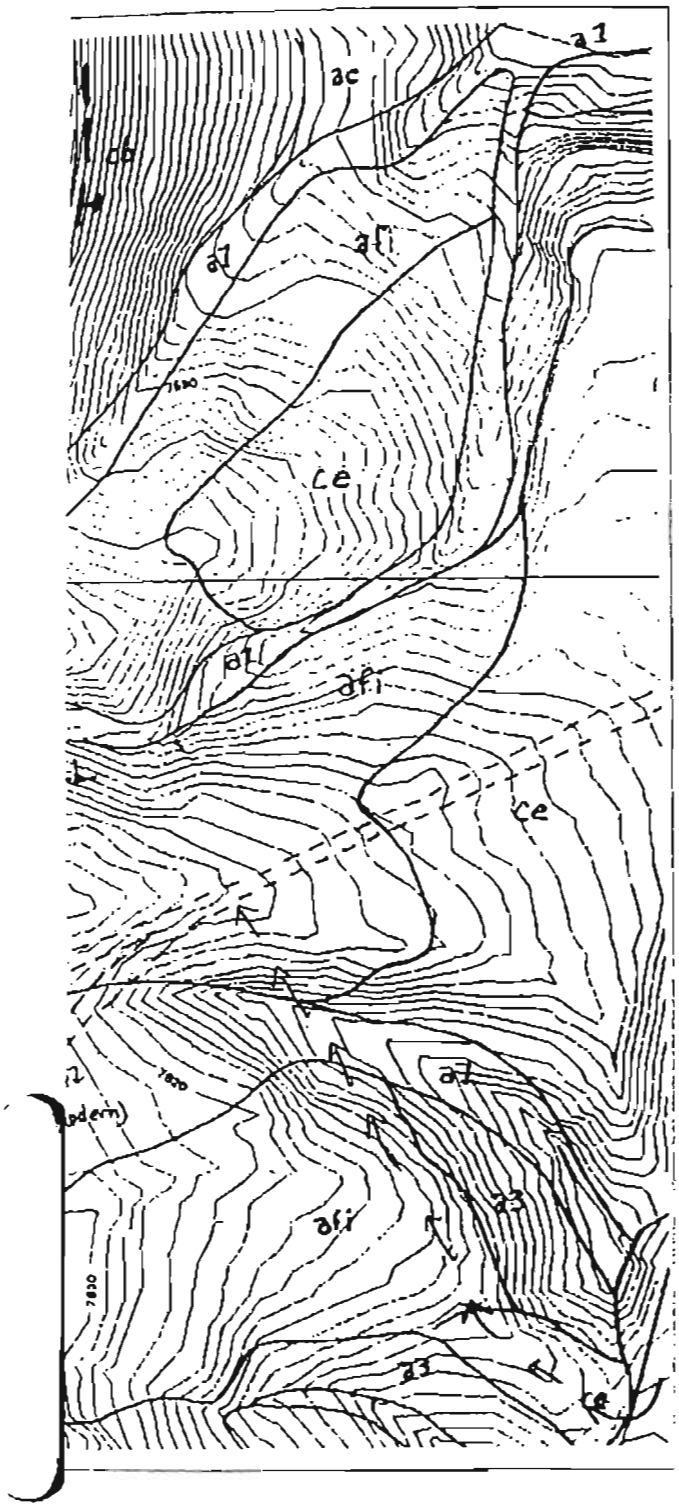

		Correlative Units of Reneau (1996)
	Holocene	
t	talus	
a1	modern alluvium	*Qal*
	Holocene and Late Pleistocene	
ac	young alluvium and colluvium	*Qfy*
	Late Pleistocene	
ce	El Cajete pumice	*Qec*
	Mid-Late Pleistocene	
cb	bouldery colluvium	*Qc*
cm	megablock colluvium	*Qc*
afi	intermediate-age alluvial fan	*Qfi*
a3	old alluvium	*Qfo*
	Early Pleistocene	
Bs	slabs of Bandelier Tuff	*Qbt*
Bt	toppled Bandelier Tuff	*Qbt*
Bi	in-situ Bandelier Tuff	*Qbt*

Symbols

topographic scarp

inferred fault at base of scarp

exposed fault in Bandelier Tuff

landslide head scarp (dashed where obscure)

direction of slide movement

ch 6 is at right center.

200 ft

61 m

N

3.9.2 Stratigraphy:

Due to the short length of Trench 6 and the shallow depth to bedrock, only a thin stratigraphic section of colluvium and fissure fill was exposed (Fig. 24). The surface colluvium (unit 1) is the same loose, friable colluvium with the pale beige-white silt matrix as exposed at the surface of most other 1997 and 1998 trenches. Underlying this colluvium is a series of poorly-consolidated stony deposits with a friable, pinkish gray to light reddish brown matrix. The uppermost unit (2a) is an older Holocene colluvium containing clasts weakly imbricated downslope. Unit 2b is better sorted, and in places (e.g. east of 2.5 mH) has a basal lag gravel that is clearly channeled into underlying deposits. This deposit represents a transition between overlying slopewash and underlying fluvial deposition on the colluvial apron. Unit 2c is similar to unit 2a, but underlies unit 2b in the western 1/3 of the trench.

Unit 3 includes a small colluvial wedge at 8-9 mH (unit 3a) and a more lenticular colluvial deposit with a basal stone line in the eastern 1/3 of the trench (unit 3Btb1). Both of these subunits overlie unit 4, which has been strongly affected by soil formation. In the western 2/3 of the trench where the depth to bedrock is only 0.5-1.5 m, unit 4?Btb is a stony colluvium with a matrix of red clay. In the eastern 1/3 of the trench unit 4 is a nearly clast-free fissure fill with a sandy silt texture. The few clasts have a downslope orientation, so this fissure fill was probably deposited by sheetwash coming down the scarp.

Two older fissure fill units (5 and 6) are similar in texture and inferred origin to unit 4, but have stronger soil development. Unit 6 consists of two facies, unit 6a (massive, clast-poor distal colluvium) and unit 6b (clast-rich proximal colluvium derived from a fault free face).

Bandelier Tuff is exposed along the entire length of the trench, but the lithology in the deep fissure (eastern 1/3 of the trench) is different than the tuff farther west. The lowest 1.5 m of the trench walls in the deep fissure expose a soft, unwelded, light beige weathered tuff. This tuff is so soft that, during excavation of this part of the trench, we thought the backhoe was still digging through unconsolidated fissure fill. The tuff contains abundant, distinctive elliptical inclusions of gray-purple pumice that range from 0.5-2 cm in diameter. The lithology of this tuff is similar to that of the tuff exposed at the top of the Pajarito fault scarp north of Highway 4 (unit F of Rogers, 1995; unit 5 of Reneau and Broxton, 1995).

In contrast, the western 2/3 of the trench exposes a hard gray welded variety of tuff, similar to that exposed at the ground surface on the lower scarp face. This lithology resembles unit E of Rodgers, or unit 4 of Reneau and Broxton (1995).

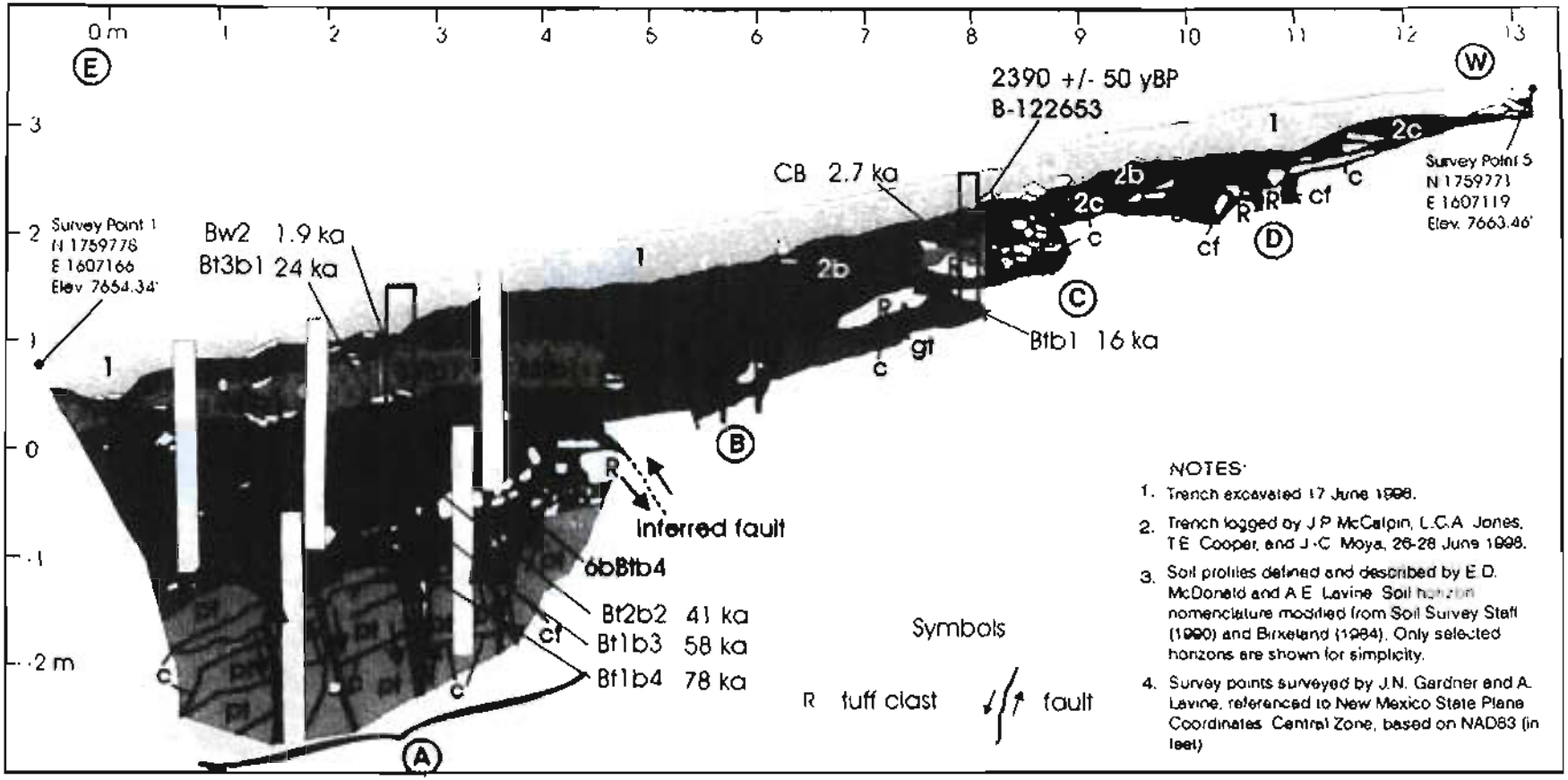

NOTES:

1. Trench excavated 17 June 1998.
2. Trench logged by J.P. McCalpin, L.C.A. Jones, T.E. Cooper, and J.-C. Moya, 26-28 June 1998.
3. Soil profiles defined and described by E.D. McDonald and A.E. Lavine. Soil horizon nomenclature modified from Soil Survey Staff (1990) and Birkeland (1984). Only selected horizons are shown for simplicity.
4. Survey points surveyed by J.N. Gardner and A. Lavine, referenced to New Mexico State Plane Coordinates, Central Zone, based on NAD83 (in feet).

Symbols

R tuff clast

fault

1	light gray gravelly sand; Holocene SLOPEWASH COLLUVIUM
2b	pinkish gray stratified gravelly sand; older Holocene SLOPEWASH
2a	light reddish brown massive gravelly sand, older Holocene COLLUVIUM
2c	similar to unit 2a, but older than unit 2b
3a	pale brown sandy gravel, COLLUVIAL WEDGE
3Btb1	red textural B horizon developed on gravelly COLLUVIUM
4Btb2	red textural B horizon developed on silty fissure fill
4?Btb	red textural B horizon developed on stony colluvium
5Btb3	strong red textural B horizon developed on silty fissure fill
6aBtb4	red textural B horizon developed on distal colluvium
6bBtb4	textural B horizon developed on proximal colluvium
gt	hard gray welded Bandelier Tuff, Unit 4 of Reneau and Broxton, 1995
cf	crack fill composed of red clay
xt	shattered, weathered tuff containing pumice clasts
pl	light beige weathered tuff containing gray-purple pumice clasts; Unit 5 of Reneau and Broxton, 1995
c	thin seams of red-brown clay

SCALE

0 1 2 meters

GEO-HAZ Consulting, Inc.

LOS ALAMOS NATIONAL LABORATORY
PAJARITO FAULT, 7 SCATTERED TRENCHES, SUMMER 1998

TRENCH 6-South Wall

DATE Dec 1998	FIGURE 24
DWG. NO. F:\GEOHAZ\LANL\PAJARITO98\TRENCH6.CDR	

3.9.3 Soils:

The younger units that span the length of the trench (units 1 and 2) contain a surface soil with an A/Bw or A/CB profile (Table 2). PDI of this soil is 6.8-8.4, which is similar to that of the surface soils in the other six trenches. In the deep fissure, fissure fill units 3, 4, 5, and 6 contain buried soils 1, 2, 3, and 4, respectively. Buried soils 1 and 2 are thick enough to contain multiple B horizons, whereas thinner buried soils 3 and 4 are only defined as a single Bt horizon. Cumulative PDI at the base of buried soils 1 through 4 is 35.0, 49.7, 62.8, and 76.0, respectively. By comparison, the post-El Cajete soil of Reneau and McDonald (1994, Table 2-10) has a PDI of 69.4. Accordingly, the bases of buried soils 3 and 4 should be approximately coeval with the El Cajete pumice. However, no El Cajete pumice was found in the trench, despite its presence on the same intermediate-age fan surface only 50 m farther east.

3.9.4 Structure:

Trench 6 exposes four deformation zones, the largest of which (zone A) has created the deep fissure in the eastern 1/3 of the trench. This zone is defined by blocks of soft tuff in the lowest 1.5 m of the trench, which have been tilted to a 20°-25° east dip, and faulted by vertical to steeply west-dipping normal faults. The blocks between the faults are 0.5-0.8 m wide and resemble the series of east-tilted domino blocks in 1998 Trench 5 and 1997 Trench 6. None of the block-bounding faults can be traced into the overlying fissure fill deposits, and none of the soil horizon boundaries appear to be displaced.

The western margin of the deep fissure, which separates the deep from the shallow part of the trench, is a complex structural zone. As shown on the trench log (Fig. 24) a block of gray welded tuff (gt) overlies the soft pumice-bearing tuff (pt). However, the small area of gt mapped on this headwall is probably not in-situ. The area consists of angular blocks of gray tuff separated by seams of red clay 2-10 cm thick. In some cases a weak stratification can be traced from one clast to the adjacent one, indicating that the deposit was more a brecciated zone of tuff with clay infill, than a colluvial deposit. However, our correlation of the soft beige tuff (unit pt) with Reneau and Broxton's (1995) Unit 5 and the hard gray tuff (unit gt) with their underlying unit, Unit 4, requires a fault with considerable vertical displacement at the western margin of the fissure. For example, the contact between Reneau and Broxton's Units 4 and 5 is mapped at the crest of the fault scarp approximately 60 m above Trench 6. In order to downfault Unit 5 to its observed position in Trench 6, a cumulative vertical displacement of 60 m must occur between the western margin of the fissure and the scarp crest; however, much of this could be accommodated by faults on the scarp face itself. No large-displacement fault was exposed in the trench headwall at 4-5 mH, despite 1/2 day of hand-digging in that area. However, based on analogy with 1998 Trench 5 and 1997 Trench 6, the zone that separates in-situ tuff and east-toppled domino blocks is mainly a zone of horizontal extension, into which blocks of exotic material fall. In such a pull-apart zone it would be unlikely to encounter a well-defined shear plane.

A pull-apart origin for the western margin of the fissure is supported by the style of deformation in fault zone B, which looks like an extensional fissure or graben. Elsewhere along the Pajarito fault such tensional openings are observed at the ground surface

upslope of fault and topple zones, and become wider in aperture as the topple zone is approached (see photograph in McCalpin, 1997, p. 34).

Fault zone C coincides with a 0.5 m-high vertical step in the bedrock trench floor at ca. 9 mH. This slightly overhanging step bounds the western edge of an anomalous pocket of imbricated clasts, which is interpreted as a colluvial wedge (unit 3a). The top of the wedge coincides with unit 2c on the upthrown side of the fault, indicating that unit 2c is also faulted. The fault can be discontinuously traced into unit 2b, but does not displace the top of that unit.

Fault zone D is another pull-apart or graben structure filled with a combination of tuff blocks and red clay. This zone does not disrupt unit 2c.

3.9.5 Geochronology

Dating control in Trench 6 comes from two detailed soil profiles (Table 2) and a single radiocarbon date (Table 3). The 2.6 m-deep soil profile in the deep fissure contains the surface soil and four buried soils, with PDI age estimates of 1.9, 24, 41, 58, and 78 ka, respectively. The oldest soil, dated at 78 ka, rests directly atop Bandelier Tuff which is 1.1 Ma. Therefore, either there was a long hiatus of nondeposition and/or erosion between 1.1 Ma and the beginning of fissure-fill deposition at 78 ka, or the age estimate of 78 ka for the cumulative soil formation does not include long time periods in which deposition or erosion were dominant. This same age relation occurred at every trench excavated in 1997 that exposed Bandelier Tuff on the downthrown fault block, i.e., the cumulative age of soil formation in sediments atop the tuff fell far short of 1.1 Ma. In some 1997 trenches the discrepancy was attributed to periods of erosion in the fissure/graben fill section, even though distinctive unconformities were hard to see due to the strong soil development. In Trench 6 at least two units (2b, 3Btb1) are clearly erosionally channelled into lower units, so unconformities do exist here.

The second soil profile in the upper part of the trench describes an attenuated (1.3 m thick) section of stony colluvium atop tuff. Cumulative PDI of the soils lying atop the tuff are only 16 ka, indicating that this location has generally been a site of erosion rather than deposition and soil formation. The base of the surface soil dates at ca. 2.7 ka, and charcoal from the middle of the surface soil dates at 2390 +/- 50 yr BP.

3.9.6 Paleoseismic Interpretation

3.9.6.1 Most Recent Event

The most recent event in Trench 6 occurred on fault C, which faulted unit 2c and led to deposition of (at least the upper part of) colluvial wedge unit 3a. However, if unit 2c predated the faulting event it should also be found on the downthrown block east of fault zone C, but it is not mapped there. Instead, on the downthrown block the colluvial wedge overlies unit 4?Btb. Thus, there are two timing scenarios for this faulting event. The first is that, prior to the event, unit 4?Btb comprised the ground surface and was faulted. Concurrent with deposition of the colluvial wedge, 4?Btb was stripped off the upthrown block. While this scenario explains the absence of 4?Btb on the upthrown block, it does

not explain how the upper part of the colluvial wedge is now juxtaposed against unit 2c across the fault. The second scenario is that the lower part of the colluvial wedge is equivalent to unit 2c, and the upper part is the true colluvial wedge. However, even this scenario requires that either unit 4?Btb was earlier stripped off the upthrown block, or it was never deposited there. If a faulting event post-dated formation of soil 4?Btb, the colluvial wedge would be composed of recycled B horizon material, rather than the loose, pale brown sandy gravel it is composed of.

In summary, the sequence of events that best explains the geometric relations across fault zone C is: (1) faulting prior to deposition of unit 4?Btb that downdropped the block east of fault C; this created the accommodation space in which unit 4 colluvium was deposited. No colluvium then existed west of fault C; (2) deposition of unit 2c as a lenticular wedge that pinched out at ca. 7.5 mH; this wedge makes up the lower half of unit 3a; (3) faulting of unit 2c and deposition of the upper half of unit 3a as a scarp-derived colluvial wedge, derived from erosion of part of unit 2c from the upthrown block; (4) deposition of unit 2b, which is bracketed by a PDI date on the base of horizon CB of 2.7 ka (range 2.1-3.4 ka) and by a radiocarbon date directly above unit 2b of 2390± 50 yrBP (C-14 years). The fracture mapped as extending up into unit 2b has no vertical displacement, and is interpreted as a growth crack above the fault. The MRE is thus bracketed between about 2.4-2.7 ka and 16 ka (the PDI age estimate for unit 4?Btb).

Earlier faulting events created only ambiguous stratigraphic evidence with poor dating control. For example, the western boundary fault of the deep fissure truncates unit 5Btb3, and juxtaposes two different facies of unit 4 (the finer 4Btb2 vs. the coarser 4?Btb). The western edge of unit 3Btb1 is also juxtaposed against unit 4?Btb, but this could be a steep depositonal contact. The base of unit 2b is clearly eroded into the fault plane. Thus this faulting event is younger than unit 5Btb3 (dated at 41 ka by PDI) and older than unit 2b (dated at 2.7 ka at PDI). This age range is so broad that it does not provide a very useful age constraint; in fact, with only the constraint that the event predates unit 2b, it could be the same event observed on fault C.

Faulting of the domino blocks must be very old, given that the contact between soils b3 (58 ka by PDI) and b4 (78 ka by PDI) is not displaced. Unit 6b is clearly the proximal colluvial wedge deposited soon after faulting, and unit 6a thins drastically over the easternmost domino block (Fig. 24). The present geometries of both units 6a and 6b could have resulted from a single faulting event, in which movement of the easternmost (exposed) domino block creates a 0.4 m-high upslope-facing scarp. This scarp was then buried by the accumulating distal colluvium of unit 6a. Although this is the simplest explanation, it is also possible that displacement on this domino block post-dated unit 6a, and that half of the thickness of unit 6a was then stripped from atop the domino before deposition of parent material 5. We prefer the scenario of one faulting event before unit 6a because: (1) there is only one proximal colluvial wedge in the fissure; and (2) the thinned section of unit 6a atop the eastern domino block shows no shear fabric. Therefore, the single faulting event would predate units 6a/6b (ca. 78 ka) and post-date the Bandelier Tuff.

Neither units 4 or 5 in the fissure fill contain a proximal colluvial facies, so it is not clear that they accumulated after a faulting event. For example, unit 5 is planar and of

uniform thickness and texture, unlike units 6a/6b. This geometry and sedimentology suggest that unit 5 was deposited as a blanket in the fissure by slopewash or rillwash processes. Unit 5 could be the only preserved remnant of a colluvial blanket that mantled the entire scarp face, and is only preserved in the fissure due to later down-dropping.

Unit 4 has a peculiar geometry for a fissure fill, in that it thickens to the east. This thickening suggests that unit 4 is buttressed against an upslope-facing domino fault block of tuff somewhere east of the trench. If true, this structural relation would suggest that the fissure was deepened and a large buttress formed downslope, sometime after the formation of soil 5Btb3, and unit 4 filled in this structural "hole". Such a faulting event would explain the truncation of soil 5Btb3 on the western edge of the fissure. Units younger than 4 (3Btb1, 2a) in the fissure are clearly fluvial channel deposits that cannot be directly related to faulting.

In summary, there is evidence for at least three faulting events in Trench 6. The youngest event immediately predates unit 2b and postdates buried soil 1, bracketing it about 2.7-16 ka. The penultimate event predates unit 4 and postdates unit 5 bracketing it between 41-58 ka. The earliest event is older than unit 6a/6b (78 ka) and younger than 1.2 Ma.

4. INTERPRETATION

4.1 Timing of the Most Recent Faulting Events

The MRE in Trenches 4, 5, and 6 predates the surface soil and youngest stratigraphic unit (typically colluvium) and post-dates the youngest of the buried soils, or at least the parent material that hosts that soil. The age constraints are shown graphically in Fig. 25. The cumulative PDI value for the surface soil is assumed to closely approximate the total time since initial deposition of the soil parent material, there being no evidence for unconformities or erosion within that parent material. Thus, PDI-based age estimates on the surface soils form minimum age constraints for the MRE. Where radiocarbon dates were obtained from the surface soil they are in good agreement with soil PDI dates (e.g. Trench 4@ 5.4 mH, PDI= 1.3-2.1 ka, C-14= 216-620 cal yrBP, 736-1170 cal yrBP; Trench 6@ 8 mH, PDI= 2.1-4.3 ka, C-14= 1738-2269 cal yrBP).

The MRE in Trench 4 (event Z_4?) deformed the colluvium at the head of the trench, but due to the penetrative compressional style of deformation, it is unkown whether this "event" refects an earthquake, an earthquake-induced landslide, or a nonseismic landslide. Regardless of origin, this deformation event is younger than the deformed beds of unit 1cBw (dated by small pieces of intrusive? charcoal as 840 +/- 50 C-14 yr BP) but older than the surface soil (age 1.7-3 ka by PDI). On Fig. 25 the 840 yr date is assumed to be erroneously young and is not used as the maximum bracketing age.

The MRE in Trench 5 (event Z5) is similarly bracketed between the age of the surface soil (2.4-3.7 ka) and that of buried soil 1 (19-30 ka). The MRE in Trench 6 (event Z6) occurred before 2.1-3.4 ka (age of the surface soil) and after 16-24 ka (age of buried soil 1).

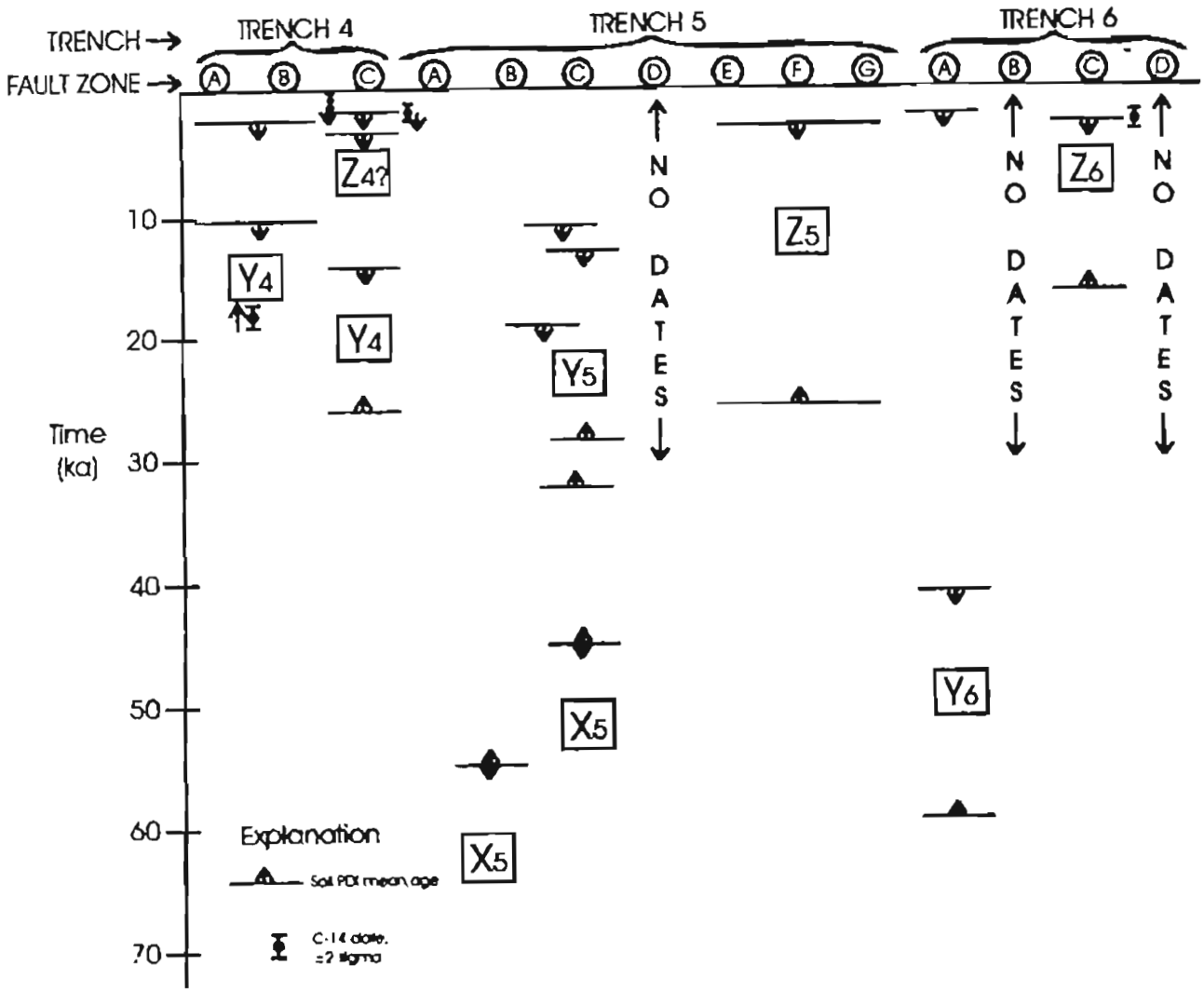

Fig. 25. Space-time diagram of faulting events in Trenches 4, 5, and 6.

All of the limiting dates cited above overlap in the age range 3.7-11 ka. This age span is suffuciently large that the MREs in Trenches 4, 5, and 6 could be different events, although their age ranges do overlap. More importantly, the age range is older than that of the MRE from 1997 trenches 3, 4, 7, and 7a. In those trenches the MRE was bracketed by 17 radiocarbon dates and four PDI age estimates (McCalpin, 1998, p.102) between about 1260 and 2290 cal yrBP. In contrast, the MREs in 1998 trenches 4-6 are bracketed by only 3 radiocarbon dates but by 10 PDI age estimates (Fig. 25). The minimum age constraints from PDI in a given soil tend to be older than the radiocarbon samples from that soil, particularly when the latter are converted to calender years. For example, in Trench 4@ 5.4 mH the beginning of surface soil formation is dated at 1.3-2.1 ka, whereas charcoal from near the base of the soil dates at 840± 50 C-14, and 276-620 cal. yrBP

In trench 4@ 6.5 mH, the beginning of surface soil formation is dated at 2.4-3.8 ka, whereas charcoal from near the base of the soil dates at 1420±50 C-14 yrBP, or 736-1170 cal. yrBP. A somewhat similar situation occurs in Trench 6@ 8 mH, where the surface soil has a PDI age of 2.1-3.4 ka, compared to a radiocarbon age of 2370± 50 C-14 yrBP, or 1738-2269 cal. yrBP.

Overall, the calendar-corrected radiocarbon dates from 1998 trenches tend to be many hundred to a few thousand years younger than the PDI estimates for beginning of soil formation (680-1824 years younger in T4@ 5.4 mH; 1230-3064 years younger in T4@ 6.5 mH; 362-1662 years younger in T6@ 8 mH). Thus, if we compare the closest minimum age constraints on the MRE from the 1997 trenches (1260-2310 cal. yr. BP) with those from the 1998 trenches (471-1972 cal. yrBP) using only calendar-corrected C-14 dates, we see the age range is similar.

We were fortunate in the 1997 trenches to expose faulted Holocene, carbon-bearing deposits in Trenches 4, 7, and 7A, whereas in Trench 3 the youngest faulted unit was a buried soil that began developing ca. 20 ka. The 1998 trenches are like 97 Trench 3 in this respect, that the maximum age constraint on the MRE is the time at which the youngest (faulted) buried soil began to develop, rather than the more preferable times of: (1) when it ceased to develop after faulting and burial; or (2) when the uppermost faulted parent material was deposited. Thus, the maximum age constraints in Fig. 25 are not as closely limiting as the minimum age constraints.

Given this asymmetry in age constraints from the 1998 trenches, it is permissable that the MRE in Trenches 4-6 is the same Holocene event as at the 1997 Trenches 3, 4, 7, and 7a.

4.2 Recurrence Intervals Between Paleoearthquakes

Only a single recurrence interval can be calculated for each trench, based on the time between the MRE and penultimate event (PE). In Trench 4, the PE is bracketed by soil PDI dates of 8-13 ka (mean 11 ka) and a radiocarbon date of 29.5 ka. The time span between this event and the MRE (1.4-3 ka to 11-17 ka) could be as long as 27.5 ka, as short as 0 ka, with a mean value of ca. 12 ka (MRE= 8.1 ka, PE= 20 ka). Note, however, that the MRE at Trench 4 may not represent a tectonic event. The span between the minimum limiting ages for each event is 5 ka (8ka minus 3 ka) to 11.6 ka (13 ka minus 1.4 ka), which is our preferred range for recurrence at this site.

In Trench 5 all we know with certainty is that the PE on fault C is younger than buried soil 2, which began forming between 20 and 55 ka. and older than buried soil 1, which began forming between 8.7 and 24 ka (Table 2). Note that the age ranges for buried soils 1 and 2 based on three different soil profiles overlap, although of course they do not overlap in any one profile. The MRE is slightly older than the surface soil (2.4-3.7 ka) and much younger than the inception of buried soil 1 formation (8.7-24 ka.). The PE, in contrast, is best contrained by PDI age estimates from the profile @ 30.7 mH, which is not a fault zone (as occurs at 31.6 mH) or on a stripped upthrown fault block (as occurs at 32.7 mH). At 30.7 mH the PE is bracketed between 15-24 ka and 25-40 ka, with the former constituting the closer constraint. Thus, although the time between the MRE and PE could conceivably be as short as 0 ka, or as long as 37.6 ka (40 ka minus 2.4 ka), given the close minumum age constraints on both events as 2.4-3.7 ka and 15-24 ka respectively, a more likely duration for the interval is in the range of 11.3-21.6 ka.

In Trench 6, the MRE is dated between 2.1-3.4 ka and 13-20 ka (closer to the former), and the PE is bracketed by soils dated at 32-51 ka and 46-74 ka (note the age overlap). The time span between the minimum age constraints for the MRE and PE thus ranges from 28.6 ka (32 ka minus 3.4 ka) to 48.9 ka (51 ka minus 2.1 ka).

In summary, the best estimates of the length of time between the MRE and PE based on the closer minimum limiting ages, range from 5-11.6 ka in Trench 4, 11.3-21.6 ka in Trench 5, and 28.6-48.9 ka in Trench 6. These values relfect the variablility among the size and activity of structures at the three trench sites. At Trench 4, a 6 m-high scarp has been created by deforming strata all most all of which are younger than the El Cajete pumice. Thus, the short recurrence estimates of 5-11 ka suggest that the Western Splay fault has been quite active in the latest Quaternary. In contrast, the fault at Trench 6 has not even created a scarp at the bedrock/alluvium contact and since 1.2 Ma has only managed to create a fissure with 2.5 m of fill in it. Given the poor geomorphic expression of this fault (it was identified only due to erosion by artificial runoff from Highway 4) it appears that it is not a major structural element of the fault zone, and thus the longer estimated recurrences (28.6-48.9 ka) may not record every faulting event on the PFZ.

Trench 5 forms an intermediate case, in that the fault has accumulated 10 m of vertical displacement on the Bandelier Tuff, but much of that displacement appears to be old. For example, most of the net vertical displacement accumulated before the formation of buried soil 2 (32-54 ka), with only minor displacements (e.g. 15-20 cm on faults E, F1, and G) since that time. The impression one receives is that this fault was a major active structure prior to (and during) the deposition of 4 m-thick unit 2l in the "lower pocket", and to a lesser degree later when the domino faults were active. However, even this latter period predates buried soil 2. Subsequent to formation of buried soil 2 the domino faults have ceased movement, and the only younger fault movements have occurred on fault zone C. A similar evolution has affected the "upper pocket", where prior to buried soil 2 a deep fissure formed by recurrent opening and deposition, whereas subsequent to buried soil 2 only minor (10-20 cm) movement has occurred on selected faults. The implication of this evolution is either: 1) the locus of faulting has shifted away from this fault since 32-54 ka, or 2) the latest two earthquakes on the PFZ have created small-displacement faulting spread across all the structures of the PFZ, but no large displacements on any one

fault. This latter scenario is compatible with the evidence of scattered but small displacements across the seven-trench transect of 1997.

The single recurrence interval measured between the MRE and PE does not allow us to estimate how variable recurrence on the Pajarito fault might be through geologic time. At other paleoseismic sites worldwide where multiple consecutive paleoearthquakes have been dated, the coefficient of variation (standard deviation/mean) of the successive recurrence times converges to about 0.35 as the record lengthens (McCalpin and Slemmons, 1998). Thus, for a fault with a mean (long-term) recurrence interval of 10 ka, about 2/3 of recurrence intervals over time would fall within one standard deviation about the mean (i.e., between 6.5 and 13.5 ka), and 95% would fall within two standard deviations from the mean (i.e., between 3 and 17 ka). This method of approximating the variability in recurrence could be applied if we knew the long-term mean recurrence on the Pajarito fault, but our single measurement is only one sample drawn from a population that may include 50 post-1.2 Ma paleoearthquakes, so it is not a very robust estimator of the long-term mean. Wong et al (1995) estimated a long-term mean recurrence of ca. 20 ka for the Pajarito fault. If that value is accurate, and the COV of recurrence approximates 0.35, then the single recurrence interval dated in Trench 4 (5-11.6 ka) falls within the one-sigma limits. The 11.3-21.6 ka interval estimate from Trench 5 falls around the one and two sigma limits. In contrast, the 28.6-48.9 ka recurrence estimate from Trench 6 falls well beyond the two-sigma limits, and suggests that perhaps this trench does not record all the paleoearthquakes experienced on the Pajarito fault.

4.3 Displacement Per Event on the Pajarito Fault

Our seven scattered trenches of 1998 were not located to optimize measurements of displacement per event on the entire PFZ, but rather to optimize identification and dating of young faulting events on specific fault strands. Even in each trench some complications arise in measuring net displacement. In Trench 4, the MRE involved penetrative deformation and folding (?) at the head of the trench, so no discrete fault displacement could be measured. During the PE the two subvertical faults at either end of the trench display opposite 20 cm displacements, while the unit 4/5 contact has a vertical separation of 2-2.5 m across deformation zone B. However, due to the presence of a slump at this location, it is unclear what structure is responsible for the vertical separation. For example, McCalpin et al (1992) mapped areas along the Hansel Valley, UT fault scarp where the fault scarp had failed during coseismic slumping, and the height of the compound scarp thus formed was greater than the vertical component of fault displacement (Fig. 26). Such a scenario might explain how the 6 m-high fault scarp at Trench 4 could be created by only 2-2.5 m of vertical displacement in the deposits underlying the scarp. Given the ambiguous nature of the structures in Trench 4, we cannot make confident estimates of displacement per event.

The MRE in Trench 5 was accompanied by vertical displacements of 20 cm on fault E, 20 cm on fault F1, and ca. 10-15 cm on fault G, for a total of 50-55 cm. If our correlation of unit 7 along the trench is correct, the latest displacement in the lower pocket occurred during the PE, and amounted to 1.4-2.8 m.

In Trench 6, the MRE led to depostion of the 40 cm-thick colluvial wedge (unit 3a) at the base of fault C, which has a net vertical displacement on tuff of 50 cm. Based on the absence of unit 4 on the upthrown block we interpreted at least one event prior to the MRE, which had to have at least 15 cm displacement to account for unit 4 on the downthrown block. Therefore, the MRE on fault C (the only fault active during the event) had a net displacement of ca. 35 cm. Displacements during older events are more difficult to estimate, due to ambiguity about the sequence of events. For example, if we assume that unit 6 in the deep fissure accumulated after a single faulting event, the 57 cm-thick colluvial wedge implies down-to-the-east vertical displacement of 0.6-1.2 m. This displacement would be partially offset by the 40 cm down-to-the-west net displacement on the easternmost domino block, resulting in a net vertical displacement of 0.2-0.8 m.

In summary, the net vertical displacement reconstructed for various events ranges from 0.2- 0.8 m, to 0.35 m, 0.5- 0.55 m, and 1.4 -2.8 m in Trenches 5 and 6. On a given fault, then, the typical displacement in recent events was <= 0.5 m. Such small displacements may explain why physical evidence such as colluvial wedges is not well preserved along the Pajarito fault in general. By comparison, the MRE in 1997 Trenches 3 and 7 had caused 1.0 m and 1.1 m of antithetic (down-to-the-west) displacement, while 1997 Trench 1 had a possible Holocene displacement of 0.7 m, and 1997 Trench 5 had a similar small (<50 cm) recent displacement. These results indicate that the vertical coseismic displacement on any one fault strand in the PFZ seldom exceeds 1 m.

During the MRE, cumulative displacement is estimated as 0.5-0.55 m in Trench 5 and 0.35 m in Trench 6. These displacements constitute minimum estimates of the displacement across the entire Pajarito fault at a given location along strike, because they only represent displacement on one of many fault strands that may have moved in the MRE. If we assume that the displacements cited above represent the average displacement along strike in the MRE, then empirical equations of Wells and Coppersmith (1994, normal faults only) predict an earthquake magnitude (Mw) of 6.5-6.6 and a rupture length of 25-28 km. The latter is within the range of scenario rupture lengths used by Wong et al (1995). However, these estimates of magnitude and rupture length are minimums because the displacements estimates are minumums.

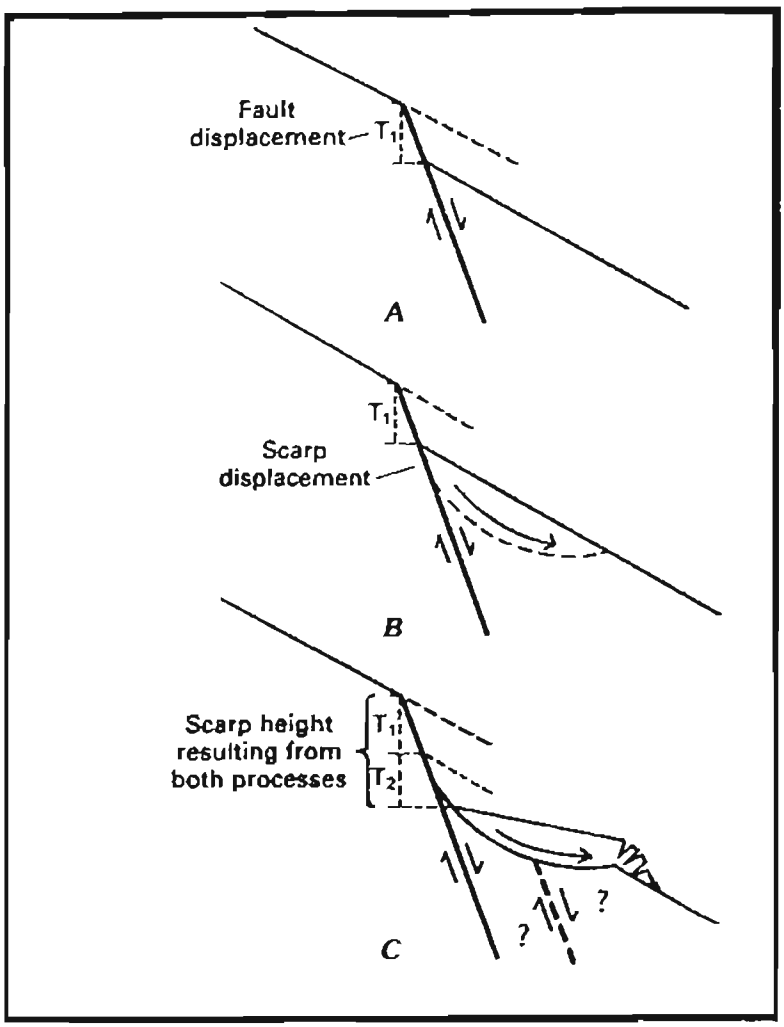

Fig. 26. Schematic cross-sections of the Hansel Valley, UT fault scarp affected by coseismic slumping. A- surface rupture creates a fault scarp with height T1; B- During seismic shaking a rotational slump forms; C- After slumping, total scarp height includes components from tectonic surface rupture (T1) and from the slump headscarp (T2). The dashed and queried fault in C represents a scenario in which the slump forms directly over the tectonic fault, and thus the resulting scarp is 100% slump headscarp. From McCalpin et al. 1992, Fig. 13).

5. CONCLUSIONS AND RECOMMENDATIONS

5.1 Conclusions

The Pajarito fault is a structurally complex zone that underlies an abnormally high and steep fault scarp, and presents a challenge to the traditional methods of paleoseismology. Based on our first field season of trenching (1997), it appeared that a Holocene displacement event had ruptured the Pajarito fault, but that evidence of such rupture was well preserved only where scarps faced upslope (McCalpin, 1998). On east- facing scarps the evidence for Holocene rupture was much more ambiguous, and could be interpreted as the result of tree- throw. The Holocene surface- faulting event was dated in 1997 Trenches 3, 4, 7, and 7a at between 1260 and 2290 cal. yr BP. Vertical displacement during the MRE could be estimated most accurately at antithetic scarps, where the cumulative displacement was 2.1 m down-to-the-west. The MRE was presumably accompanied by an equal or greater amount of down-to-the-east displacement, perhaps as much as 3.1-5.2 m (for explanation, see McCalpin, 1998), but due to erosion on steep east-facing scarps the evidence of such displacements was poorly preserved.

The 1998 trenches were placed either across lineaments or east-facing (synthetic) fault scarps, and evidence of a relatively small-displacement (35-55? cm) Holocene paleoearthquake was detected in Trenches 4, 5, and 6. This MRE is bracketed between the age of the surface soil (2-3 ka by PDI, 0.5-2 ka by C-14) and the age of the youngest buried soil (12-20 ka by PDI). The younger part of this age span overlaps that of the MRE dated in the 1997 trenches, but given the larger age uncertainties associated with the 1998 PDI age estimates compared to the 1997 radiocarbon chronology, we cannot unambiguously correlate the 1997 and 1998 MREs.

PDI age estimates carry uncertainties from the PDI chronofunction curve of McDonald (1999) (which relates PDI to soil development time), but also sources internal to the method, such as those that return PDI values that are sometimes contradictory with stratigraphic position or with radiocarbon dates, as in Trench 4. When PDI age estimates conflict with radiocarbon dates from the same horizon, the PDI age estimates are invariably older. As pointed out by reviewer F.H. Swan, "Soil forming processes vary locally depending on slope aspect, slope angle, drainage, etc. Soil formation is probably accelerated at the break in slope below scarps.....". Thus, much of the uncertainty concerning the age of the MRE and PE exposed in the 1998 trenches arises from the assumptions and limitations of the PDI dating method.

5.2 Implications of the 1997 and 1998 Trench Results on Quaternary Slip Rates for the Pajarito Fault

According to the Final Report of the Seismic Hazards Evaluation of the Los Alamos National Laboratory (WCFS, 1995), the net slip rate of the Pajarito fault is the most important input parameter in the PSHA. WCFS (1995) calculated a range of slip rates for the Pajarito fault, based on: (1) the average height of the fault scarp (81 m); (2) a spatially-averaged long-term vertical slip rate of 81m/1.2 Ma, or 0.07 mm/yr; and (3) net

slip on a 70-degree rake of 123% of the vertical slip rate, or 0.086 mm/yr (WCFS, 1995, Table 7-1, footnote 9). To account for short-term variations in slip rate, McCalpin (1995) suggested a space-for-time substitution utilizing the variability of short- vs. long term slip rates on many faults in the Basin and Range and Rio Grande rift provinces. WCFS adapted this approach the Pajarito fault and calculated the following slip rates for the Pajarito fault:

Table 4. Slip rates used for the Pajarito fault in the WCFS 1995 Logic Tree

Net Slip Rate (mm/yr)	Probability[1]	Percentile[2]
0.01	0.1	5th
0.05	0.2	20th
0.09	0.4	50th
0.20	0.2	80th
0.95	0.1	95th

[1] Probability used on the PSHA logic tree
[2] Cumulative percentile assuming a space-for-time substitution; see Wong et al. (1995), Fig. 7-26

Based on the 1997 trenches, the net slip rate for the last seismic cycle (between the MRE and PE) is 0.06-0.21 mm/yr. Thus, even the fastest slip rate suggested by the 1997 trenching and geochronology data is already covered in the WCFS 1995 logic tree, at a probability of roughly 20%.

The 1998 trench data indicate that at Trench 5, the MRE released 50-55 cm of vertical slip that accumulated over a period of 11.3-21.6 ka, for a slip rate of 0.023-0.049 mm/yr on that fault strand. These slip rates are in the lower part of the range cited in Table 1, but of course they only represent the slip on one of three major fault strands at this latitude on the Pajarito fault. Of the two other fault strands, the westernmost is the Western Splay fault that was partially exposed by Trench 4. There a 6 m-high scarp has been created by a combination of folding, slumping, and/or faulting on a fan surface that post-dates the El Cajete pumice. The slip rate implied by a 6 m scarp in 50-60 ka deposits is 0.1-0.12 mm/yr. This slip rate falls near the center of the range cited in Table 4. However, it must be admitted that some of the 6 m of total scarp height may represent toe thrusting of a landslide. The vertical separation between correlated 30-43 ka strata across the center of the trench is only 2-2.5 m. This separation implies a vertical slip rate of only 0.046-0.083 mm/yr, which is in the lower part of the range cited in Table 4. If the slip rates on the Western Splay fault and the Trench 5 scarp are summed (which represents 2 of the 3 major fault strands at this latitude), the net vertical slip rate is 0.069-0.132 mm/yr. These rates approximately straddle the midpoint of the distribution cited in Table 4. An unknown additional component of slip during the MRE may have occurred on the 25 m-high fault scarp downslope from Trench 5, but that structure has not been trenched. Nevertheless, the net slip rate across 2/3 of the Pajarito fault south of Pajarito Canyon during the most recent seismic cycle appears to fall in about the midddle of the range of estimates made by Wong et al. (1995).

The slip rates cited above only represent the latest seismic cycle, and slip rates during previous seismic cycles may have varied from this value, in the same general way that recurrence intervals vary through time.

5.3 Timing of the MRE on the PF, GMF, and RCF

A separate issue is whether the 4-6 ka event on the Guaje Mountain fault, and the 8 (23?) ka event on the Rendija Canyon fault, also involved seismogenic rupture of the Pajarito fault. The 1.5 ka to 2.5 ka MRE deduced for the Pajarito fault from the 1997 trenches does not overlap in time with a 4-6 ka event, whereas the 2-3 ka to 12-20 ka MRE from the 1998 trenches does overlap the 4-6 ka event. Thus, if the 1998 MRE is the same as the 1997 MRE, then neither is the same event as the 4-6 ka MRE on the Guaje Mountain fault. Alternatively, if the 1998 MRE is a different event than the 1997 MRE, then it could conceivably be the same event as the 4-6 ka MRE on the Guaje Mountain fault, or it could be different than either the 1997 MRE or the Guaje Mountain fault MRE. In any case, if we assume that the 4-6 ka date on the Guaje Mountain fault MRE is correct, then the 1997 MRE, 1998 MRE, and Guaje Mountain fault MRE cannot all represent the same faulting event. Thus, the current dating control suggests that either: (1) the Guaje Mountain fault can rupture without rupturing the Pajarito fault, which is a possibility contained within the Wong et al. 1995 logic tree, or (2) two Holocene ruptures occurred on different parts of the Pajarito fault, with a boundary somewhere between Pajarito Canyon (northern known extent of the 1998 MRE) and Los Alamos Canyon (1997 MRE). This latter possibility is equivalent to having a fault segment boundary between Pajarito and Los Alamos Canyons. None of the 22 rupture scenarios in the Wong et al. (1995, Fig. 7-25) logic tree contain such a segment boundary, although several show a segment boundary at Los Alamos Canyon.

The current age control on the MRE on the Rendija Canyon fault is insufficient to permit a correlation with events on the PF, either from our 1997 or 1998 trenches. For example, if the 8 ka date is correct, then this event did not rupture any of the 1997 trenches on the PF. However, a date of 8 ka does fall within the rather broad age limits for the MRE from the 1998 trenches. Again, we must conclude that, if the 1998 MRE correlates with the Rendija Canyon fault MRE, then the 1998 MRE must be a different event than the 1997 MRE on the Pajarito fault. If it does not correlate with the Rendija Canyon fault MRE, then the Rendija Canyon fault can rupture independently of the PF.

Thus, it appears that under either correlation scenario between the Pajarito fault and Rendija Canyon fault, or the Pajarito fault and Guaje Mountain fault, that we must retain the possibility that ruptures may occur on the Rendija Canyon fault and Guaje Mountain fault that do not rupture the PF, as is contained in the Wong et al. (1995) logic tree.

5.4 Recommendations

The two field seasons of trenching on the Pajarito fault have answered several key questions as to the accuracy of slip rates and appropriateness of structural and behavioral scenarios for the PFZ, as included in the Wong et al. (1995) logic tree. The only remaining unanswered question at present is whether the dates currently cited for the MREs on the

Guaje Mountain fault and Rendija Canyon fault are correct. At the beginning of the 1997 trenching studies, the paleoseismic histories of the Guaje Mountain fault and Rendija Canyon fault, with one well-dated trench site on each, were better known than that of the Pajarito fault. At that time, of the four trenches of Wong et al. (1995) on the Pajarito fault, one exposed no faults, two were in a suspected landslide block (Fig. 2b, top), and the fourth exposed only small-displacement structures of the basal fault zone that could not be well-dated. At present we have excavated 14 trenches on the Pajarito fault and have constructed space-time diagrams of ruptures covering the past 10 ka (for the 1997 trenches) and 70 ka (for the 1998 trenches). Thus, at this point the limitation in correlating paleoearthquakes among the Pajarito fault, Guaje Mountain fault, and Rendija Canyon fault arises from two sources: (1) the general absence of deposition between ca. 4 and 20 ka on the Pajarito fault scarp, and (2) the limited trench and geochronology data on the Guaje Mountain and Rendija Canyon faults.

Therefore, future paleoseismic investigations (if undertaken) should aim at these two data gaps. First, sites should be examined on the Pajarito fault where early Holocene-late Pleistocene deposition may have occurred in association with faulting, such as the grabens at the head of the scarp north of Water Canyon and Canon de Valle, and the graben along West Jemez Road. Second, one to two additional trenches should be excavated across the Guaje Mountain fault and Rendija Canyon fault to confirm the timing of the MRE (and possibly the PE) that is now based on only a single trench site on each fault. If the additional trenches on each fault yields dates comparable with the existing dates, then the paleoseismic history will probably be as well constrained as can be expected (given the inherent limitations imposed by field conditions), and no further paleoseismic studies are indicated. If the second trench on one or both faults yields dates on the MREs that conflict with the present age ranges, then the dating effort in those second trenches must be sufficiently sophisticated that the new dates will supercede the old dates, and permit a confident correlation between the MREs (and possibly PEs) among the Pajarito fault, Guaje Mountain fault, and Rendija Canyon fault.

6. REFERENCES

Aitken, M. J., and Bowman, S. G. E. 1975, Thermoluminescence dating: Assessment of alpha particle contribution. Archaeometry, 17, 132-138.

Balescu, S. and Lamothe M., 1992, The blue emissions of K-feldspar coarse grains and its potential for overcoming TL age underestimates: Quaternary Science Reviews, v. 11, p. 45-51.

Blong, R.J. and Gillespie, R., 1978, Fluvially transported charcoal gives erroneous 14-C ages for recent deposits: Nature, v. 271, p. 739-741.

Broxton, D.E. and Reneau, S.L., 1995, Stratigraphic nomenclature of the Bandelier Tuff for environmental restoration project at Los Alamos National Laboratory: Los Alamos National Laboratory Report LA-13010-MS, Los Alamos, NM, 21 p.

Gardner, J.N., Baldridge, W.S., Gribble, R., Manley, K., Tanaka, K., Geissman, J.W., Gonzalez, M. and Baron, G., 1990, Results from seismic hazards trench #1 (SHT-1), Los Alamos Seismic Hazards Investigations, Los Alamos National Laboratory Report No. EES1-SH90-19, 57 p.

Gardner, J.N. and Reneau, S.L., unpublished, Unpublished in-progress mapping of faults in the vicinity of Los Alamos National Laboratory: Los Alamos National Laboratory, NM.

Godfrey-Smith, D. I., Huntley, D. J. and Chen, W.-H., 1988, Optical dating studies of quartz and feldspar sediment extracts: Quaternary Science Reviews v. 7, p. 373-380.

Harden, J.W., 1982, A quantitative index of soil development from field descriptions--Examples from a chronosequence in central California: Geoderma, 28:1-28.

Harden, J.W. and Taylor, E.M., 1983, A quantitative comparison of soil development in four climatic regimes: Quaternary Research, v. 20, p. 342-359.

Hecker, S. and Schwartz, D.P., 1994, The characteristic earthquake revisited; geological evidence of the size and location of successive earthquakes on large faults: U.S. Geological Survey Open-File Report 94-568, p. 79-80.

Huntley, D. J., and Wintle, A. G., 1981,The use of alpha scintillation counting for measuring Th-230 and Pa-231 contents of ocean sediments. Canadian Journal of Earth Sciences, 18, 419- 432.

Huntley, D. J., Hutton, J. T. and Prescott, J. R., 1993, The stranded beach-dune sequence of south-east sout Australia. A test of thermoluminescence dating, 0-800 ka: Quaternary Science Reviews v. 12, p. 1-20.

Kelson, K.I., Hemphill-Haley, M.A., Olig, S.S., Simpson, G.D., Gardner, J.N., Reneau, S.L., Kolbe, T.K., Forman, S.L. and Wong, I.G., 1996, Late Pleistocene and possibly Holocene displacement along the Rendija Canyon fault, Los Alamos County, New Mexico, in New Mexico Geological Society Guidebook, 47th Field Conference, Jemez Mountains Region, p.

Kolbe, T., Sawyer, J., Gorton, A., Olig, S., Simpson, D., Fenton, C., Reneau, S., Carney, J., Bott, J., and Wong, I., 1994, Evaluation of the potential for surface faulting at the proposed mixed waste disposal facility, TA-67: unpublished report submitted by Woodward-Clyde federal Services, Oakland, CA to Los Alamos National Laboratory, Los Alamos, NM.

Kolbe, T., Sawyer, J., Springer, J., Olig, S., Reneau, S., Hemphill-Haley, M. and Wong, I., 1995, Evaluation of the potential for surface faulting at TA-63: unpublished report submitted by Woodward-Clyde federal Services, Oakland, CA to Los Alamos National Laboratory, Los Alamos, NM.

Lettis, W.R. and Swan, F.H. III, 1997, Review of paleoseismic trenches (No. 1 through 7) along a transect across the Pajarito fault zone south of Los Alamos Canyon, September 17, 18, and 19, 1997: unpublished letter report submitted by Wm. Lettis & Associates and Geomatrix Consultants, Inc. to Los Alamos National Laboratory, Oct. 15, 1997, 8 p.

McCalpin, J.P., 1995, Frequency distribution of geologically-determined slip rates for normal faults in the western USA: Bulletin of the Seismological Society of America, v. 85, no. 6, p. 1867-1872

McCalpin, J.P. (ed.), 1996a, Paleoseismology: Academic Press, New York, 583 pp.

McCalpin, J.P., 1996b, Field Techniques in Paleoseismology, Chapter 2 in McCalpin, J.P. (ed.), Paleoseismology: Academic Press, New York, p. 33-84.

McCalpin, J.P., 1997, Geomorphology and structure of the Pajarito fault zone west of Los Alamos National Laboratory, New Mexico: unpublished report submitted to Los Alamos National Laboratory, Los Alamos, NM, by GEO-HAZ Consulting, Inc., Estes Park, CO, April 9, 1997, 54 p.

McCalpin, J.P., 1998, Late Quaternary faulting on the Pajarito fault, west of Los Almaos National Laboratory, north-central New Mexico; Results from the transect of seven trenches excavated in 1997; Final Report: unpublished report submitted to Los Alamos National Laboratory. Los Alamos, NM by GEO-HAZ Consulting, Inc., Estes Park, CO, Aug. 31, 1998, 112 p. Plus appendices.

McCalpin, J.P. and Slemmons, D.B., 1998, Statistics of paleoseismic data: unpublished Final Technical Report submitted to U.S. Geological Survey, Reston, VA by GEO-HAZ

Consulting, Inc., Estes Park, CO, Contract 1434-HQ-96-GR-02752, March 20, 1998, 62 p.

McCalpin, J.P., Robison, R.M. and Garr, J.D., 1992, Neotectonics of the Hansel Valley-Pocatello Valley corridor, northern Utah and southern Idaho, in Gori, P.L. and hays, W.W. (eds.), Assessment of regional earthquake hazards and risk along the Wasatch Front, Utah: U.S. Geological Survey Professional Paper 1500-G, p. G1-GG18.

McDonald, E.V., 1999, LANL seismic hazard trench investigations: Soil stratigraphy and pedologic age estimates for Late Quaternary faulting on the Pajarito fault, west of Los Alamos National Laboratory; Results from 1997 and 1998 trench excavations: unpublished report submitted to Los Alamos National Laboratory, Los Alamos, NM, by Desert Research Institute, Reno, NV, Feb. 1999, 82 p

Olig, S.S., Kelson, K.I., Gardner, J.N., Reneau, S.L. and Hemphill-Haley, M.A., 1996, The earthquake potential of the Pajarito fault system, New Mexico, in New Mexico Geological Society Guidebook, 47th Field Conference, Jemez Mountains Region, p. 143-152.

Pantosti, D., Schwartz, D.P. and Valensise, G., 1993, Paleoseismology along the 1980 surface rupture of the Irpina fault; implications for earthquake recurrence in the southern Appennines, Italy: Journal of Geophysical Rserach, v. 98, p. 6561-6577.

Pezzopane, S.K. and Dawson, T.E., 1996, Fault displacement hazard; a summary of issues and information, in Whitney, J.E. (ed.), Seismotectonic framework and characterization of faulting at Yucca Mountain, Nevada: report by U.S. Geol. Survey, Denver, CO submitted to US Dept. of Energy, Contract DE-AC04-94AL85000, 3 vols

Reneau, S.L., 1996, West Jemez geomorphology: unpublished map produced by S.L. Reneau for Los Alamos National Laboratory, FIMAD Plot ID g105108, scale 1:5,686.

Reneau, S.L. and McDonald, E.V., 1996, Landscape history and processes on the Pajarito Plateau, northern New Mexico: Fieldtrip Guidebook, Rocky Mountain cell, Friends of the Pleistocene, 12-15 Sept. 1996, Los Alamos, NM, 179 pp.

Reneau, S.L., Gardner, J.N. and Forman, S.L., 1996, New evidence for the age of the youngest eruptions in the Valles caldera, New Mexico: Geology, v. 24, p. 7-10.

Rogers, M.A., 1995, Geologic map of the Los Alamos National Laboratory Reservation: New Mexico Environment Department, Santa Fe, NM.

Taylor, E.M., 1988, Instructions for the soil development index template- Lotus 1-2-3: U.S. Geological Survey Open-File Report 233A.

Vogel, J.C., Fuls, A., Visser, E. and Becker, B., 1993, Praetoria calibration curve for short lived samples: Radiocarbon, v. 35, p. 73-8

Wong, I. and 16 others, 1993, Seismic hazards evaluation of the Los Alamos National Laboratory, Draft Final Report: submitted to Los Alamos National Laboratory by Woodward Clyde Federal Services, June 1, 1993, 3 vols.

Wong, I. and 16 others, 1995, Seismic hazards evaluation of the Los Alamos National Laboratory, Final Report: submitted to Los Alamos National Laboratory by Woodward Clyde Federal Services, 25 Feb. 1995, 3 vols.

APPENDIX 1

Seismic refraction survey results.

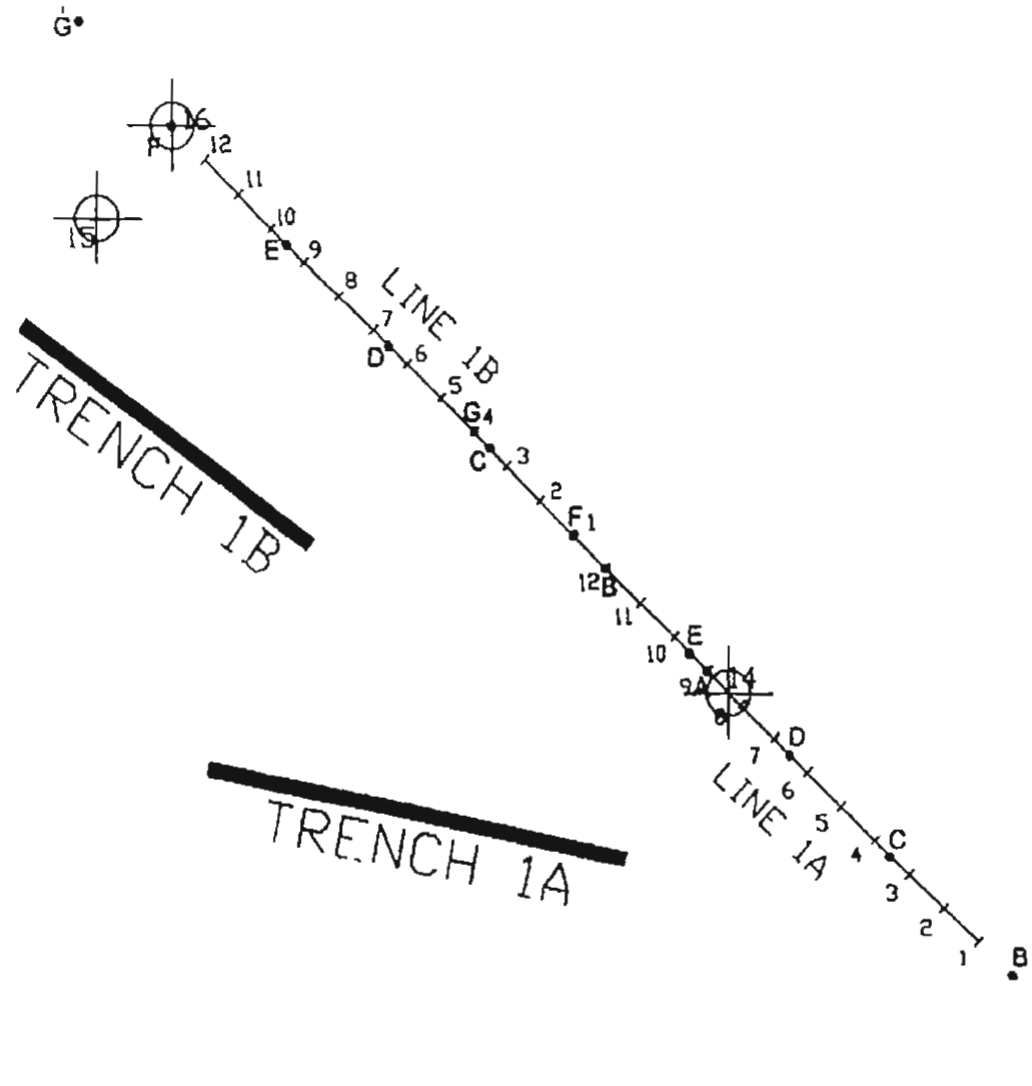

Geophone

A Shot Point

NORTH

FIGURE 1-A
Trench 1A-1B - Lines 1A-1B Location Map
LANL Pajarito Fault Project
August 1998

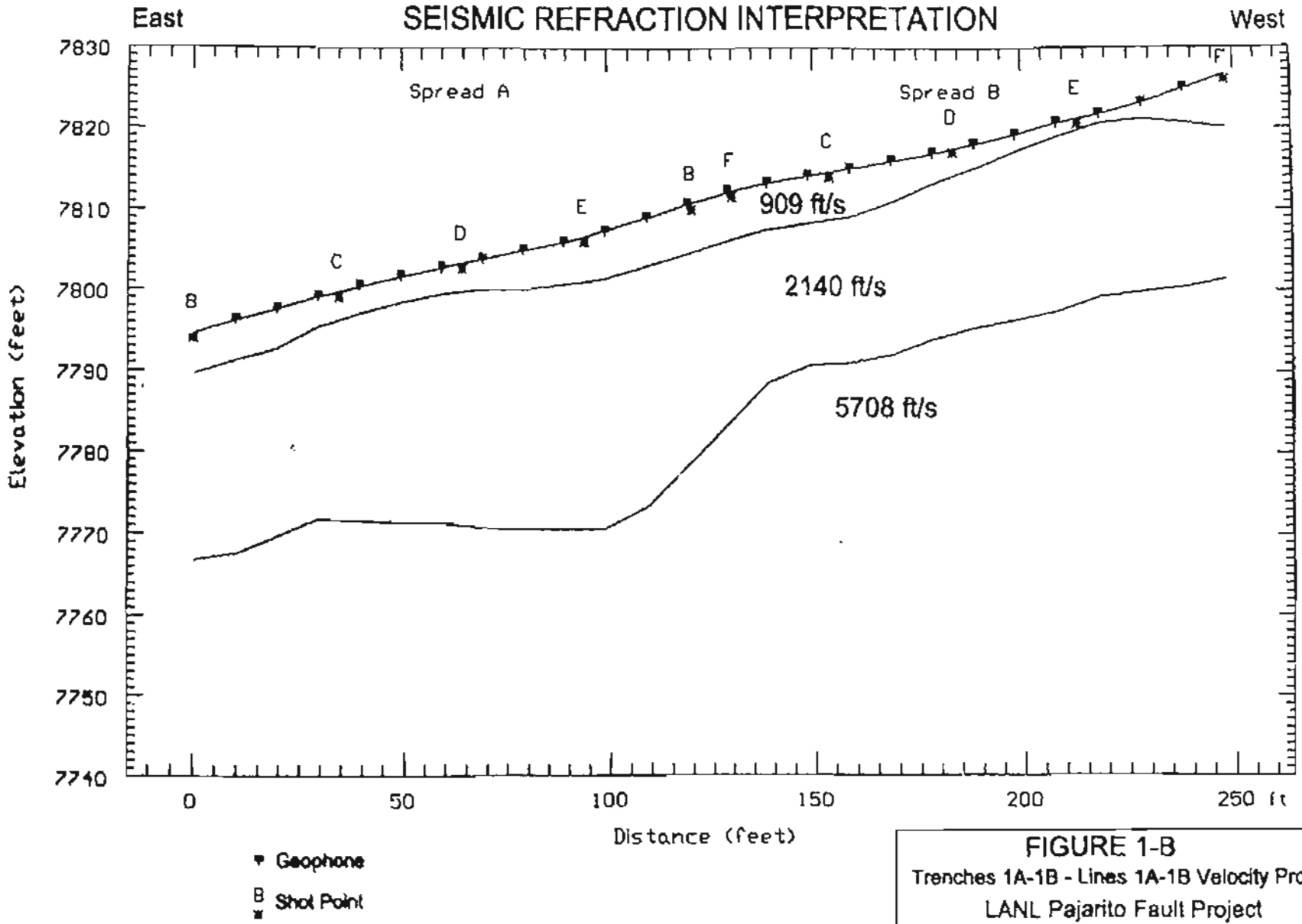

FIGURE 1-B
Trenches 1A-1B - Lines 1A-1B Velocity Profile
LANL Pajarito Fault Project
August 1998

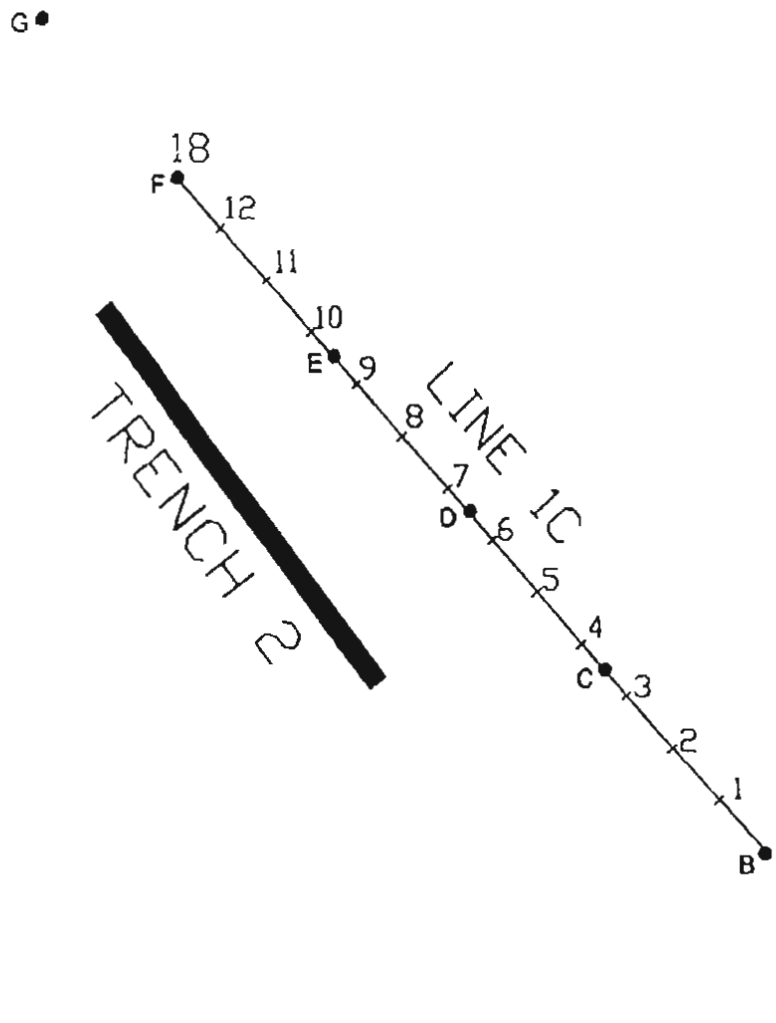

FIGURE 2-A
Trench 2 - Line 2 Location Map
LANL Pajarito Fault Project
August 1998

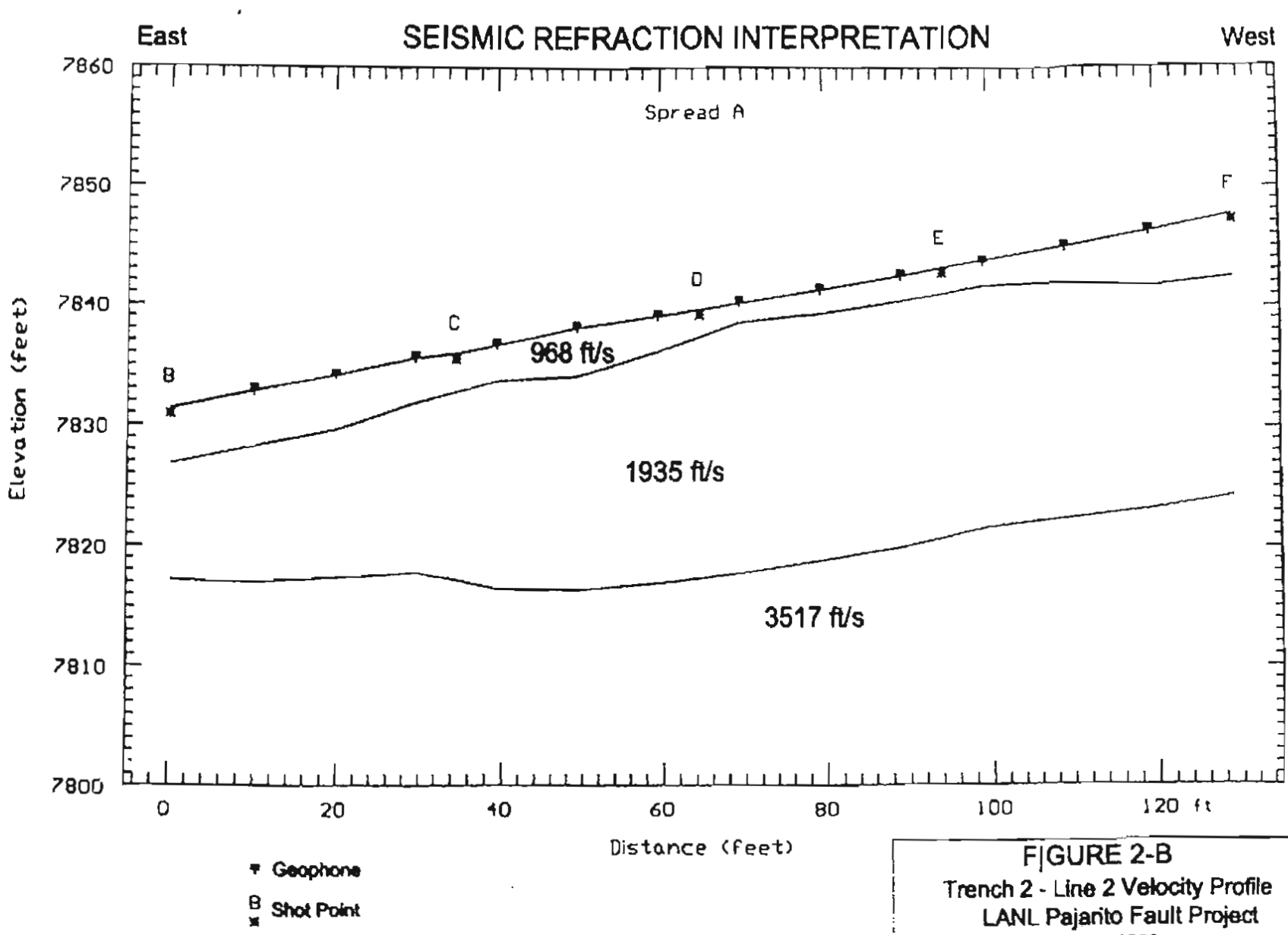

FIGURE 2-B
Trench 2 - Line 2 Velocity Profile
LANL Pajarito Fault Project
August 1998

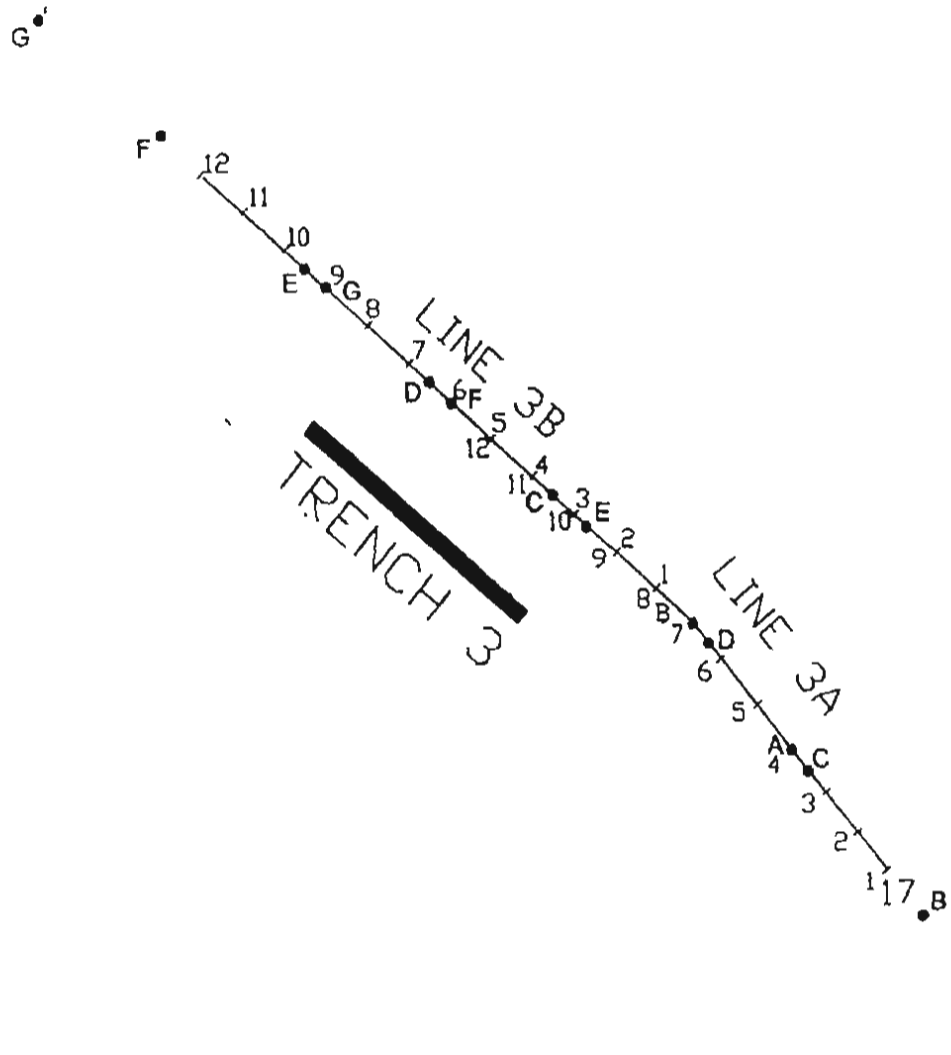

FIGURE 3-A
Trench 3 - Line 3A-B Location Map
LANL Pajarito Fault Project
August 1998

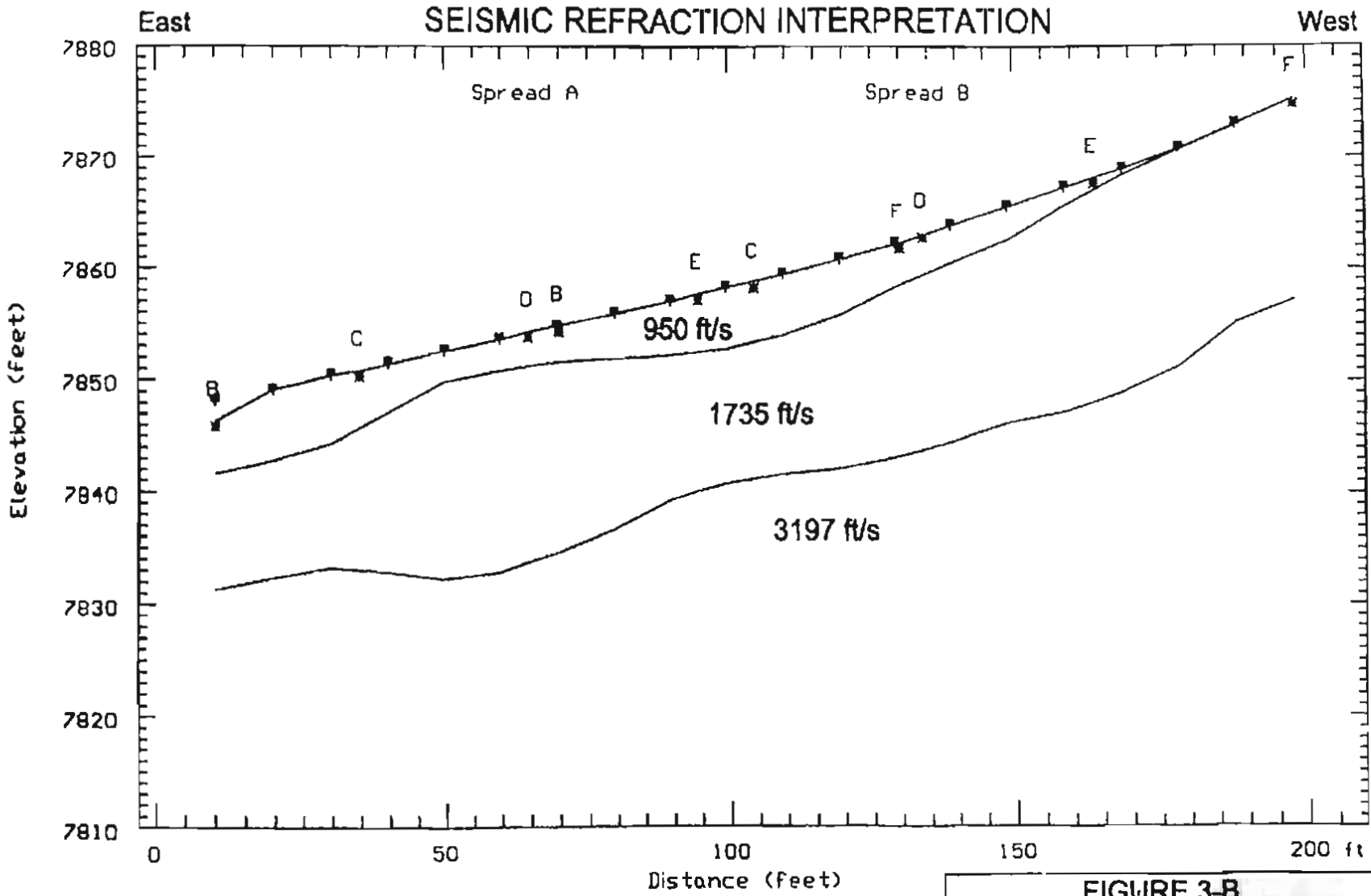

FIGURE 3-B
Trench 3 - Lines 3A and 3B Velocity Profile
LANL Pajarito Fault Project
August 1998

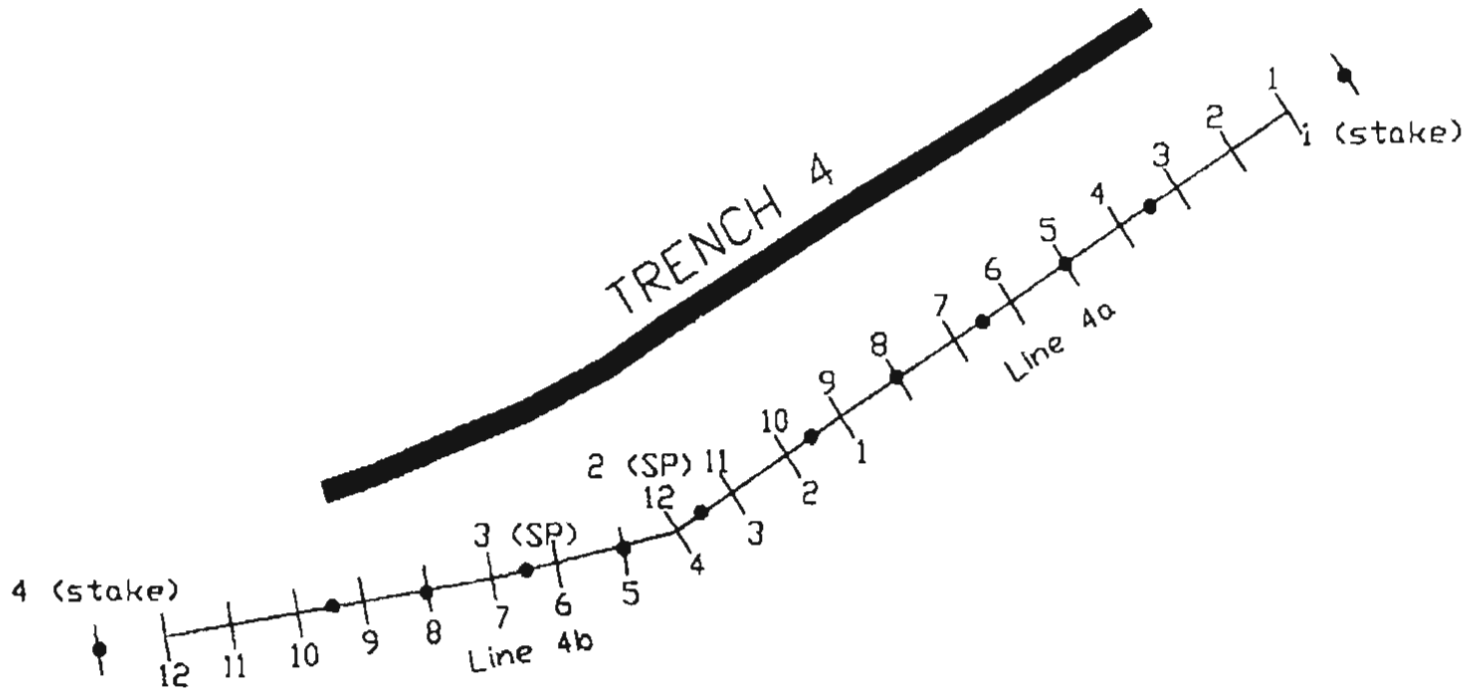

Geophone

Shot Point

FIGURE 4-A

Trench 4 - Line 4a, 4b Location Map

LANL Pajarito Fault Project

August 1998

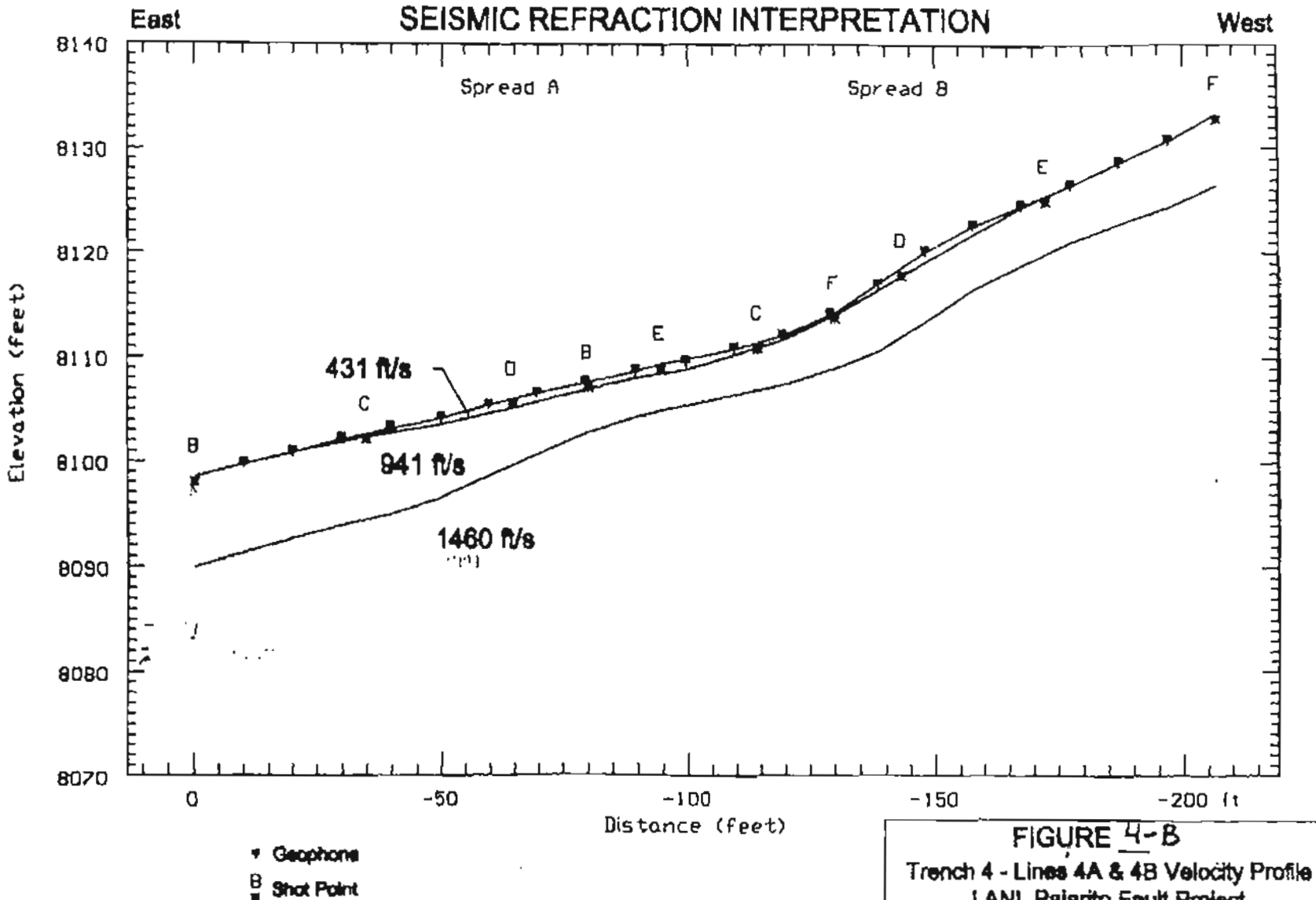

FIGURE 4-B
Trench 4 - Lines 4A & 4B Velocity Profile
LANL Pajarito Fault Project
August 1998

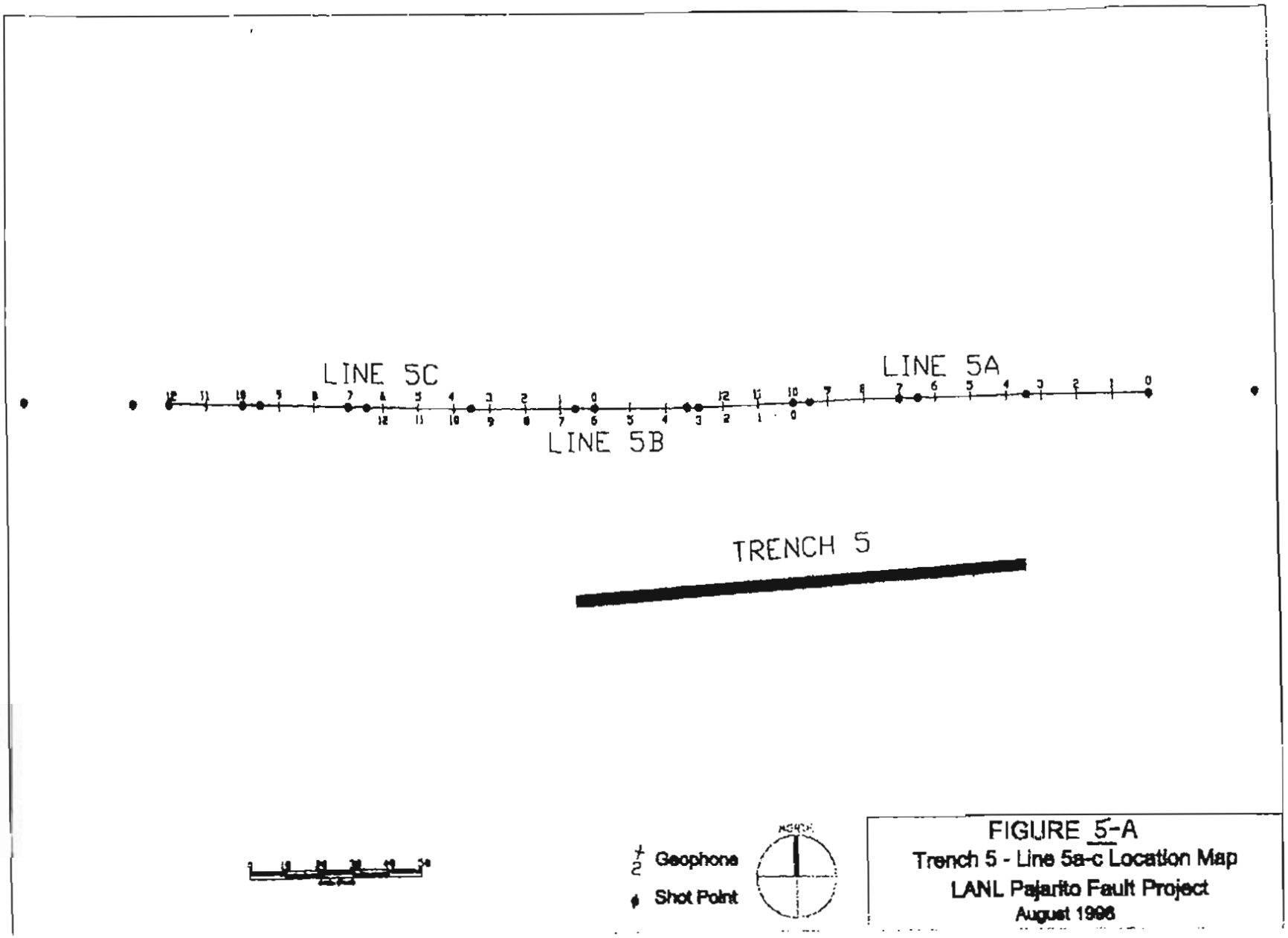

FIGURE 5-A
Trench 5 - Line 5a-c Location Map
LANL Pajarito Fault Project
August 1998

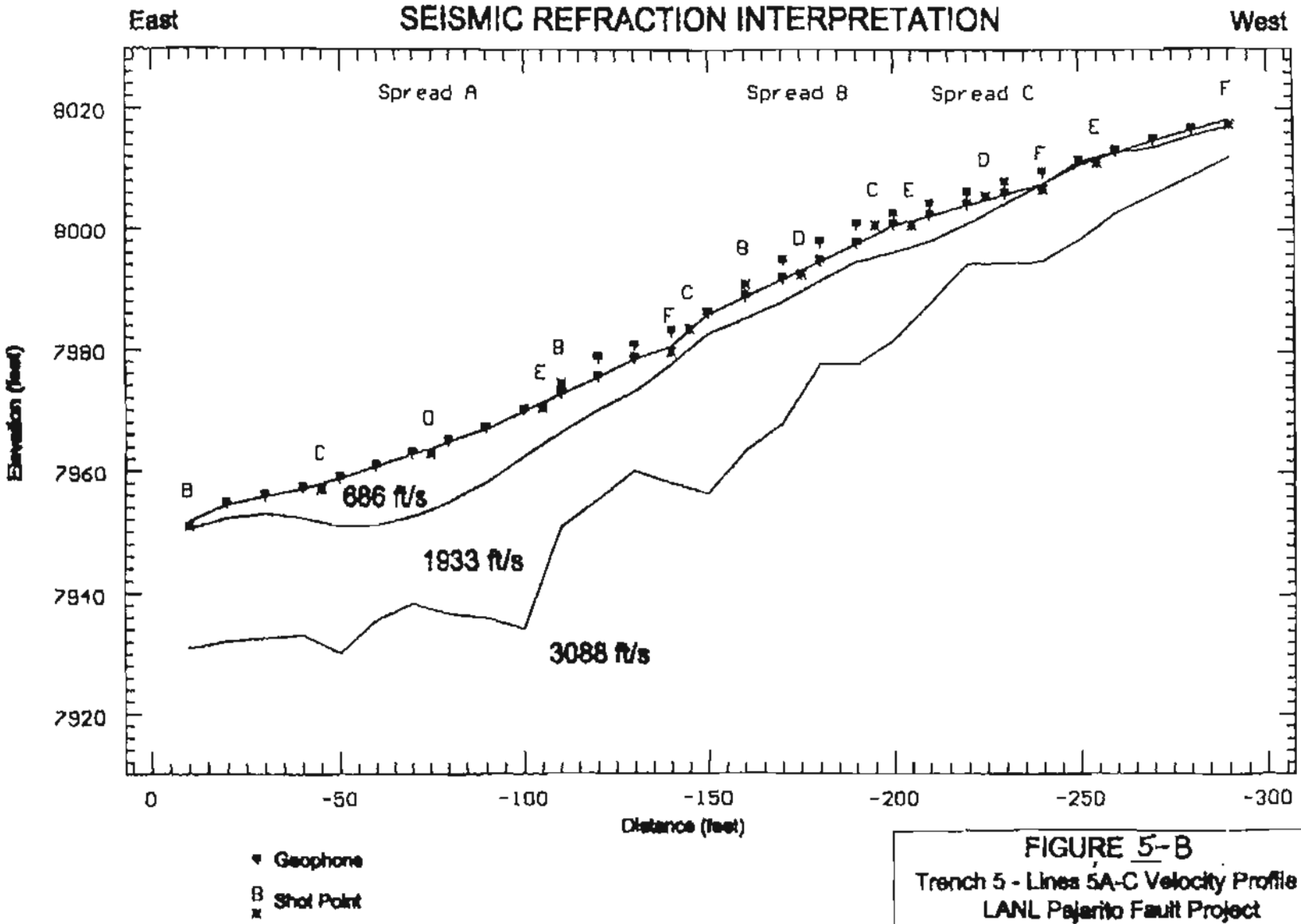

FIGURE 5-B
Trench 5 - Lines 5A-C Velocity Profile
LANL Pajarito Fault Project
August 1998

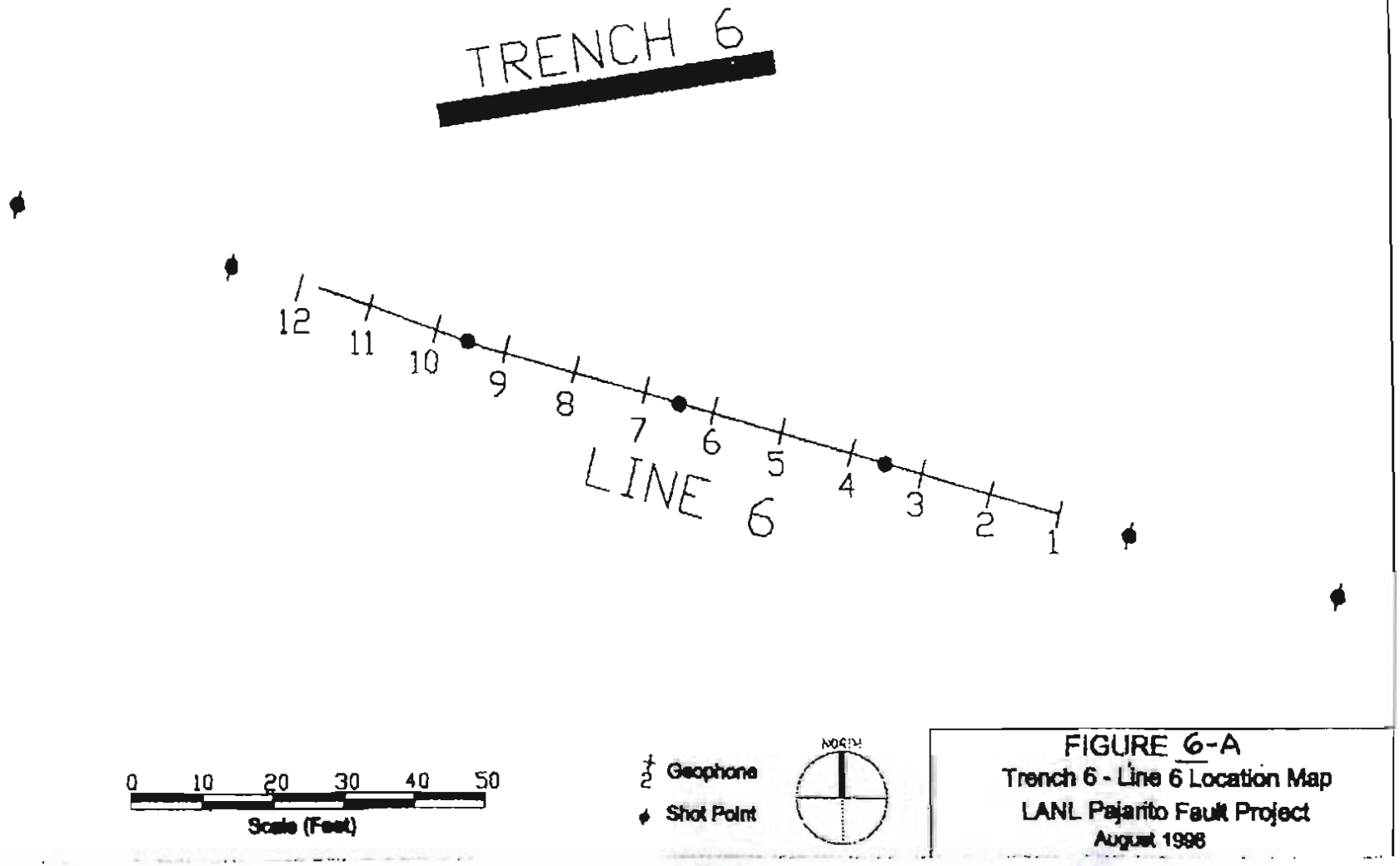

FIGURE 6-A
Trench 6 - Line 6 Location Map
LANL Pajarito Fault Project
August 1998

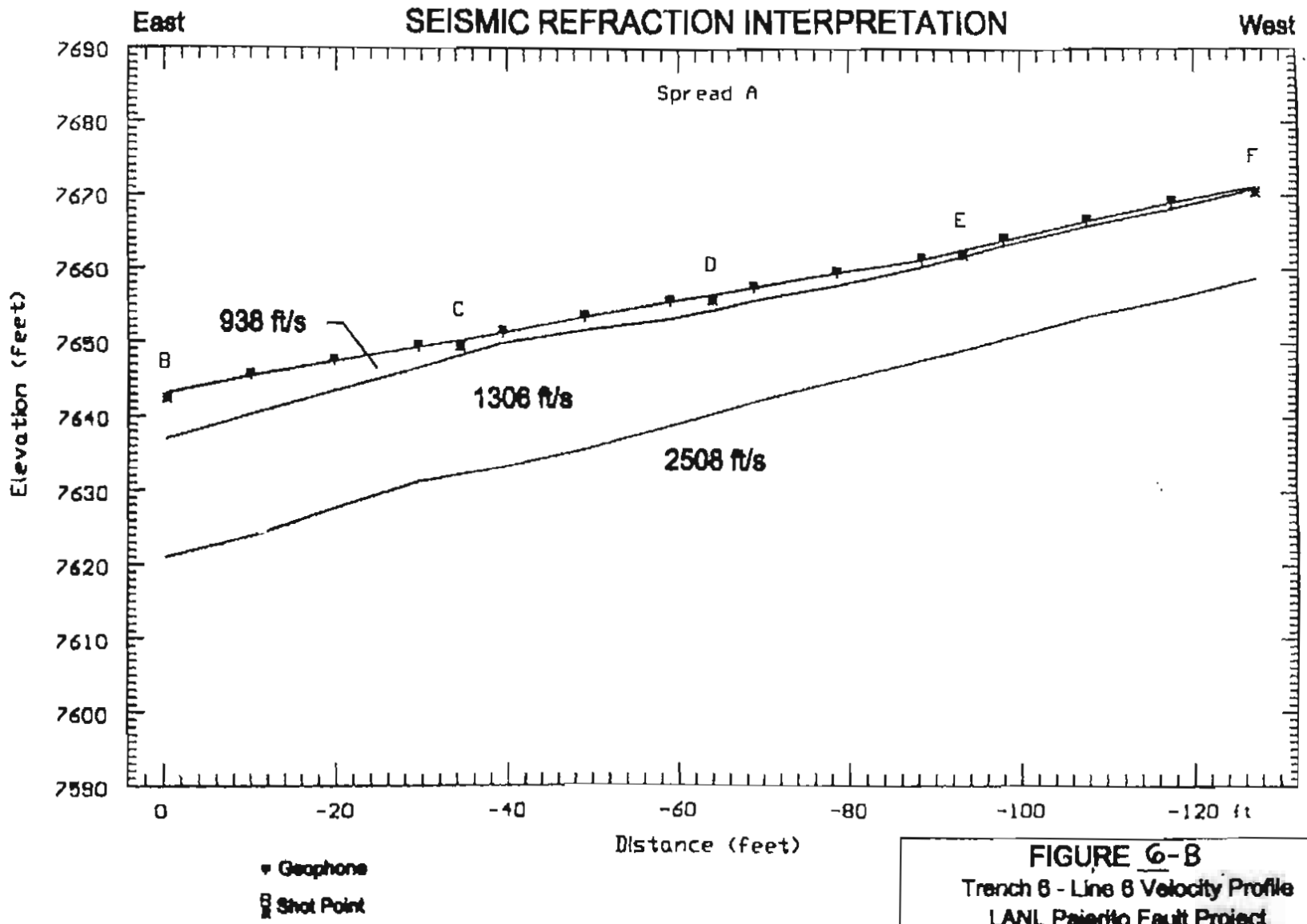

FIGURE 6-B
Trench 6 - Line 6 Velocity Profile
LANL Pajarito Fault Project
August 1998

APPENDIX 2

Report by PaleoResearch Labs, on content of radiocarbon samples

EXAMINATION OF SOIL FROM LOS ALAMOS, NEW MEXICO

E,

Kathryn Puseman
Paleo Research Laboratories
Denver, Colorado

Paleo Research Labs Technical Report 98-83

Prepared For

Geo-Haz Consulting, Inc.
Estes Park, Colorado

September 1998

INTRODUCTION

Bulk soil samples were recovered from trenches excavated as part of a paleoseismic study near Los Alamos, New Mexico. Botanic components and detrital charcoal were identified, and potentially radiocarbon datable material was separated.

METHODS

The samples were floated using a modification of the procedures outlined by Matthews (1979). Each sample was added to approximately 3 gallons of water. The sample was stirred until a strong vortex formed, which was allowed to slow before pouring the light fraction through a 150 micron mesh sieve. Additional water was added and the process repeated until all visible macrofloral material was removed from the sample (a minimum of 5 times). The material which remained in the bottom (heavy fraction) was poured through a 0.5 mm mesh screen. The floated portions were allowed to dry.

The light fractions were weighed, then passed through a series of graduated screens (US Standard Sieves with 4 mm, 2 mm, 1 mm, 0.5 mm and 0.25 mm openings to separate charcoal debris and to initially sort the remains. The contents of each screen were then examined. Charcoal pieces larger than 1 mm in diameter were broken to expose a fresh cross-section and examined under a binocular microscope at magnifications up to 140x. The remaining light fraction in the 4 mm, 2 mm, 1 mm, 0.5 mm, and 0.25 mm sieves was scanned under a binocular stereo microscope at a magnification of 10x, with some identifications requiring magnifications of up to 70x. The material which passed through the 0.25 mm screen was not examined. The coarse or heavy fractions also were screened and examined for the presence of botanic remains.

Macrofloral remains, including charcoal, were identified using manuals (Core et al. 1976; Martin and Barkley 1973; Panshin and Zeeuw 1980; Petrides and Petrides 1992) and by comparison with modern and archaeological references. The term "seed" is used to represent seeds, achenes, caryopses, and other disseminules. Remains from both the light and heavy fractions were recorded as charred and/or uncharred, whole and/or fragments. Because charcoal and possibly other botanic remains were to be sent for radiocarbon dating, clean laboratory conditions were used during the flotation and identification to avoid contamination. All instruments were washed between samples, and samples were protected from contact with modern charcoal.

DISCUSSION

The sampled trenches were located three to four miles west of Los Alamos, New Mexico. The project area is dominated by ponderosa pine (Pinus ponderosa), with very little understory vegetation present. Six samples from three trenches were examined.

Sample 98T4-5 contained pieces of probable Pinus (charcoal (Tables 1 and 2), which were submitted for radiocarbon dating. The sample also contained pieces of charred vitrified tissue and small, charred bark fragments. Vitrified material has a shiny,

glassy appearance due to fusion by heat. Uncharred roots, rootlets, and an unidentified hardwood twig fragment represent modern plants. Sclerotia, an insect chitin fragment, and rock/gravel also were present. Sclerotia are commonly called "carbon balls". They are small, black, solid or hollow balls that range from 0.5 to 4mm in size. Sclerotia are associated with mycorrhizae fungi, such as Cenococcum graniforme, that have a mutualistic relationship with tree roots. Sclerotia are the resting structures of the fungus, identified by Dr. Kristina Vogt, Professor of Ecology in the School of Forestry and Environmental Studies at Yale University. Many trees are noted to depend heavily on mycorrhizae and may not be successful without them. "The mycelial strands of these fungi grow into the roots and take some of the sugary compounds produced by the tree during photosynthesis. However, mycorrhizal fungi benefit the tree because they take in minerals from the soil, which are then used by the tree" (Kricher and Morrison 1988:285). Sclerotia appear to be ubiquitous and are found with coniferous and deciduous trees including Abies (fir), Juniperus communis (common juniper), Larix (larch), Picea (spruce), Pinus (pine), Pseudotsuga (Douglas fir), Acer pseudoplatanus (sycamore maple), Alnus (alder), Betula (birch), Carpinus caroliniana (American hornbeam), Carya (hickory), Castanea dentata (American chestnut), Corylus (hazelnut), Crataegus monogyna (hawthorn), Fagus (beech), Populus (poplar, cottonwood, aspen), Quercus (oak), Rhamnus fragula (alder bush), Salix (willow), Sorbus (chokecherry), and Tilia (linden) (McWeeney 1989:229-130; Trappe 1962).

Small pieces of charred bark and conifer charcoal from sample 98T4-6 were combined and submitted for radiocarbon dating. The conifer charcoal most likely represents local pine trees; however, the charcoal pieces were too small for a positive Pinus identification. Uncharred rootlets, sclerotia, and rock/gravel were the only other remains to be recovered.

Sample 98T4-7 contained small pieces of conifer charcoal that were submitted for radiocarbon dating. This sample also yielded a charred vitrified tissue fragment, uncharred rootlets, sclerotia, and rock/gravel.

Sample 98T5-1 contained pieces of Pinus charcoal, charred bark fragments, uncharred rootlets, sclerotia, and rock/gravel. The Pinus charcoal was sent for radiocarbon dating.

Three small pieces of charred bark were the only charred remains present in sample 98T5-2, although these pieces of bark were too small for radiocarbon dating. An uncharred Pinus needle fragment and uncharred rootlets represent modern plants. Non-floral remains include very small uncharred bone fragments and rock/gravel.

Sample 98T6-1 yielded sufficient probable Pinus charcoal for radiocarbon dating. Three vitrified tissue fragments were the only other charred remains to be recovered. Uncharred remains include modern Pinus bark scale fragments, roots, and rootlets. The sample also contained sclerotia, a few worm casts, and rock/gravel.

SUMMARY AND CONCLUSIONS

Flotation of samples from trenches near Los Alamos, New Mexico, resulted in recovery of Pinus charcoal, probable Pinus charcoal, conifer charcoal, and charred bark fragments that were submitted for AMS radiocarbon dating. Only sample 98T5-2 yielded insufficient quantities of charred material for dating. Conifer charcoal present in these samples most likely represents local pine trees, but the fragments were too small for a positive Pinus identification.

TABLE 1
MACROFLORAL REMAINS FROM TRENCHES NEAR LOS ALAMOS, NEW MEXICO

Sample No.	Identification	Part	Charred W	Charred F	Uncharred W	Uncharred F	Weights/ Comments
98T4-5	Liters Floated						1.3 L
	Light Fraction Weight						7.03 g
	FLORAL REMAINS:						-
	Bark			9			0.006 g
	Vitrified tissue			12			0.020 g
	Roots					X	
	Rootlets					X	Moderate
	Sclerotia				X		Moderate
	CHARCOAL/WOOD:						
	cf. Pinus	Charcoal					
	Unidentified hardwood twig	Wood					
	NON-FLORAL REMAINS:						
	Insect	Chitin				1	
	Rock/Gravel					X	Moderate
98T4-6	Liters Floated						1.15 L
	Light Fraction Weight						5.79 g
	FLORAL REMAINS:						
	Bark			9			0.006 g
	Rootlets					X	Numerous
	Sclerotia				X		Moderate
	CHARCOAL/WOOD:						
	Conifer	Charcoal		6			0.003 g
	NON-FLORAL REMAINS:						
	Rock/Gravel					X	Moderate
98T4-7	Liters Floated						1.0 L
	Light Fraction Weight						3.83 g
	FLORAL REMAINS:						
	Vitrified tissue			1			0.014 g
	Rootlets					X	Moderate
	Sclerotia				X		Few
	CHARCOAL/WOOD:						
	Conifer	Charcoal		13			0.013 g
98T4-7	NON-FLORAL REMAINS:						
	Rock/Gravel					X	Moderate
98T5-1	Liters Floated						0.8 L
	Light Fraction Weight						6.84 g
	FLORAL REMAINS:						
	Bark			8			0.007 g
	Rootlets					X	Numerous
	Sclerotia				X		Moderate
	CHARCOAL/WOOD:						
	Pinus	Charcoal		10			0.031 g
	NON-FLORAL REMAINS:						
	Rock/Gravel					X	Moderate
98T5-2	Liters Floated						1.1 L
	Light Fraction Weight						5.21 g

	FLORAL REMAINS:						
	Bark			3			<0.001 g
	Pinus	Needle				1	
	Rootlets					X	Few
	NON-FLORAL REMAINS:						
	Bone < 1 mm					X	Moderate
	Rock/Gravel					X	Moderate
98T6-1	Liters Floated						1.35 L
	Light Fraction Weight						15.02 g
	FLORAL REMAINS:						
	Vitrified tissue			3			0.002 g
	Pinus	Bark scale				X	Numerous
	Roots					X	
	Rootlets					X	Numerous
	Sclerotia				X		Few
	CHARCOAL/WOOD:						
	cf. Pinus	Charcoal		7			0.016 g
98T6-1	NON-FLORAL REMAINS:						
	Rock/Gravel					X	Moderate
	Worm casts				X		Few

W = Whole
F = Fragment
X = Presence noted in sample
g = grams

TABLE 2
INDEX OF MACROFLORAL REMAINS RECOVERED IN SAMPLES FROM LOS ALAMOS

Scientific Name	Common Name
FLORAL REMAINS:	
Pinus	Pine
Sclerotia	Small, black, solid or hollow balls associated with mycorrhizae fungi, such as Cenococcum graniforme
CHARCOAL/WOOD:	
Conifer	Cone-bearing, gymnospermous trees and shrubs, mostly evergreens, including the pine, spruce, fir, juniper, cedar, yew, and cypress
Pinus	Pine

REFERENCES CITED

Core, H. A., W. A. Cote, and A. C. Day
1976 Wood Structure and Identification. Syracuse University Press, Syracuse, New York.

Kricher, John C. and Gordon Morrison
1988 A Field Guide to Ecology of Eastern Forests. Houghton Mifflin Company, Boston and New York.

Martin, Alexander C. and William D. Barkley
1973 Seed Identification Manual. University of California Press, Berkeley.

Matthews, Meredith H.
1979 Soil Sample Analysis of 5MT2148; Dominguez Ruin, Dolores, Colorado. Appendix B IN The Dominguez Ruin: A McElmo Phase Pueblo in Southwestern Colorado by Alan D. Reed. Bureau of Land Management Cultural Resource Series No. 7, Denver, Colorado.

McWeeney, Lucinda
1989 What Lies Lurking Below the Soil: Beyond The Archaeobotanical View of Flotation Samples. IN North American Archaeologist Vol.10(3) 227-230. Baywood Publishing Co., Inc.

Panshin, A. J. and Carl de Zeeuw
1980 Textbook of Wood Technology. McGraw-Hill Book Co., New York.

Petrides, George A. and Olivia Petrides
1992 A Field Guide to Western Trees. Houghton Mifflin Co., Boston, Massachusetts.

Trappe, James M.
1962 Fungus Associates of Ectotrophic Mycorrhizae. IN The Botanical Review. U.S. Department of Agriculture, Washington, D.C.

APPENDIX 3

Explanation for reconnaissance geologic map of the main Pajarito fault scarp west of LANL (Reneau, 1996)

Qal	Holocene stream alluvium
Qal2	late Pleistocene stream alluvium (terraces)
Qbt	Bandelier Tuff (1.2 Ma)
Qc	colluvium (Quaternary, undivided)
Qec	El Cajete Pumice (ca. 50-60 ka)
Qfo?	Older alluvial fan, early-mid Pleistocene
Qfi	Intermediate-age alluvial fan, mid-Pleistocene (pre El Cajete)
Qfy	Young alluvial fan (Holocene and late Pleistocene; post El Cajete)
Qoal	Older stream alluvium, early-mid Pleistocene